1996

The development and validation of conjugate imaging techniques in the automated reproduction of three dimensional coordinates from multiple camera images

Allan B. Carman

University of Wollongong

THE DEVELOPMENT AND VALIDATION OF CONJUGATE IMAGING TECHNIQUES IN THE AUTOMATED REPRODUCTION OF THREE DIMENSIONAL COORDINATES FROM MULTIPLE CAMERA IMAGES

A thesis submitted in partial fulfilment of the

requirements for the award of the degree of

HONOURS MASTER OF SCIENCE

from

THE UNIVERSITY OF WOLLONGONG

by

ALLAN B. CARMAN, BAppSc.

DEPARTMENT OF BIOMEDICAL SCIENCE

1996

ABSTRACT

The dimensional quantitative analysis of human motion requires the reproduction of three dimensional coordinates from multiple camera images. In current photogrammetric systems the ability to identify and track individual camera image points imposes limitations on the accuracy and complexity of human motion analysis. Current photogrammetric systems are limited by the number of cameras, three dimensional segments, markers per segment, and the complexity of movement possible due to the increased difficulty and time required to reproduce three dimensional coordinates. The automated reconstruction and tracking of three dimensional coordinates may overcome these limitations by removing the necessity to track and identify two dimensional camera coordinates. The aims of the present research were firstly, to identify limitations and practical problems associated with the use of conjugate imagery in the reproduction of three dimensional coordinates, and secondly, to identify and implement techniques involving conjugate imagery for the automated reproduction of three dimensional coordinates. The methods and procedures developed in the current research provides the basis for future research into automated three dimensional tracking. Four criterion measures, i) Conjugate Point Error, ii) Lab Point Standard Error, iii) Lab Point Error, and iv) Lab Point Paired Error, were established for determining the validity of conjugate image points. Based on the criterion measures an algorithm was developed which accurately reproduced three dimensional coordinates and conjugate image points for a 55 point marker system viewed in four cameras (digitisation error $< 0.2\%$, laboratory point separation $\geq$ 6cm.). The success of the algorithm was dependent on the digitisation error, laboratory point separation, and the number of laboratory points appearing in two camera images. The present research has shown the applicability of conjugate imagery in the automated reproduction of three dimensional coordinates from multiple camera images, a well as the viability of this approach in the automated three dimensional tracking of camera image data to achieve an increase in accuracy and complexity of human movement analysis.

ACKNOWLEDGEMENTS

The author wishes to gratefully acknowledge the following people for their assistance during the cause of this thesis.

A special thank you must go to Dr. Peter Milburn for his expert supervision, guidance and continued support which made this thesis possible and saw it reach its conclusion.

Thank you also goes to Julie Steele, Mark Andrews, and fellow students at the University of Wollongong for their encouragement during the course of this study.

Finally, in appreciation for everthing, thank you to my family.

TABLE OF CONTENTS

Page

List if Figures....vi
List of Tables....vii

1.0 Introduction....1

1.1 Statement of the problem....1

1.2 Aim....3

1.3 Purpose....4

1.4 Approach to solving the problem....4

1.5 Review of literature....6

1.5.1 Photogrammetry....7
1.5.2 Stereoscopic configuration and expected accuracy....15
1.5.3 Collinearity and epipolar imagery....28
1.5.4 Collinearity and perspective cross-ratio theory....30
1.5.5 Rigid body mechanics....32
1.5.5.1 Body fixed axes....33
1.5.5.2 Rigid body axes in rigid body mechanics....34
1.5.5.3 Accuracy of rigid body location....40

1.6 Motion analysis systems....42

1.7 The role of automated three dimensional coordinate reproduction in three dimensional identification and tracking....45

2.0 Methodology....48

2.1 Assumptions....48

2.2 Passpoint criteria....48

2.2.1 Maximum criterion values....50
2.2.2 Laboratory point reduction....51

2.3 Mathematical procedures....52

2.3.1 Least squares solution....52
2.3.2 Conjugate imagery in human motion analysis....60
2.3.3 Paired image point normalisation....63

2.4 Test data 67

2.5 Three dimensional reproduction algorithm 72

2.5.1 Three dimensional point generation 72
2.5.2 Three dimensional point reduction : amongst object points of multiple image points 74
2.5.3 Three dimensional point reduction : amongst object points of paired image points 75
2.5.4 Algorithm summary 75

3.0 Results 77

3.1 Lab Point Error 77

3.1.1 Lab Point Error and two camera image points 80
3.1.2 Lab Point Error and camera to laboratory point angle 82

3.2 Lab Point Standard Error 84

3.3 Conjugate Point Error 92

3.4 Reproduction of three dimensional coordinates 99

4.0 Discussion 101

4.1 Accuracy of three dimensional coordinate reproduction 101

4.2 Performance of passpoint criteria 104

4.2.1 Lab Point Standard Error 104
4.2.2 Conjugate Point Error 106
4.2.3 Lab Point Paired Error 110
4.2.4 Coincidence with another set of collinear lines 110

4.3 Three dimensional reproduction algorithm 111

4.4 Future research 115

5.0 Summary and Conclusion 119

6.0 References 123

Appendix I Error factor in stereoscopic configuration 126
Appendix II Test data 147
Appendix III Three dimensional reproduction algorithm 155
Appendix IV Video data 159

LIST OF FIGURES

1 Relationship between film plane, comparator plane and object space 8
2 Camera configuration 16
3 Error factor 27
4 Conjugate imagery 29
5 Perspective cross-ratio theory 31
6 Body fixed axes 34
7 Eularian two axis rotation 36
8 Conjugate point error 49
9 Paired conjugate image points 50
10 Camera perspective centre 56
11 Laboratory boundary 61
12 Image point to epipolar line 63
13 Camera image plane axes 70
14 Paired conjugate image points; angle and Lab Point Error 83
15 Normalisation curve; angle and Lab Point Error 85
16 Paired conjugate image points; angle and Normalised Lab Point Error 86
17 Conjugate Point Error and camera distance 96
18 Conjugate Point Error and angle 98
19 Image point error and reproduction error 108
20 Test data set up 147
21 Three dimensional reproduction algorithm - schematic 155
22 Three dimensional point generation 156
23 Three dimensional point reduction : amongst object points from multiple image points 157
24 Three dimensional point reduction : amongst object points of paired image points 158

LIST OF TABLES

1 The RMS values of residual errors of image coordinates using the DLT method for various photographic set ups, with and without the inclusion of non-linear film deformation and lens distortion 19
2 Predicted errors of object space coordinates as derived from formulae for various photographic set ups, with and without the inclusion of non-linear film deformation and lens distortion 25
3 Measured errors of object space coordinates 41
4 Measured errors of rigid body spatial parameters 42
5 Lab Point Error, with 0.18% introduced error in camera image data 77
6 Lab Point Error, with 0.35% introduced error in camera image data 77
7 Lab Point Error, with 0.53% introduced error in camera image data 78
8 Lab Point Error, with 0.70% introduced error in camera image data 78
9 Lab Point Error, analysis of variance between cameras 79
10 Lab Point Error for paired cameras, with 0.35% introduced error in camera image data 81
11 Lab Point Error, analysis of variance between camera pairs with 0.35% introduced error in camera image data 82
12 Un-normalised Lab Point Standard Error, with 0.18% introduced error in camera image data 87
13 Un-normalised Lab Point Standard Error, with 0.35% introduced error in camera image data 87
14 Un-normalised Lab Point Standard Error, with 0.53% introduced error in camera image data 87
15 Un-normalised Lab Point Standard Error, with 0.70% introduced error in camera image data 88
16 Un-normalised Lab Point Standard Error, analysis of variance between cameras 89
17 Normalised Lab Point Standard Error, with 0.18% introduced error in camera image data 89
18 Normalised Lab Point Standard Error, with 0.35% introduced error in camera image data 90
19 Normalised Lab Point Standard Error, with 0.53% introduced error in camera image data 90
20 Normalised Lab Point Standard Error, with 0.70% introduced error in camera image data 90
21 Normalised Lab Point Standard Error, analysis of variance between cameras 91
22 Conjugate Point Error, with 0.18% introduced error in camera image data 93
23 Conjugate Point Error, with 0.35% introduced error in camera image data 93
24 Conjugate Point Error, with 0.53% introduced error in camera image data 94
25 Conjugate Point Error, with 0.70% introduced error in camera image data 94
26 Conjugate Point Error, analysis of variance between cameras 95
27 Conjugate Point Error, distance from camera perspective centre to midpoint in laboratory space 97
28 Video camera, Conjugate Point Error 100

29 Video camera, Lab Point Standard Error....100
30 Error factor....127
31 Laboratory boundary....148
32 Camera positions....148
33 Camera 1; image plane coordinates relative to laboratory space and image plane of the eight calibration markers....149
34 Camera 2; image plane coordinates relative to laboratory space and image plane of the eight calibration markers....150
35 Camera 3; image plane coordinates relative to laboratory space and image plane of the eight calibration markers....150
36 Camera 4; image plane coordinates relative to laboratory space and image plane of the eight calibration markers....151
37 Camera 5; image plane coordinates relative to laboratory space and image plane of the eight calibration markers....151
38 Camera 6; image plane coordinates relative to laboratory space and image plane of the eight calibration markers....152
39 Camera 7; image plane coordinates relative to laboratory space and image plane of the eight calibration markers....152
40 Camera 8; image plane coordinates relative to laboratory space and image plane of the eight calibration markers....153
41 Test data; DLT parameters....153
42 Test data; Conjugate Point Error....154
43 Test data; Calibration markers reproduced and LPSE....154
44 Calibration cube....159
45 Camera image coordinates of calibration markers....160
46 Video data; DLT parameters....160
47 Video data; Conjugate Point Error....160
48 Video data; Calibration markers reproduced and LPSE....161
49 Video data; Camera image coordinates of body markers....162
50 Conjugate image points and reproduced laboratory coordinates....163

1.0 INTRODUCTION

A fundamental requirement in the analysis of human movement is the need to describe the orientation of limb segments and the relative rotations occurring at segmental joints. The complexity of human movement and the need for biomechanists and bioengineers to make an accurate and at times detailed assessment of movement has led to the use of three dimensional photogrammetry and mechanical modelling techniques to record and quantify the motion of limb segments.

The quantitative assessment of human movement provides a powerful tool for gaining indirect information and insight into human motion that may not otherwise be obtained. As such it is widely used in ergonomic, biomechanical, medical, bioengineering, and related fields. Advantages of this form of assessment include, obtaining a permanent record of the movement, the ability to view the movement at your own speed, obtaining a large array of kinematic and kinetic descriptions of the motion, and enabling a statistical and graphical analyses.

1.1 Statement of the problem.

Three dimensional quantitative analysis of human motion utilises analytical photogrammetry and rigid body mechanics to reproduce human motion from multiple camera images. Analytical photogrammetric techniques are required to reproduce three dimensional coordinate data from multiple two dimensional camera coordinates while rigid body dynamical techniques utilise the three dimensional coordinates of markers placed on each body segment to define the position of that segment in three dimensional space.

The Direct Linear Transformation (DLT) technique (Abdel-Aziz & Karara, 1974) is a commonly used photogrammetric model for the reproduction of three dimensional

coordinates in biomechanical studies. The DLT equations require a minimum of two image points to be identified in their respective camera images so that their corresponding three dimensional coordinates can be determined. At present limitations exist in the reproduction of three dimensional data that stem from automated digitising systems' inability to consistently identify points in two dimensional camera images. Even when the commonly used approach of tracking each camera view into two dimensional path information is adopted, the results can be a large number of path segments that need to be manually identified and pieced together. Problems include the uncertainty of the presence of any individual laboratory point (object point) in a given camera image and the identification of image points that lie in close proximity or temporarily obscure another point. The magnitude of the identification task and time required increases markedly with an increase in number of cameras, number of segments, number of markers per segment, and complexity of the movement.

Rigid body techniques allow the three dimensional position of a segment to be determined from known positions of at least three markers placed on that segment. This is achieved by defining a local body-fixed axis system for each rigid body. The translational and rotational vectors which define the local axis in turn define the three dimensional position of the segment. For each segment a minimum of three externally placed markers are required to locate the local coordinate system in three dimensional space. However, more markers are recommended to offset individual marker movements and a least squares solution found. The use of six to ten external markers has been recommended for reproducing joint angles between two joint coordinate systems (Hussain 1977).

Limitations in the ability to identify points in different camera images have resulted in limitations in the accuracy and complexity of human movement analysis. These limitations in accuracy and complexity are brought about by strategies to reduce the total number of markers and complexity of movement of markers in the different camera images. The total number of external markers used in movement analysis is

often reduced by decreasing the number of three dimensional segments and/or reducing the numbers of markers per segment. Commercially available motion analysis systems often limit their protocol to the minimum number of three markers per segment at the expense of accuracy. To reduce the complexity of marker movement the complexity of the three dimensional motion under investigation is often reduced or limited to a two dimensional analysis, leading to limitations and assumptions in the research methodology.

Even with these limitations in accuracy and complexity of motion, the reproduction of three dimensional coordinates can still become time consuming and a difficult proposition if segment markers move in close proximity of one another or cross one another's path in a camera's field of view.

1.2 Aim.

The aims of this project were as follows:

(i) to identify limitations and practical problems associated with the use of conjugate imagery in the identification of conjugate points in multiple camera images when applied to the analysis of human motion;

(ii) to identify procedures to facilitate the automated identification of conjugate image points and the reproduction of three dimensional coordinates from multiple camera images when applied to the analysis of human motion; and

(iii) to implement these procedures in an application for automated reproduction of three dimensional coordinates for the analysis of human motion.

1.3 Purpose.

The purpose of the project was, firstly, to increase the accuracy of three dimensional spatial location thereby increasing the accuracy of the analysis of human motion through an increase in the numbers of external markers placed on each body segment, and secondly, to enable the analysis of more complex human movements.

The desired results would be achieved through improvements in the ability to identify camera image points visible in multiple two dimensional camera images.

1.4 Approach to solving the problem.

The development of an automated three dimensional analysis system capable of tracking more than the minimum number of three individual marker per segment would overcome many of the limitations in accuracy and complexity of current motion analysis systems. This algorithm would need to match respective marker points in different camera images and track the paths of the three dimensional points. Such an automated three dimensional tracking procedure would potentially eliminate the necessity to track and identify individual markers in two dimensional camera images and leave the process of generation of three dimensional path information to the computer algorithm.

The success of an automated three dimensional tracking algorithm would determine the extent to which manual intervention was required and the speed and ease at which three dimensional data could be generated. An increase in accuracy could be achieved by an increase in the number of external markers placed on the segment. An increase in complexity of studies undertaken as well as a wider use of three dimensional movement analysis would also result from an increase in the ability to reproduce three dimensional coordinate data.

Despite advances in automated digitisation, such as infrared illumination of retro-reflective markers coupled with electronic processing of video images, little has appeared in the literature as to alternative approaches that might be adopted in the automated reproduction and tracking of three dimensional coordinates. Such investigations into the automated reproduction and tracking of three dimensional coordinates have the potential to address current limitations in accuracy and complexity of human motion analysis and stimulate further research in this area.

The present study has applied conjugate imaging techniques to the development of procedures for the automated reproduction of three dimensional coordinates from multiple camera images. The present study brings together imaging techniques that have previously been used in stereophotogrammetry and will establish its applicability and viability to the automated reproduction of three dimensional coordinates in the study of human motion. In the implementation of procedures developed in the study, limitations and practical problems associated with the use of conjugate imagery in the automated reproduction of three dimensional coordinates will have been established.

The result of this study will be the development of an algorithm for the automated reproduction of three dimensional coordinates from camera image data. This algorithm and the techniques developed represent the first stage in the development of a complete three dimensional tracking algorithm. The role of automated three dimensional coordinate reproduction in the analysis of human motion and in three dimensional tracking of markers directly from camera image data are discussed in section 1.5. However, with further development of the algorithm and the addressing of problems identified in this study, a robust three dimensional tracking algorithm can be subsequently developed.

In summary, this study will utilise imaging techniques to develop protocols and procedures for the automated reproduction of three dimensional coordinates, show the viability of the approach in the analysis of human motion, and provide the

fundamental techniques required for the development of automated three dimensional tracking. The purpose is to significantly improve the ability of computer systems to identify image points in different camera images which in turn will increase the accuracy and complexity currently attainable in the analysis of human motion.

1.5 Review of literature.

The photogrammetric and mathematical techniques used in three dimensional quantification of human movement have developed out of disciplines such as surveying, mathematics, engineering and medicine. Stereophotogrammetry involves the reconstruction of three dimensional coordinate data from two dimensional points taken from multiple camera images using various analytical photogrammetric techniques. In biomechanical literature the Direct Linear Transformation (DLT) technique developed by Abdel-Aziz and Karara (Cappozzo, 1985; Miller, et al., 1980; Shapiro, 1978) is the most commonly used photogrammetric model for the reproduction of three dimensional coordinates.

Rigid body mechanics allows us to define the three dimensional orientation of a rigid body in space by knowing the three dimensional locations of marker points located on that limb segment. By representing the human body as a linked rigid body model we can apply the principles of rigid body mechanics to describe the motions that are occurring between the segments. The combination of mechanics and photogrammetry will therefore allow one to carry out the quantitative analysis of human motion by a process of recording the motion on film or video and then being able to reproduce the motion from multiple camera images. Of importance to the analysis of human motion is an anatomical expertise in the formulation of the rigid body model and in interpretation and implementation of the results. Model design should be specific to the application that it represents and the processes that are occuring in the system, and results of the modelling process need to be related to the functioning of the system to give insight into the system.

This review of literature will bring together the various techniques from a variety of disciplines relevent to this study. Firstly a background to photogrammetry and the development of the DLT photogrammetric technique will be presented along with its advantages, limitations and accuracies. This will be followed by an explanation of stereometric configuration and a more detailed look at configuration in relation to the expected accuracy of photogrammetric systems; concepts which are important to the ability to reproduce three dimensional coordinates. The next two sections give explanations of epipolar geometry and its role in limiting the search area in camera images, as well as a brief mention of perspective cross ratio theory in establishing distances along perspectively related lines. Rigid body mechanics is then introduced and includes the role of body fixed axis, the reproduction and accuracy of spatial parameters describing segment location, and the combination of photogrametric and rigid body equations in a least squares approach to obtaining spatial parameters directly from two dimensional image coordinates. The next section is devoted to motion analysis systems and present techniques used for the reproduction of three dimensional coordinates from two dimensional image coordinates. An explanation is given of the limitations inherent in these techniques and the limitations they impose on the accuracy and complexity of human movement analysis. Finally the role of automated reproduction of three dimensional coordinates in human motion analysis is given followed by how the auotomated reproduction of three dimensional coordinates may be achieved and its role in overcoming the present limitations in the accuracy and complexity of human motion analysis.

1.5.1 Photogrammetry.

A photograph may be considered a momentary record of the of light rays which travel from three dimensional space (object space) through the camera lens system and are recorded on photographic film (Wong, 1980). The photographic film, located on the image plane of the camera, gives a permanent record of the incident light rays at a moment in time. Each point visible in object space has a unique map onto the two dimensional image plane of the camera (Miller, et.al., 1980), which describes the

fundamental condition of collinearity, which states that the projection centre, image point and object point lie on the same straight line (Figure 1). In practice, two dimensional measurements are not taken directly from the image plane but rather from a projection, considered a reproduction of the bundle of light rays recorded on film, by an optical comparator (Miller, et al., 1980; Wong, 1980). A comparator is any device for taking measurements from photographic film, such as a film projector and digitisation tablet commonly used in cinematographic analysis or computerised image processor in an automated video analysis system. The photographic axis (also called photo axis or comparator axis) is any axis system on the projected image from which two dimensional photographic coordinates (also called photo coordinates or comparator coordinates) are taken (Figure 1).

Figure 1. Relationship between film plane, comparator plane and object space.

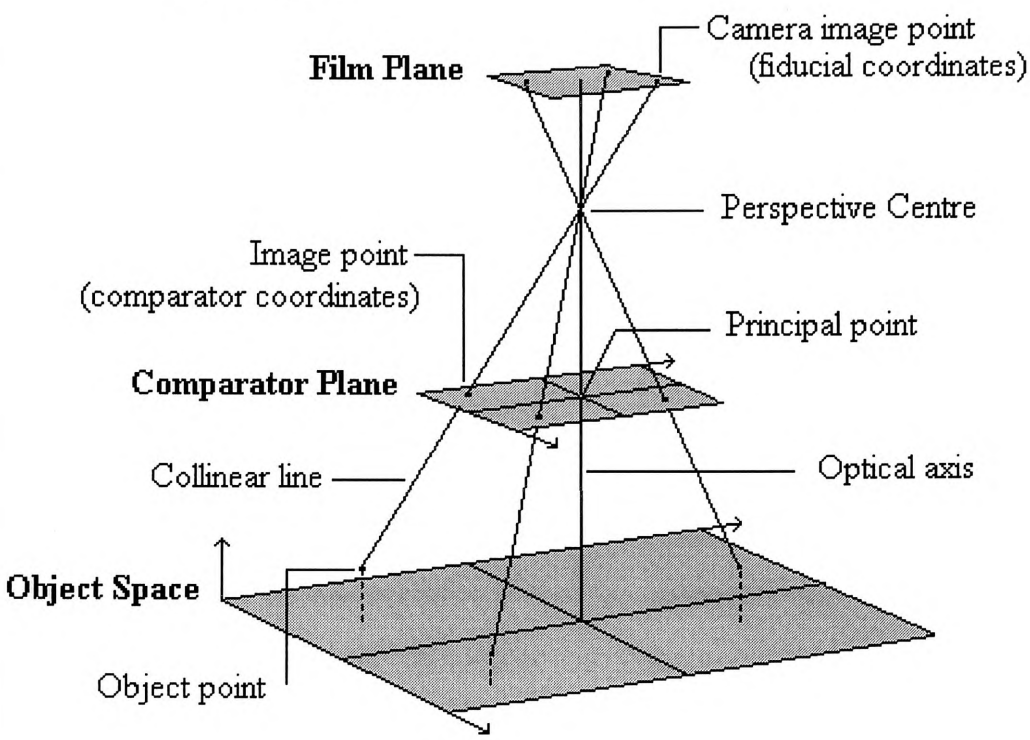

The reproduction of three dimensional points from comparator coordinate data is not achieved by a direct transformation as the projection of a single image point back onto object space will not result in a map onto a unique point but rather onto a line in

object space. Traditional photogrammetric techniques involve two transformations to arrive at object space coordinates (Abdel-Aziz & Karara, 1974; Miller, et al., 1980; Shapiro, 1979; Wong, 1980). In the first transformation, known as interior orientation, comparator coordinates are mapped onto the camera image plane (fiducial coordinates) as well as correcting for linear and non-linear lens distortion and film deformation (Wong, 1980). Internal orientation requires knowledge of the focal length, location of the camera principal point and distortion characteristics of the lens system and therefore restricting its application to metric cameras (Shapiro, 1979). Metric cameras are equipped with four or eight fiducial landmarks which are permanently fixed in the camera housing, each of which leaves a fiducial landmark on the film (Wong, 1980). The purpose of the fiducial points is to locate the camera principal point and define fiducial axes on the comparator image. The second transformation, known as exterior orientation, establishes a projective relationship between fiducial coordinates and three dimensional object space coordinates based on the condition of collinearity (Abdel-Aziz & Karara, 1974; Miller, et al., 1980; Wong, 1980).

The use of metric cameras imposes several limitations on the widespread application of the traditional photogrammetric model. Disadvantages of metric cameras include having fixed focal lengths, a limited field of view, and the fact that they are expensive (Shapiro, 1979). By comparison, non-metric cameras have no internal image coordinate system so the first transformation is not possible (Abdel-Aziz & Karara, 1974; Shapiro, 1979). Karara (1980) listed the disadvantages of using non-metric cameras as having lenses that are designed for high resolution at the expense of high distortion, instability of interior orientation, lack of fiducial landmarks, and the absence of level bubbles and orientation provisions which precludes the determination of exterior orientation before exposure.

In order to use the traditional photogrammetric techniques with non-metric cameras and provide a more flexible photogrammetric model, Abdel-Aziz and Karara (Abdel-Aziz & Karara, 1974; Miller, et al., 1980; Shapiro, 1979) combined the two

traditional photogrammetric transformations into one linear transformation called the Direct Linear Transformation (DLT) method. In the method of Abdel-Aziz & Karara (1974) the model for interior orientation, which corrected for linear components of lens distortion and film deformation, took the following form:

$$\bar{x}_i - \bar{x}_0 = a_1 + a_2 x_i + a_3 y_i \qquad (1.5.1.1)$$

$$\bar{y}_i - \bar{y}_0 = a_4 + a_5 x_i + a_6 y_i \qquad (1.5.1.2)$$

Where:

$\bar{x}_i, \bar{y}_i$ = image coordinates of point i.
$\bar{x}_0, \bar{y}_0$ = image coodinates of the camera principal point.
x_i, y_i = comparator coordinates of point i.
$a_1, a_2 \ldots a_6$ = transformation constants.

The second transformation in the method of Abdel-Aziz & Karara (1974) was expressed as the following:

$$\begin{bmatrix} \bar{x}_i - \bar{x}_0 \\ \bar{y}_i - \bar{y}_0 \\ -C \end{bmatrix} = \lambda_i \begin{bmatrix} m_{11} & m_{12} & m_{13} \\ m_{21} & m_{22} & m_{23} \\ m_{31} & m_{32} & m_{33} \end{bmatrix} \cdot \begin{bmatrix} X_i - X_o \\ Y_i - Y_o \\ Z_i - Z_o \end{bmatrix} \qquad (1.5.1.3)$$

which can be put in the following form:

$$\bar{x}_i - \bar{x}_0 = -C. \frac{m_{11}(X_i - X_o) + m_{12}(Y_i - Y_o) + m_{13}(Z_i - Z_o)}{m_{31}(X_i - X_o) + m_{32}(Y_i - Y_o) + m_{33}(Z_i - Z_o)} \qquad (1.5.1.4)$$

$$\bar{y}_i - \bar{y}_0 = -C. \frac{m_{21}(X_i - X_o) + m_{22}(Y_i - Y_o) + m_{23}(Z_i - Z_o)}{m_{31}(X_i - X_o) + m_{32}(Y_i - Y_o) + m_{33}(Z_i - Z_o)} \qquad (1.5.1.5)$$

Where:

$\bar{x}_i, \bar{y}_i$ = image coordinates of point i.
$\bar{x}_0, \bar{y}_0$ = image coordinates of the camera principal point.
X_i, Y_i, Z_i = object space coordinates of point i.
X_0, Y_0, Z_0 = object space coordinates of the camera perspective centre.
C = camera constant.
m_{jk} = coefficients of transformation.
λ_i = scale factor.

Abdel-Aziz & Karara (1974) combined the equations (1.5.1.1), (1.5.1.2), (1.5.1.4) and (1.5.1.5) to form the DLT equations. The DLT method eliminates the need for fiducial landmarks and the calculation of internal orientation and is therefore applicable to non-metric cameras. The DLT equations take the following form:

$$x_i - L_1X_i - L_2Y_i - L_3Z_i - L_4 + L_9x_iX_i + L_{10}x_iY_i + L_{11}x_iZ_i = 0 \qquad (1.5.1.6)$$

$$y_i - L_5X_i - L_6Y_i - L_7Z_i - L_8 + L_9y_iX_i + L_{10}y_iY_i + L_{11}y_iZ_i = 0 \qquad (1.5.1.7)$$

Where

x_i, y_i = comparator coordinates of point i.
X_i, Y_i, Z_i = object space coordinates of point i.
$L_1 \ldots L_{11}$ = DLT parameters.

The eleven DLT parameters combine the constants of inner and outer orientation and account for the linear components of lens distortion and film aberration (Abdel-Aziz & Karara, 1974; Shapiro, 1979). To establish the eleven DLT parameters for a given camera configuration a minimum of six well-spaced control points are needed. A control point is a marker that has known object space and comparator coordinates. Each control point results in two equations incorparating the eleven DLT parameters. Generally more than six control points are used to provide a least squares estimate of the DLT parameters. Miller, et al. (1980) recommended a minimum of ten control

points be used and these should be placed throughout the region in which the body was to move. Similarly, Shapiro (1979) recommended the use of twelve to twenty control points to calculate the DLT parameters. With known DLT parameters, the DLT equations (1.5.1.6) and (1.5.1.7) will provide a direct map from object point coordinates to comparator coordinates. With a minimum of two cameras the DLT equations (1.5.1.6) and (1.5.1.7) can be used to calculate object space coordinates from conjugate comparator coordinates. Increased accuracy can be obtained with the use of more than two cameras with a least squares solution to produce the three unknown (X_i,Y_i,Z_i) object space coordinates.

When the DLT method was originally presented in 1971 the equations did not involve interior orientation constants (Karara, 1980) and relied on the eleven DLT coefficients to account for the linear components of lens distortion and film aberration (Abdel-Aziz & Karara, 1974; Karara, 1980). The DLT equations (1.5.1.6) and (1.5.1.7) considered the image coordinates to be free of non-linear components of lens distortion and film aberration. Abdel-Aziz & Karara (1974) expanded the DLT equations to include internal orientation constants and to account for non-linear components of lens distortion and film aberration. Lens distortion from a perfectly centered lens is symmetrical about the optical axis of the lens system and the point of symmetry would coincide with the principal point of the image plane, hence called symmetrical lens distortion. Asymmetric lens distortion refers to the decentering of lens elements. With the inclusion of systematic errors, the relationship between comparator and image coordinates can be expressed as:

$$\bar{x}_i = x_i - \Delta x_i \qquad (1.5.1.8)$$

$$\bar{y}_i = y_i - \Delta y_i \qquad (1.5.1.9)$$

Where:

Δx_i, Δy_i = correction in comparator coordinates to account for non-linear components of lens distortion and film aberration for point i.

When investigating the accuracy of the DLT method with non-metric cameras Abdel-Aziz & Karara (1974) found that the modelling of the non-linear components of lens distortion and film deformation could be satisfactorily achieved by the following model:

$$\Delta x_i = \tilde{x}_i . K_1 . r_i^2 \qquad (1.5.1.10)$$

$$\Delta y_i = \tilde{y}_i . K_1 . r_i^2 \qquad (1.5.1.11)$$

Where:

K_1 = coefficient of symmetrical lens distortion.
r_i = length of vector from the point of symmetry to point i.
$\tilde{x}_i = x_i - \bar{x}_s$.
$\tilde{y}_i = y_i - \bar{y}_s$.
$\bar{x}_s, \bar{y}_s$ = point of symmetry relative to the comparator coordinate axes.

It was shown by Abdel-Aziz & Karara (1974) that in non-metric cameras asymmetric lens distortion was relatively small when the principal point was taken as the reference point for symmetrical lens distortion. They also showed that the inclusion of corrections for asymmetric lens distortion in the above model provided no significant improvement in accuracy of the DLT method. In the above model, the principal point was used as the point of symmetry in the calculation of symmetrical lens distortion. The mathematical model of the DLT equations that account for non-linear lens distortion and film aberration in image coordinates has the following form:

$$A\tilde{x}_i K_1 r_i^2 + x_i + L_1 X_i + L_2 Y_i + L_3 Z_i + L_4 + L_9 x_i X_i + L_{10} x_i Y_i + L_{11} x_i Z_i = 0 \qquad (1.5.1.12)$$

$$A\tilde{y}_i K_1 r_i^2 + y_i + L_5 X_i + L_6 Y_i + L_7 Z_i + L_8 + L_9 y_i X_i + L_{10} y_i Y_i + L_{11} y_i Z_i = 0 \qquad (1.5.1.13)$$

Where:

$$A = L_9X_i + L_{10}Y_i + L_{11}Z_i + 1.$$

Abdel-Aziz & Karara (1974) provided a means of calculating the camera principal point in non-metric cameras directly from the DLT coefficients. The location of the camera principal point relative to the comparator axis is necessary to provide an approximation to the point of symmetry for use as a reference point for symmetric and asymmetric lens distortions. Abdel-Aziz & Karara first assumed the image axes and comparator axes were parallel, resulting in the following relationship:

$$\bar{x} - \bar{x}_0 = \lambda_1(x - x_0) \qquad (1.5.1.14)$$

$$\bar{y} - \bar{y}_0 = \lambda_2(y - y_0) \qquad (1.5.1.15)$$

Where:

x_o, y_o = principal point relative to comparator axes.
λ_1,λ_2 = constants.

Abdel-Aziz & Karara (1974) substituted the equations (1.5.1.14) and (1.5.1.15) into the exterior orientation equations (1.5.1.4) and (1.5.1.5) respectively and the DLT equations deduced. By manipulation of the expressions for the eleven DLT parameters, the following equations that relate the DLT parameters to the camera principal point were obtained;

$$x_o = (L_1L_9 + L_2L_{10} + L_3L_{11}) / (L_9^2 + L_{10}^2 + L_{11}^2) \qquad (1.5.1.16)$$

$$y_o = (L_5L_9 + L_6L_{10} + L_7L_{11}) / (L_9^2 + L_{10}^2 + L_{11}^2) \qquad (1.5.1.17)$$

1.5.2 Stereoscopic configuration and expected accuracy.

The accuracy of a photogrammetric system is determined by the accuracy of the object space coordinates that it reproduces (Abdel-Aziz & Karara, 1974; Marzan, 1977). In the case of non-metric cameras, accuracy is a function of:

(i) The residual error in comparator coordinates, which is corrected for by various models of lens distortion and film deformation;
(ii) The accuracy of object space control points, which are used in camera calibration for establishing DLT and internal orientation parameters;
(iii) The scale of the photos; and,
(iv) The configuration of the camera system (Abdel-Aziz & Karara, 1974; Marzan, 1977).

The scale of a photograph refers to the ratio between distances on the photograph and distances in object space, and is usually expressed as the ratio of principal distance of the camera (C) divided by the object distance (D) (Figure 2). The configuration of a photogrammetric system describes the physical relationship between a camera stereo-pair in object space and refers to the exterior orientation of the system. The configuration of a photogrammetric system is usually described by the base, the object distance and the convergence (Marzan, 1977). The base distance refers to the distance between the two exposure stations; the object distance refers to the perpendicular distance from the base to the centre of object space; and the convergence refers to the angle formed by the two camera axis, either measured individually for each camera or as a combined angle (Marzan, 1977). When the two camera axes are parallel, convergence is equal to zero and we have the normal case of photography. When the two axes are not parallel we have the convergent case.

In the normal case, Abdel-Aziz & Karara (1974) and Marzan (1977) noted that the error in object coordinates (X,Y,Z) decreases with increasing photo scale (C/D), while the error in the Z component of the object space, which was directed along the

line bisecting the two cameras perspective centres, decreased with increasing base to object distance ratio (B/D) (Figure 2). In the normal case the base distance (B), which is the separation between the two cameras, is limited by the size of the image, the photo scale (C/D) and the required overlap of the two photos. The minimum object distance (D) is a function of the depth of field required for the object. In the special convergent case where both camera axes are directed towards the central point, Abdel-Aziz & Karara (1974) and Marzan (1977) found that as the angle of convergence (ϕ) increased, the error directed along the bisector of the two cameras (Z) decreased. Similarly the error directed along a line perpendicular to the bisector, but in the plane of the two cameras (X), increased while the error directed along a line normal to the plane of the two cameras and the direction of movement (Y) remained constant.

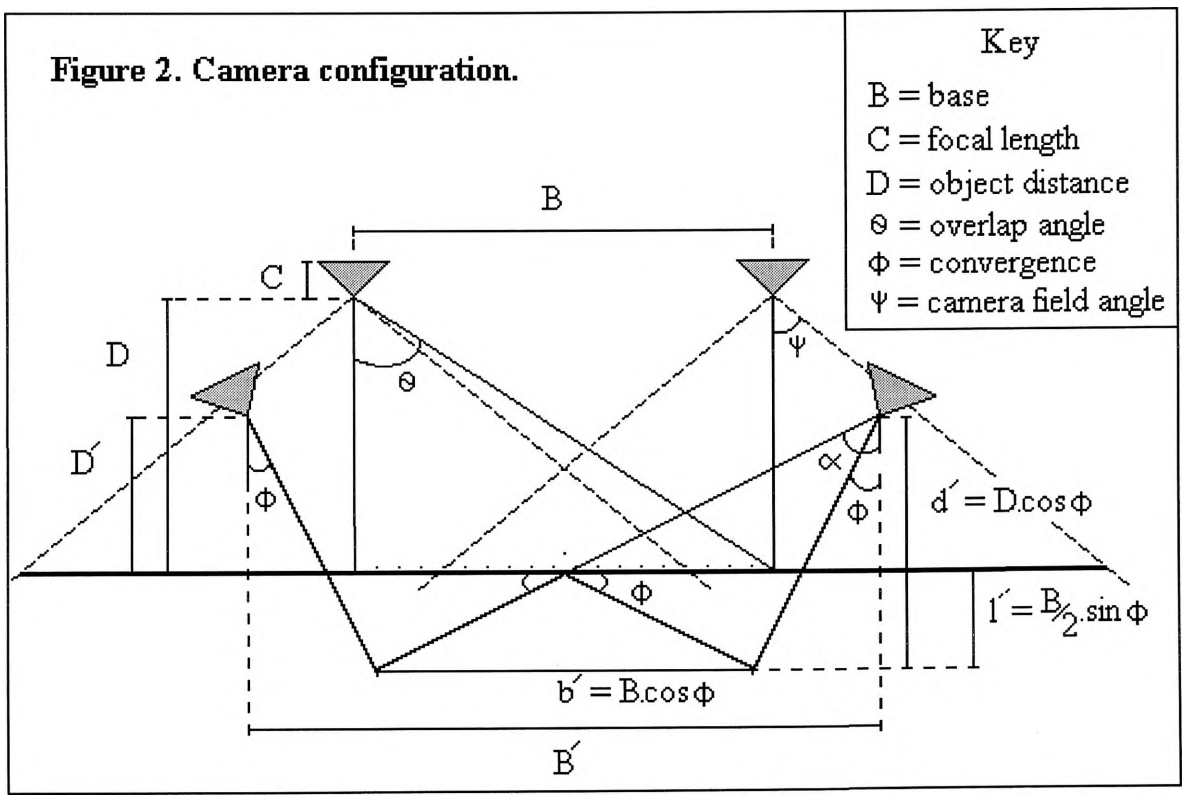

In the convergent case, where the lengths B and D remain constant and the angle of convergence is varied, Abdel-Aziz & Karara (1974) found that when the focal axes were directed towards the central object space ($\phi = \theta$) the errors in the components of

object space (X,Y,Z) were at their maximum. They recommended that the normal case of photogrammetry be used if possible, otherwise the angle of convergence must be kept as small as possible, with the focal axis directed as far as possible from the line of the central point in object space. Marzan (1977) pointed out that Abdel-Aziz & Karara made their conclusions based on the assumption that a fixed base to object distance ratio (B/D) was maintained with the introduction of convergence. However, Marzan (1977) noted that with the introduction of convergence (ϕ) there was an accompanying decrease in object distance (D) and an increase in base distance (B) provided the same photo scale (C/D) and overlap were maintained. To enable the comparison of one configuration with another, Marzan (1977) introduced the idea of an "equivalent normal case" in which different camera configurations, although varying in base distance (B), object distance (D) and convergence (ϕ), maintained the same photo scale (C/D) and overlap angle (θ). The normal case which also maintained this relationship was referred to as the "equivalent normal case". The overlap angle was defined by Marzan (1977) as:

$$\tan\theta = \frac{B}{D} \qquad (1.5.2.1)$$

Marzan (1977) derived general formulae to evaluate the accuracy of close range photogrammetry. These general formulae expressed the object space coordinate errors (m_X,m_Y,m_Z) as a function of the image coordinate error (m), the photo scale (C/D), the convergence (ϕ), and the overlap angle (θ) for any symmetrical configuration:

$$m_X = \frac{D}{\sqrt{2}.C} \cdot \frac{m}{(1 - {}^1/_2.\tan\theta.\sin\phi).\cos\phi} \qquad (1.5.2.2)$$

$$m_Y = \frac{D}{\sqrt{2}.C} .m \qquad (1.5.2.3)$$

$$m_Z = \frac{\sqrt{2}.D}{C} \cdot \frac{m}{\tan\theta.\cos^2\phi + 2.\sin\phi} \qquad (1.5.2.4)$$

With the position error $m_T = \sqrt{(m^2_X + m^2_Y + m^2_Z)}$

we have :

$$m_T = \frac{D}{C} .m. \text{ (Error Factor)} \qquad (1.5.2.5)$$

Where:

$$\text{Error Factor} = \sqrt{\frac{1}{2(1-{}^1/_2.\tan\theta.\sin\phi)^2.\cos^2\phi} + \frac{1}{2} + \frac{2}{(\tan\theta.\cos^2\phi + 2.\sin\phi)^2}} \qquad (1.5.2.6)$$

From the above formulae Marzan (1977) made the following observations:

(i) The standard errors in object space coordinates were inversely proportional to the average photo scale, (C/D);

(ii) The standard errors in object space coordinates were functions of the overlap angle (θ) and the convergence (ϕ); and

(iii) The standard errors in object space coordinates were directly proportional to the error in image coordinates (m), with the value of m varying from one system to another.

Of the parameters that describe the standard errors in object space coordinates, the error in image coordinates (m) is the most difficult to predict. The accuracy of m determines the accuracy of the formulae and the ability to predict the accuracy of the photogrammetric system (Marzan 1977). The value of m is specific to the photogrammetric system and Marzan listed the determinants of (m) as:

(i) the characteristics of the camera-lens-film combination;

(ii) the precision of the data reduction instrument;

(iii) the user's ability to obtain data from the instrument; and

(iv) the data processing techniques employed.

Results obtained by Abdel-Aziz & Karara (1974) for values of the RMS of residual errors in image coordinate obtained from different photogrammetric systems are presented in Table 1.

Table 1. The RMS values of residual errors of image coordinates using the DLT method for various photographic set ups, with and without the inclusion of non-linear film deformation and lens distortion.

Camera	Focal Length (mm)	Image Format (mm)	RMS (μm)†	
			model #1††	model#2†††
Kodak Instamatic 154	43	12x12	43.0	15.2
Crown Graphic	135	120x100	18.4	11.5
Honeywell Pentax Spotmatic	50	36x24	27.0	3.9
Hasselblad 500 C	80	55x55	30.8	6.1
Hasselblad MK 70 *	60	55x55	4.6	4.6

Reproduced from Abdel-Aziz & Karara (1974).

† The average of the root mean square residual error of image coordinate data obtained from ten photographs taken with each camera.

†† Without the inclusion of non-linear film deformation and lens distortion in the DLT equations.

††† With the inclusion of non-linear film deformation and lens distortion in the DLT equations

* Metric camera where internal orientation was utilised.

Marzan (1977) concluded that with an increasing angle of convergence, thereby increasing the base object distance ratio, the accuracy of object space coordinates increased up to a certain point after which further convergence would result in subsequent deterioration in accuracy. In comparison with the convergent cases, there

exists a corridor of convergences for which the accuracy obtained will be better than that of the 'equivalent normal case'. As the overlap angle (θ) increases, the overlap and/or the camera field angle (φ) also increase and there is a subsequent decrease in convergence at which optimal configuration is obtained. Optimal convergence is less with increasing camera field angle (φ). For the special convergent case where the camera axes are directed towards the central object point the optimum configuration was achieved at an angle of convergence of 45 degrees. This was said to be the case for any camera used and was independent of overlap angle (θ) or camera field angle (φ).

Marzan (1977) presented tables containing the error factor (from equation 1.5.2.6) for varying degrees of convergence and overlap. The table allowed for computation of the object positional error of a point for a given system or determination of the convergence required to achieve a given accuracy in object coordinates.

Considering indeterminacy and the error factor (1.5.2.6), the error in the object space x-coordinate (1.5.2.2) approaches infinity whenever:

$$(1 - {}^{1}/_{2}.\tan\theta.\sin\phi).\cos\phi = 0 \qquad (1.5.2.7)$$

which results when

$$\cos\phi = 0 \qquad (1.5.2.8)$$

or

$$\tan\theta.\sin\phi = 2 \qquad (1.5.2.9)$$

From Figure (2) one can obtain the following relationships:

$$b' = B.\cos\phi \qquad (1.5.2.10)$$

$$d' = D.\cos\phi \qquad (1.5.2.11)$$

$2.l' = B.\sin\phi$ (1.5.2.12)

By substitution of equation (1.5.2.1) into (1.5.2.9) and using the relationships expresesd in (1.5.2.10), (1.5.2.11) and (1.5.2.12), equation (1.5.2.9) takes the form:

$$\frac{B.2.l'}{D.B} = 2 \quad \text{or simply} \quad l' = D \qquad (1.5.2.13)$$

Summarising equations (1.5.2.8) and (1.5.2.13), the error in the x-coordinate of object space approaches infinity as convergence (ϕ) approaches 90 degrees regardless of overlap angle (θ) or when l' becomes equal to D. The later condition requires that $B \geq 2D$ (Figure 2). These points of indeterminacy are not supported by graphical comparisons of the configurations.

In re-arranging the equations by Marzan (1977) the relationships between image coordinate errors and the error in the central object point can be defined as:

$$m_X = \frac{D'}{\sqrt{2}.C} \frac{1 + \tan\alpha.\tan\phi}{(1 - \tan(\alpha - \phi).\tan\phi)} .m \qquad (1.5.2.14)$$

$$m_Y = \frac{D'}{\sqrt{2}.C} \frac{\sec\phi}{(1 - \tan(\alpha - \phi).\tan\phi)} .m \qquad (1.5.2.15)$$

$$m_Z = \frac{\sqrt{2}.D'D'}{C.B'} \frac{1 + \tan\alpha.\tan\phi}{(1 - \tan(\alpha - \phi).\tan\phi)} .m \qquad (1.5.2.16)$$

Making use of the relationship:

$$\tan(\alpha - \phi) = \frac{\sin(\alpha - \phi)}{\cos(\alpha - \phi)} = \frac{\sin\alpha.\cos\phi - \cos\alpha.\sin\phi}{\sin\alpha.\sin\phi + \cos\alpha.\cos\phi} \qquad (1.5.2.17)$$

The factors in equations (1.5.2.14) and (1.5.2.16) involving ϕ and α can be rewritten in the form:

$$\frac{1+\tan\alpha.\tan\phi}{(1-\tan(\alpha-\phi).\tan\phi)} = \frac{\cos\alpha.\cos\phi+\sin\alpha.\sin\phi}{\cos\alpha.\cos\phi} \cdot \frac{\cos(\alpha-\phi).\cos\phi}{\cos(\alpha-\phi).\cos\phi-\sin(\alpha-\phi).\sin\phi}$$

$$= \frac{\sin^2\alpha.\sin^2\phi+\cos^2\alpha.\cos^2\phi+2\sin\alpha.\sin\phi.\cos\alpha.\cos\phi}{\cos^2\alpha.\cos^2\phi+\cos^2\alpha.\sin^2\phi}$$

$$= \cos^2\phi+\tan^2\alpha.\sin^2\phi+2\tan\alpha.\sin\phi.\cos\phi$$

$$= (\cos\phi+\tan\alpha.\sin\phi)^2 \qquad (1.5.2.18)$$

Similarly it can be shown that the factor in equation (1.5.2.15) involving ϕ and α, can be rewritten in the form:

$$\frac{\sec\phi}{(1-\tan(\alpha-\phi).\tan\phi)} = (\cos\phi+\tan\alpha.\sin\phi) \qquad (1.5.2.19)$$

From Figure (2) it can be seen:

$$B' = B.\cos\phi+2D.\sin\phi \qquad (1.5.2.20)$$

$$D' = D.\cos\phi-{}^{B}/_{2}.\sin\phi \qquad (1.5.2.21)$$

By definition and using the relationships (1.5.2.20) and (1.5.2.21):

$$\tan\alpha = \frac{B'}{2D'} = \frac{B.\cos\phi+2D.\sin\phi}{2D.\cos\phi-B.\sin\phi} \qquad (1.5.2.22)$$

By substitution of (1.5.2.22) into (1.5.2.19) and making use of the relationship (1.5.2.17) one obtains:

$$\cos\phi+\tan\alpha.\sin\phi = \cos\phi+\frac{B.\cos\phi+2D.\sin\phi}{2(D.\cos\phi-{}^{B}/_{2}.\sin\phi)}.\sin\phi$$

$$= \frac{2D\cos^2\phi+B\cos\phi.\sin\phi-B\cos\phi.\sin\phi+2D\sin^2\phi}{2(D.\cos\phi-{}^{B}/_{2}.\sin\phi)}$$

$$= \frac{D}{D'}$$

In agreement with Marzan (1977), equations (1.5.2.18) and (1.5.2.19) can be rewritten as:

$$\frac{1 + \tan\alpha.\tan\phi}{(1 - \tan(\alpha - \phi).\tan\phi)} = \left(\frac{D}{D'}\right)^2 \qquad (1.5.2.23)$$

$$\frac{\sec\phi}{(1 - \tan(\alpha - \phi).\tan\phi)} = \frac{D}{D'} \qquad (1.5.2.24)$$

With the substitution of equations (1.5.2.23) and (1.5.2.24) into equations (1.5.2.14), (1.5.2.15) and (1.5.2.16) we obtain:

$$m_X = \frac{D.D}{\sqrt{2}.C.D'} .m \qquad (1.5.2.25)$$

$$m_Y = \frac{D}{\sqrt{2}.C} .m \qquad (1.5.2.26)$$

$$m_Z = \frac{\sqrt{2}.D.D}{C.B'} .m \qquad (1.5.2.27)$$

Further substitution of equations (1.5.2.20) and (1.5.2.21) into equations (1.5.2.25), (1.5.2.26) and (1.5.2.27) results in the following:

$$m_X = \frac{D}{\sqrt{2}.C} \frac{1}{(\cos\phi - {}^1/_2.\tan\theta.\sin\phi)} .m \qquad (1.5.2.28)$$

$$m_Y = \frac{D}{\sqrt{2}.C} .m \qquad (1.5.2.29)$$

$$m_Z = \frac{D}{\sqrt{2}.C} \frac{1}{(\sin\phi + {}^1/_2.\tan\theta.\cos\phi)} .m \qquad (1.5.2.30)$$

With the position error $m_T = \sqrt{(m^2_X + m^2_Y + m^2_Z)}$

we have :

$$m_T = \frac{D}{\sqrt{2}.C} .m.(\text{Error Factor}) \qquad (1.5.2.31)$$

Where:

$$\text{Error Factor} = \sqrt{\frac{1}{(\cos\phi - {}^1/_2.\tan\theta.\sin\phi)^2} + 1 + \frac{1}{(\sin\phi + {}^1/_2\tan\theta.\cos\phi)^2}}$$

(1.5.2.32)

Utilising the results of Abdel-Aziz & Karara (1974) presented in Table 1, position errors in object space coordinates have been calculated using equations (1.5.2.28), (1.5.2.29) and (1.5.2.30) and are presented in Table 2.

The values of the error factor determined from equation (1.5.2.32) for overlap angles and convergence angles ranging from 0-90 degrees are presented in Appendix I. The normal case of photography corresponds to zero convergence ($\phi = 0$) and the special convergent case where camera axes are directed towards the central object point corresponds to zero overlap angle ($\theta = 0$). By inspection of equation (1.5.2.32) and Appendix I, there exist points of indeterminacy in the calculation of object space coordinates.

Table 2. Predicted errors of object space coordinates as derived from formulas for various photographic set ups, with and without the inclusion of non-linear film deformation and lens distortion.

Camera	RMS (mm)					
	model #1*			model #2**		
	X	Y	Z	X	Y	Z
Kodak Instamatic 154	4.43	3.89	6.61	1.57	1.37	2.34
Crown Graphic	0.60	0.53	0.90	0.38	0.33	0.56
Honeywell Pentax Spotmatic	2.39	2.10	3.57	0.35	0.30	0.52
Hasselblad 500 C	1.82	1.60	2.72	0.36	0.32	0.54
Hasselblad MK 70†	0.20	0.18	0.30	0.20	0.18	0.30

Note: Adapted from Abdel-Aziz & Karara (1974), the convergent case of photography was used with a base distance of 3.75 meters and an object distance of 5.5 meters and angle of convergence of 15 degrees.

* Without the inclusion of non-linear film deformation and lens distortion in the DLT equations.

** With the inclusion of non-linear film deformation and lens distortion in the DLT equations.

†Metric camera where internal orientation was utilised.

Indeterminacy in equation (1.5.2.32) will result when:

$$\cos\phi - {}^{1}/_{2}.\tan\theta.\sin\phi = 0 \qquad (1.5.2.33)$$

or

$$\sin\phi + {}^{1}/_{2}.\tan\theta.\cos\phi = 0 \qquad (1.5.2.34)$$

From equation (1.5.2.33) and substitution of equation (1.5.2.1) and (1.5.2.21):

$$\cos\phi - {}^{1}/_{2}.\tan\theta.\sin\phi = 0$$

$$\Rightarrow D.\cos\phi - \frac{B.\sin\phi}{2} = 0$$

$$\Rightarrow D' = 0$$

From equation (1.5.2.34), and recognising that sin(φ), cos(φ) and tan(φ) are positive for $0 \leq \varphi \leq 90$ degrees, indeterminacy results when convergence (ϕ) = overlap angle (θ) = 0. Indeterminacy, or values approaching infinity in the standard error of object space coordinates of the central point, can result when the central point in object space and the two camera perspective centres are collinear. Therefore on the basis of equation (1.5.2.32) it can be concluded that the accuracy of object space coordinates increase as the overlap and convergence angles move further away from points of indeterminacy. Similar to the results of Marzan (1977), there exists a corridor of convergences that will produce improved accuracy over that of the equivalent normal case (Figure 3). Likewise, there also exists a corridor of convergences within which the special convergent case ($\theta = 0$) will give better accuracy than the normal case.

The normal case is obtained when the convergence is equal to zero ($\phi = 0$) and the above equations (1.5.2.28) (1.5.2.29) and (1.5.2.30) reduce to:

$$m_X = \frac{D}{\sqrt{2}.C}.m \qquad (1.5.2.33)$$

$$m_Y = \frac{D}{\sqrt{2}.C}.m \qquad (1.5.2.34)$$

$$m_Z = \frac{D}{\sqrt{2}.C}.2\cot\theta.m \qquad (1.5.2.35)$$

with:

$$\text{Error Factor} = \sqrt{2 + 4.\cot^2\theta} \qquad (1.5.2.36)$$

Figure 3. Error Factor

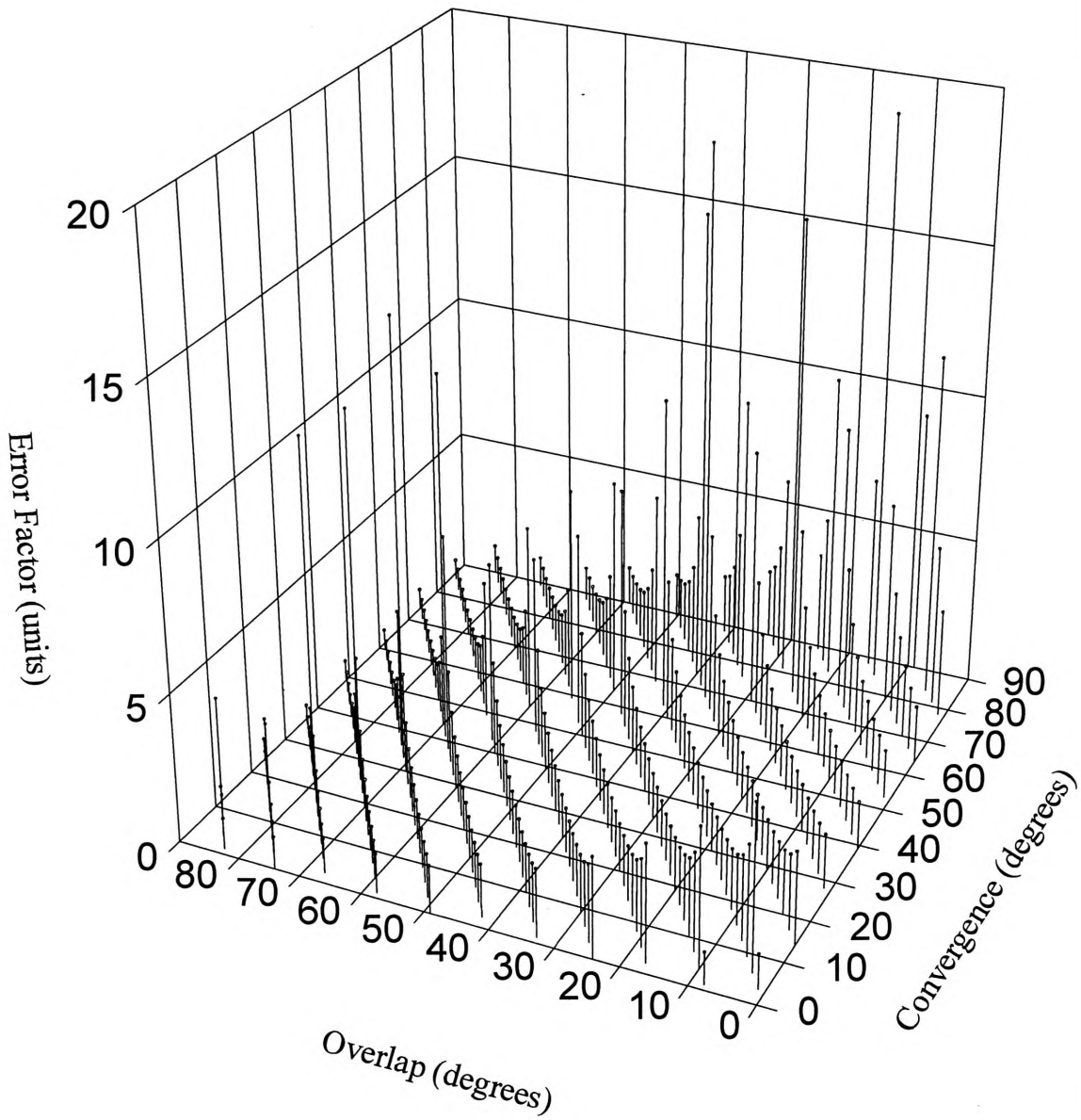

The special convergent case, when the camera axes are directed towards the central object space, is obtained when the overlap angle is equal to zero ($\theta = 0$) and the above equations (1.5.2.28), (1.5.2.29) (1.5.2.30) reduce to:

$$m_X = \frac{D}{\sqrt{2}.C} .\sec\phi.m \qquad (1.5.2.37)$$

$$m_Y = \frac{D}{\sqrt{2}.C} .m \qquad (1.5.2.38)$$

$$m_Z = \frac{D}{\sqrt{2}.C} .\mathrm{cosec}\phi.m \qquad (1.5.2.39)$$

With:

$$\text{Error Factor} = \sqrt{\sec^2\phi + 1 + \mathrm{cosec}^2\phi} \qquad (1.5.2.40)$$

1.5.3 Collinearity and epipolar imagery.

The reproduction of three dimensional points requires the identification of corresponding (conjugate) image points in two or more camera images. The determination of corresponding image points in respective camera images (image correlation) is aided by the use of epipolar geometry (Keating, 1977). Epipolar geometry makes use of the coplanarity condition which states that the two camera perspective centres, the camera image points and the respective laboratory (object) point lie on the same plane in object space (Figure 4). This plane in object space has a line of intersection with both respective camera image planes. When searching for conjugate image points in a second camera image plane the collinearity condition is used, where a single image point casts a collinear line through object space along which the corresponding object point may lie. If the collinear line is represented on

the second camera image plane, forming a conjugate epipolar line, then the search for a conjugate point will be greatly simplified by reducing the search area to a line on the second camera image plane.

Figure 4. Conjugate Imagery.

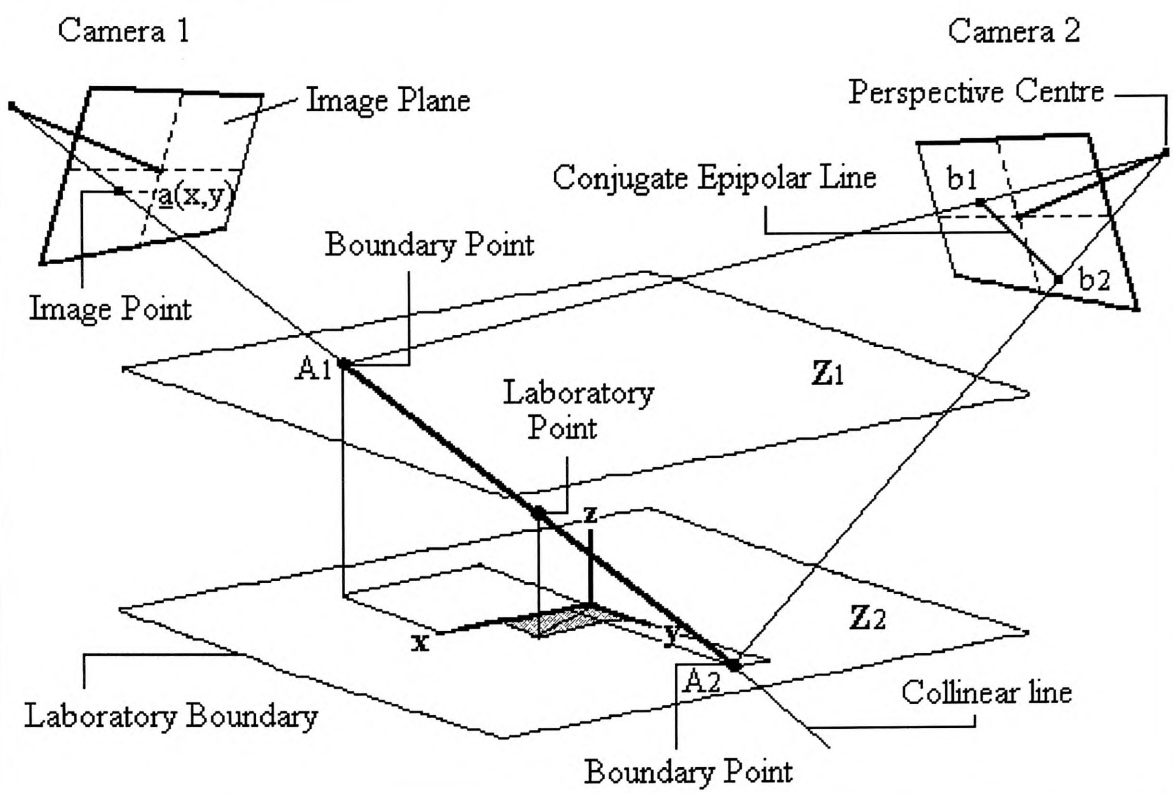

The epipolar axis refers to the line joining the two camera perspective centres (Figure 4). The epipolar plane contains the epipolar axis as well as the two camera image points and the object point. The epipolar plane is bounded by the epipolar axis and the two respective collinear lines and represents the condition of coplanarity. The two respective epipolar lines are formed by the lines of intersection between the epipolar plane and the two camera image planes.

The important concept of epipolar imagery is that conjugate points will always be found on conjugate epipolar lines (Keating, 1977). The precise location of the conjugate point on an epipolar line is dependent only on the elevation of the point in object space (Keating, 1977). The technique employed by Keating (1977) for

locating a single conjugate point, given that the camera orientation parameters are known, was as follows (Figure 4):

(i) Two elevations (Z_1 and Z_2) are chosen which define two horizontal planes which vertically bound object space. The vertical boundaries should include the expected elevation of the object point;

(ii) For a given image point $\underline{a}$ with image coordinates (x,y), the collinearity equations are solved for the first camera for each elevation, Z_1 and Z_2, in turn. Each solution involves two equations in two unknowns to give two object space coordinates, A_1 and A_2;

(iii) The two object space coordinates, A_1 and A_2, can be readily substituted into the collinearity equations of the second camera to give two image points, $\underline{b}_1$ and $\underline{b}_2$, which define the limits of the conjugate epipolar line containing the conjugate image point; and

(iv) The search for the conjugate point is now restricted to a line segment on the image plane of the second camera instead of the more usual entire image plane.

1.5.4 Collinearity and perspective cross-ratio theory.

Cross Ratio Theory describes a geometric relationship that exists between two or more perspectively related lines contained in a common plane and a series of lines projected from a common source also contained in the same plane. This situation arises when a series of collinear lines projected from a common camera perspective center are intersected by a second series of collinear lines originating from a second perspective center. Cross-ratio theory enables distances measured along one collinear line to be related to distances along any another perspectively related collinear line. The theory of cross-ratios gives the following geometric distance relationship (Figure 5):

$$\frac{\overline{13}\,/\,\overline{23}}{\overline{14}\,/\,\overline{24}} = \frac{\overline{P1P3}\,/\,\overline{P2P3}}{\overline{P1P4}\,/\,\overline{P2P4}} = K \qquad (1.5.4.1)$$

where $\overline{13}$ refers to the line segment from point 1 to point 3.

Figure 5. Perspective cross-ratio theory.

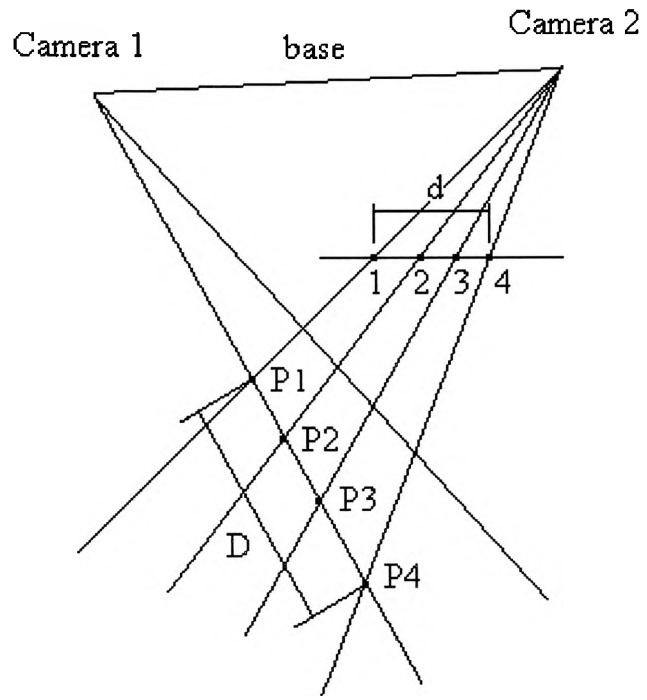

Equation (1.5.4.1) states that there exists a constant ratio (K) between distances separating points on perspectively related lines (Keating, 1977). Once the constant ratio (K) has been determined distances along one line can be converted to distances along another perspectively related line. Cross-ratio theory also provides a tool for determining changes in elevation of object points from movements along an epipolar line.

By manipulation of equation (1.5.4.1) it can be simplified to:

$$D = \frac{C_1 d + C_2}{C_3 d + 1} \qquad (1.5.4.2)$$

where:

D = unknown distance along one perspective line.

d = measured distance along another perspective line.

C_1, C_2, C_3 = cross-ratio transformation coefficients.

When any three distances along one line are determined as well as their corresponding distances along a second perspectively related line, equation (1.5.4.2) can be solved for the three unknown transformation coefficients C_1, C_2, C_3. With known coefficients (C_1, C_2, C_3) distances along one perspective line can be directly given by known distances along another perspectively related line.

1.5.5 Rigid body mechanics.

The biomechanical modelling of human motion has predominantly represented limb segments as rigid links interconnected by frictionless joints of varying degrees of freedom (Hatze, 1980; McGee, et al., 1979). This approach lends itself to the established methods of rigid body mechanics for locating individual segments in three dimensional space and for describing the relative motions that occur between each segment.

The acccuracy of locating a rigid body in space is a fundamental problem in the description of human motion. Errors in spatial parameters determine the limits to which we can measure the changes in motion occurring between limb segments. This is important, for example, when one is investigating small changes in gait due to different pathological conditions. The rigid body approach approximates a limb segment to an axis system located in three dimensional space reproduced from marker points located on the limb surface. A further limitation to the accuacy of the rigid body approach is the treatment of the motion of a limb segment as a truely rigid

body. A limb segment consists primarily of muscle, fat and other connective tissue moving about a rigid skeletal system, which can be clearly demonstrated in the slow motion view of an athlete sprinting. Soft tissue movement about the skeletal system results in further inaccuracies of segmental location in rigid body techniques. Therefore, errors in reconstructing the position of the limb segment will be even greater with greater surface movement. Reducing these limitations in accuracy is essential if one is concerned with the detection of small changes in human movement pattern from one condition to another.

1.5.5.1 Body-fixed axes.

Each rigid body in three dimensional space is represented by an orthogonal axis system which is fixed relative to the segment it defines. The location of the body-fixed axis in object space is described by a position vector (to the origin of the system) and a rotation matrix and defines the position of the segment and any point on the segment that is known relative to the body-fixed axis. In the biomechanical literature various conventions have been used to place fixed axis coordinate systems on rigid body segments as well as the rotational convention used to describe the orientation of the axis system.

Despite a right handed axis system being placed perpendicular to the sagittal, transverse and coronal/frontal planes of the individual segment (Figure 6), differences lie in defining which axis is perpendicular to which anatomical plane (Chao, 1980; Grood & Suntay, 1983; Seireg & Arvikar, 1989). A number of rotational conventions are used in the literature including Eulerian two axis (Y,X',Y''), Eulerian three axis (Pitch,Yaw, Roll), Screw axis, and more recently Floating axis. Whichever rotational convention is used, anatomically correct displacements and rotations need to be generated in order to be meaningful in the analysis of human movement. This was the major consideration prompting development of the Floating axis system by Grood & Suntay (1983). The different conventions have been shown to produce comparable results (Small, et al., 1982),

however some uniformity in biomechanical literature would facilitate the understanding and comparisons of methodologies and results (Grood & Suntay, 1983; Small, et al., 1982).

Figure 6. Body fixed axes.

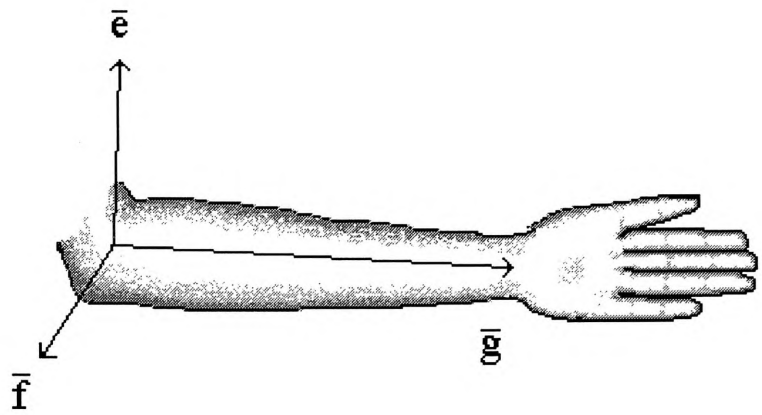

1.5.5.2 Rigid body axes in rigid body mechanics.

The location of a body-fixed reference frame and the associated rigid body segment can be established from at least three non-linear markers located on that segment (Spoor & Veldpaus, 1980). If the coordinates of the segment markers are known with respect to the body-fixed axis, as well as their coordinates relative to the inertial (object space) reference frame, then the three translations and three rotations needed to locate the body fixed axis in the inertial frame can be readily obtained (Hussain, 1977; Miller, et al., 1980).

The relationship between coordinates in the body-fixed (local) coordinates systems and the object space (inertial) coordinate system can be expressed as:

$$\begin{bmatrix} 1 \\ X \\ Y \\ Z \end{bmatrix} = [T]. \begin{bmatrix} 1 \\ a \\ b \\ c \end{bmatrix} \qquad (1.5.5.2.1)$$

where

$$[T] = \begin{bmatrix} 1 & 0 & 0 & 0 \\ X_0 & \bar{i}.\bar{e} & \bar{i}.\bar{f} & \bar{i}.\bar{g} \\ Y_0 & \bar{j}.\bar{e} & \bar{j}.\bar{f} & \bar{j}.\bar{g} \\ Z_0 & \bar{k}.\bar{e} & \bar{k}.\bar{f} & \bar{k}.\bar{g} \end{bmatrix} \qquad (1.5.5.2.2)$$

a,b,c = coordinates of point relative to local coordinate system.
X,Y,Z = coordinates of point relative to global coordinate system.
X_0, Y_0, Z_0 = origin of local cordinate system relative to global system.
$\bar{e}, \bar{f}, \bar{g}$ = orthonormal base vectors of local system.
$\bar{i}, \bar{j}, \bar{k}$ = orthonormal base vectors of global system.

The expanded form of the transformation matrix [T] depends on the rotational convention used. For the commonly used Eularian two axis convention (Figure 7), matrix [T] takes the form:

$$[T] = \begin{bmatrix} 1 & 0 & 0 & 0 \\ X_0 & \cos\phi.\cos\varphi - \sin\phi.\sin\varphi.\cos\theta & -\sin\phi.\cos\varphi - \cos\phi.\sin\varphi.\cos\theta & \sin\theta.\sin\varphi \\ Y_0 & \cos\phi.\sin\varphi + \sin\phi.\cos\varphi.\cos\theta & -\sin\phi.\sin\varphi + \cos\phi.\cos\varphi.\cos\theta & -\sin\theta.\cos\varphi \\ Z_0 & \sin\theta.\sin\phi & \sin\theta.\cos\phi & \cos\theta \end{bmatrix} \qquad (1.5.5.2.3)$$

where

φ = first rotataion about $\bar{k}$

θ = second rotataion about $\bar{i}'$

ϕ = third rotataion about $\bar{k}''$

Figure 7. Eularian two axis rotation.

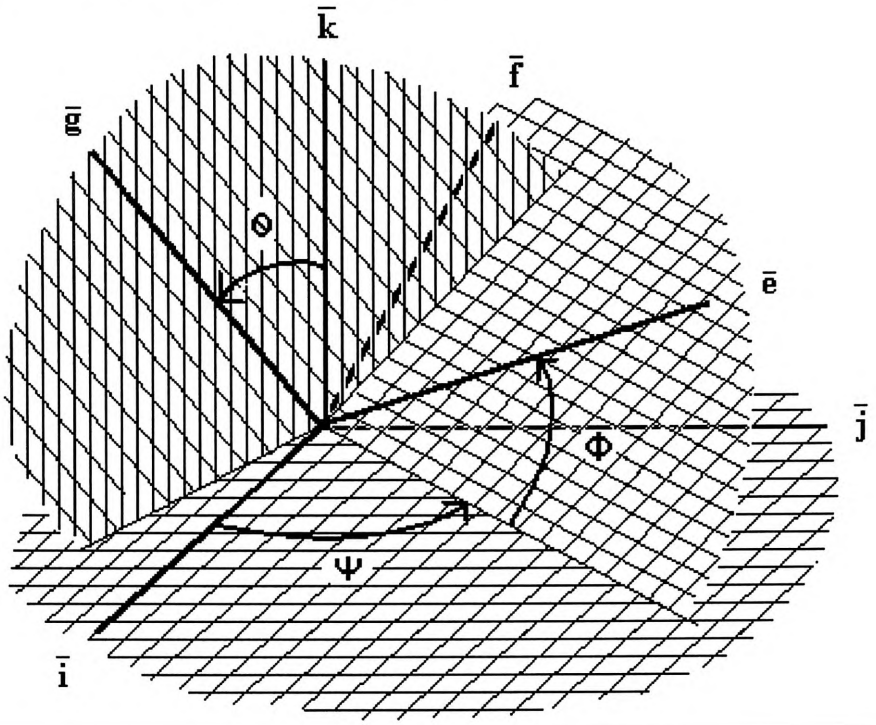

Miller, et al. (1980) combined photogrammetric DLT and rigid body transformation equations to provide a means of calculating the six spatial parameters describing the location of a rigid body from camera image data. By combining equations (1.5.1.6), (1.5.1.7) and (1.5.5.2.1) one obtains:

$$x = \frac{Nx}{Dx} \qquad (1.5.5.2.4)$$

$$y = \frac{Ny}{Dy} \qquad (1.5.5.2.5)$$

where:

$$Nx = L_4 + \begin{bmatrix} 0 & L_1 & L_2 & L_3 \end{bmatrix} \mathbf{T} \begin{bmatrix} 1 \\ a \\ b \\ c \end{bmatrix} \qquad (1.5.5.2.6)$$

$$Dx = 1 + \begin{bmatrix} 0 & L_9 & L_{10} & L_{11} \end{bmatrix} \mathbf{T} \begin{bmatrix} 1 \\ a \\ b \\ c \end{bmatrix} \qquad (1.5.5.2.7)$$

$$Ny = L_8 + \begin{bmatrix} 0 & L_5 & L_6 & L_7 \end{bmatrix} \mathbf{T} \begin{bmatrix} 1 \\ a \\ b \\ c \end{bmatrix} \qquad (1.5.5.2.8)$$

$$Dy = 1 + \begin{bmatrix} 0 & L_9 & L_{10} & L_{11} \end{bmatrix} \mathbf{T} \begin{bmatrix} 1 \\ a \\ b \\ c \end{bmatrix} \qquad (1.5.5.2.9)$$

From equations (1.5.5.2.6), (1.5.5.2.7), (1.5.5.2.8) and (1.5.5.2.9) it can be seen that the camera image coordinates (x,y) are a function of the six spatial parameters contained in the transformation matrix **T**, assuming the eleven DLT parameters for each camera ($L_1 ... L_{11}$) and the local coordinates of each body fixed marker (a,b,c) are known. Representing the transformation function, as in Miller, et al. (1980), we have:

$x_{ij} = f_{ij1}(X_0, Y_0, Z_0, \varphi, \theta, \phi)$ and

$y_{ij} = f_{ij2}(X_0, Y_0, Z_0, \varphi, \theta, \phi)$ (1.5.5.2.10)

where:

i = the local body fixed marker.

j = the camera.

Miller, et al. (1980) presents a technique for obtaining an iterative least squares solution to the six unknown spatial parameters in equation (1.5.5.2.10). Using a truncated Taylor series one obtains:

$$x_{ij} \cong f_{ij1}^{0} + \frac{\partial f_{ij1}^{0}}{\partial X_0}\Delta X_0 + \frac{\partial f_{ij1}^{0}}{\partial Y_0}\Delta Y_0 + \frac{\partial f_{ij1}^{0}}{\partial Z_0}\Delta Z_0 + \frac{\partial f_{ij1}^{0}}{\partial \varphi}\Delta\varphi + \frac{\partial f_{ij1}^{0}}{\partial \theta}\Delta\theta + \frac{\partial f_{ij1}^{0}}{\partial \phi}\Delta\phi \qquad (1.5.5.2.11)$$

$$y_{ij} \cong f_{ij2}^{0} + \frac{\partial f_{ij2}^{0}}{\partial X_0}\Delta X_0 + \frac{\partial f_{ij2}^{0}}{\partial Y_0}\Delta Y_0 + \frac{\partial f_{ij2}^{0}}{\partial Z_0}\Delta Z_0 + \frac{\partial f_{ij2}^{0}}{\partial \varphi}\Delta\varphi + \frac{\partial f_{ij2}^{0}}{\partial \theta}\Delta\theta + \frac{\partial f_{ij2}^{0}}{\partial \phi}\Delta\phi \qquad (1.5.5.2.12)$$

where:

$$\begin{aligned}
\Delta X_0 &= X_0^{\wedge} - X_0^{0} \\
\Delta Y_0 &= Y_0^{\wedge} - Y_0^{0} \\
\Delta Z_0 &= Z_0^{\wedge} - Z_0^{0} \\
\Delta\varphi &= \varphi^{\wedge} - \varphi^{0} \\
\Delta\theta &= \theta^{\wedge} - \theta^{0} \\
\Delta\phi &= \phi^{\wedge} - \phi^{0}
\end{aligned} \qquad (1.5.5.2.13)$$

The superscript 'o' indicates the evaluation of formula (1.5.5.2.10) using the current estimate of the six spatial coordinates. The calculated error (Δ) is the difference between the correct (superscript 'Λ') and the current (superscript 'o') values for the six spatial coordinates. Re-writing equations (1.5.5.2.11) and (1.5.5.2.12) in matrix form one obtains:

$$\begin{bmatrix} x_{11} - f^0_{111} \\ y_{11} - f^0_{112} \\ \vdots \quad \vdots \\ x_{ij} - f^0_{ij1} \\ y_{ij} - f^0_{ij2} \end{bmatrix} = \begin{bmatrix} \frac{\partial f^0_{111}}{\partial X_0} & \cdots & \frac{\partial f^0_{111}}{\partial \phi} \\ \frac{\partial f^0_{112}}{\partial X_0} & \cdots & \frac{\partial f^0_{112}}{\partial \phi} \\ \vdots & \vdots & \vdots \\ \frac{\partial f^0_{ij1}}{\partial X_0} & \cdots & \frac{\partial f^0_{ij1}}{\partial \phi} \\ \frac{\partial f^0_{ij2}}{\partial X_0} & \cdots & \frac{\partial f^0_{ij2}}{\partial \phi} \end{bmatrix} \begin{bmatrix} \Delta X_0 \\ \Delta Y_0 \\ \Delta Z_0 \\ \Delta \varphi \\ \Delta \theta \\ \Delta \phi \end{bmatrix} \qquad (1.5.5.2.14)$$

or

$$F_0 \cong Z_0 . \Delta\zeta \qquad (1.5.5.2.15)$$

Applying least squares techniques one then obtains:

$$\Delta\zeta = (Z_0 Z_0^T)^{-1} Z_0^T F_0 \qquad (1.5.5.2.16)$$

Using the current estimate of the six spatial parameters we solve for $\Delta\xi$, to give the error in our current estimations. An improved estimate is then obtained via equation (1.5.5.2.15). The iterative procedure continues until the values $\Delta\xi$ are below a set criterion value. To initiate the process an initial guess is required of the six spatial parameters. This can be obtained using the more traditional approach of identifying marker points in different camera views, calculating the three dimensional points from the DLT equations and then calculating the spatial parameters in the transformation matrix (1.5.5.2.3). However the estimates need to be sufficiently accurate to ensure convergence of the algorithm. Once the set of six spatial parameters are obtained for the first frame, subsequent frames can use the parameters from the previous frame as their initial estimates. This applies only if a sufficient frame rate was used.

1.5.5.3 Accuracy of rigid body location.

Hussain (1977) tested the validity and reliability of rigid body mechanics when applied to describing limb motion in controlled flexion and extension of a cadaveric monkey knee. Two stainless steel threaded skeletal pins were drilled into the tibia and femur onto which a plexiglass targets were fitted and locked in position. Ten well distributed target points were placed on each respective target. Hussain concluded the precision achievable using a Wild C-40 stereometric camera at an object distance of 1.5 meters, a base ratio of 1 and a convergent angle of 30 degrees, can be of the order ± 0.2 mm for the translational components and ± 0.2° for the rotational components of segment orientation. Higher precision could be achieved using a three camera system, with expected accuracies of ± 0.1 mm for translational components and ± 0.1° for rotational components of segment orientation. As previously mentioned, the current methodology could establish three dimensional object points with a precision of ± 0.03 mm to ± 0.5 mm in object space (Hussain 1977). The greatest error was reported in the direction normal to the photographic base, in this case the Z coordinate. The author noted a significant improvement in the Z coordinate accuracy (from 0.195 mm to 0.114 mm) and over-all location of an object point (from 0.166 mm to 0.082 mm) was achieved with the addition of a third camera. The standard errors reported in the X Y Z coordinates were ± 0.093 mm, ± 0.108 mm and ± 0.331 mm respectively (Table 3).

Miller, et al. (1980) investigated the accuracy of reproducing motion from cinematographic analysis and recommended the placement of between six to ten markers on the surface of the limb segment to improve accuracy. The redundancy was an attempt to eliminate the random motion of individual markers on the surface of the segment and solution was found via a least squares approach. The largest errors in spatial parameters were seen when only one camera was used despite placing eight markers on the segment (Table 4). The use of two cameras saw a significant improvement in accuracy. The use of eight markers was only slightly better than the use of four markers which Miller, et al. (1980) noted may have been

due to a problem with the synchronisation between cameras and the turning mechanism.

Table 3. Measured errors of object space coordinates.

Camera	RMS (mm)		
	X	Y	Z
Locam cinecamera†	1.76	4.28	4.68
Kodak Instamatic 154††	1.30	1.30	2.50
Crown Graphic††	0.41	0.34	1.29
Honeywell Pentax Spotmatic††	0.25	0.24	0.74
Hasselblad 500 C††	0.37	0.26	1.15
Hasselblad MK 70††	0.36	0.32	1.07
Wild C-40†††	0.09	0.11	0.33

† From Miller, et al. (1980) utilising a pin registered 16 mm high speed cinecamera, with image data obtained via a Vangard Motion Analyser. The convergent case of photography was used with a base of 0.8 meters and an object distance of 2.3 meters. Non-linear film deformation and lens distortion was not included in the DLT equations.

†† From Abdel-Aziz & Karara (1974), the convergent case of photography was used with a base of 3.75 meters, an object distance of 5.5 meters and a convergence of 15 degrees.

††† From Hussain (1977), utilising a stereometric camera, the normal case of photography was used with a base of 0.4 meters and an object distance of 1.27 m. Images were formed on Kodak Metalographic plates.

Table 4. Measured errors of rigid body spatial parameters.

Author	markers	cameras	RMS (mm, rad)					
			X_0	Y_0	Z_0	ϕ	θ	φ
Miller.et.al. †	8	1	1.06	9.47	6.92	0.023	0.017	0.014
Miller et.al. †	4	2	0.80	1.17	1.60	0.019	0.011	0.008
Miller et.al. †	8	2	0.73	0.96	1.49	0.019	0.014	0.010
Hussain††	10	2	0.22	0.34	0.45	0.008	0.008	0.002
Hussain††	10	3	0.12	0.16	0.22	0.003	0.004	0.001

† From Miller, et al. (1980) utilising a pin registered 16 mm high speed cinecamera, with image data obtained via a Vangard Motion Analyser. The convergent case of photography was used with a base of 0.8 meters and an object distance of 2.3 meters. Non-linear film deformation and lens distortion was not included in the DLT equations.

†† From Hussain (1977), utilising a stereometric camera, the normal case of photography was used with a base of 0.4 meters and an object distance of 1.27 m. Images were formed on Kodak Metalographic plates.

1.6 Motion analysis systems.

Considerable effort has been devoted to the development of automated motion analysis systems. Commerically-available systems include Ariel (Ariel Life Systems, USA), Elite (BTS Engineering, Italy), MacReflex (Qualisys, Sweden), Motion Analysis (Motion Analysis Corporation, Santa Rosa, USA), Peak (Peak Performance Technologies, Englewood, USA) and Vicon (Oxford Metrics, Oxford, England). These systems provide the user with the complete hardware and software required for the analysis of human motion including data collection, analysis and graphical display. Motion Analysis is one of the most extensive commercially available systems, with applications including OrthoTrak and KinTrak software packages. OrthoTrak is a three dimensional, full body gait analysis package designed for the clinical and scientific analysis of human gait. The system provides a

comprehensive description of segment and joint motions with the integration of force data for the calculation of resultant joint moments and forces. KinTrak is a general purpose three dimensional motion analysis package for analysing the motion between rigid segments, including the analysis of human motion.

A major limitation to the use of all motion analysis systems in the clinical setting is the time needed to produce an assessment of the movement which ideally would be carried out within a consultation period. To undertake a three dimensional analysis using these systems requires considerable time in patient preparation, data collection and analysis. Another factor is that some systems, by virtue of their complexity, require a specialist technician in their use. Considerable research is being done in an effort to produce a three dimensional system that will provide detailed and accurate results in a time efficient manner. Automated digitisation has removed the laborious task of manually digitising data points frame by frame for each camera image. In the case of the Motion Analysis and MacReflex systems this is achieved by the use of infrared illumination of retro-reflective markers placed on the subject with video recording of the movement and electronic processing of the video image. The efficiency of movement analysis systems have also been improved by making the systems application-specific. A set goal, as in the analysis of gait, can enable the number of three dimensional segments to be fixed as well as limiting the number and placement of segment markers. A set calibration and data collection routine can be followed and the analysis can proceed quickly as the input and desired outcomes are known in advance. The obvious disadvantage of being application-specific is that the application cannot adapt to other uses and may not accept variations from the expected input and analysis procedure. OrthoTrak is gait-specific to achieve efficiency in design, but this also means that parameters defining the pelvis and the location of hip joint centres are fixed by the computer programme.

A major difficulty and source of delay in the analysis of three dimensional motion is in the conversion of two dimensional camera image coordinates into three dimensional laboratory coordinates. The traditional approach involves the tracking of

each two dimensional camera view into two dimensional path information. Each two dimensional path in the different camera views is then identified and edited. Finally the identified two dimensional paths are combined into three dimensional paths. Considerable time can be required in the identification and tracking process. Difficulties include the uncertainty of the presence of any individual point in a given camera image and the identification of image points that move in close proximity or temporarily obscure one another. In the tracking process these difficulties can result in a confusion of paths. The complexity of the task and time required in the editing process increases markedly with the number of cameras, the number of markers and the complexity of movement. In such cases a large portion of the data processing time will be spent in the editing of paths and in the worst case, the paths may be un-retrievable.

Limitations are therefore present in present-day motion analysis systems due to the ability to identify and track image points in camera images. To overcome these limitations motion analysis systems generally limit both the number of markers by limiting the number of three dimensional segments and limiting the number of markers per segment and by having the markers well spaced. OrthoTrak and KinTrak limit the number of surface markers per three dimensional segment to three; the minimum required to locate a rigid body in three dimensional space. OrthoTrak also makes use of a rigid triangular arrangement of markers placed on the thigh and lower leg to ensure well spaced markers and to assist in the tracking process. The Motion Analysis tracking function is therefore limited to tracking up to thirty points simultaneously. The complexity of movement is also limited to predominantly sagittal plane movements.

1.7 The role of automated three dimensional coordinate reproduction in three dimensional identification and tracking.

Little information has appeared in the literature describing algorithms or techniques for the automated reproduction of individual points appearing in multiple camera images. The identification of individual marker points appearing in three dimensional space has several advantages over identifying image points in two dimensional camera views. Identifying three dimensional points is made easier by:

(i) being able to view the laboratory points from a variety of angles;
(ii) knowing which laboratory points are present and their positions relative to one another;
(iii) preforming only one tracking and identification procedure.

This is in contrast to the identification of camera images in which:

(i) the user must work with fixed two dimensional views;
(ii) the presence of individual markers is unknown and can vary throughout the movement;
(iii) tracking and identification needs to be carried out for each camera.

The application of automated three dimensional point reproduction from a single frame would lie in direct three dimensional tracking of segmental spatial parameters from two dimensional camera coordinates. A tracking procedure similar to that described by Miller, et al. (1980) may be used. In this procedure the photogrammetric equations are combined with the rigid body equations of motion to provide a direct transformation from two dimensional image coordinates to the spatial parameters describing three dimensional segmental location. This procedure requires an approximation of all the spatial parameters (in this case, six per segment) for the current frame. A least square routine is then used to adjust the spatial parameters to fit the predicted image coordinates with the measured image

coordinates for each camera. In this iterative tracking procedure the spatial parameters from the previous frame are used for the current estimate to arrive at the current spatial parameters. Miller, et al. (1980) has had success with this algorithm for reproducing the spatial parameters in human movement analysis. However, a problem arose in obtaining adequate initial approximations of the spatial parameters for the first frame. This problem may be overcome by the automated reproduction of three dimensional coordinates for a single frame. With a single frame of three dimensional coordinates, markers can be readily identified (see above) and segment axis and spatial parameters generated. A requirement in rigid body techniques for the reproduction of three dimensional segment location is a prior knowlege of segmental markers' coordinates relative to the local body axis system. These parameters could be obtained in a subject calibration procedure from automatically reproduced three dimensional coordinates of segmental and calibration markers. Again, with a single frame of three dimensional coordinates, markers can be readily identified and segmental axis and local coordinates generated. With the development of automated three dimensional coordinate reproduction it would therefore be possible to reduce the problem of tracking and identification markers in multiple two dimensional camera images to identification in just two frames of three dimensional coordinate. One frame would act as a subject calibration procedure and another frame acts as the beginning of a three dimensional tracking algorithm. The advantage of this approach in working directly with three dimensional coordinates would be realised in removing the necessity of having to identify, track and edit two dimensional coordinate data from each camera view.

The procedures and techniques developed in the current research project for evaluating the validity of conjugate image points and reproduction of three dimensional coordinates also have the potential to be incorporated into a three dimensional tracking procedure similar to that of Miller, et al.(1980). With further investigation into this approach of three dimensional tracking of spatial coordinates there is potential to improve on the results already obtained by these authors.

In summary, the automated generation of three dimensional coordinates from multiple camera images would significantly increase the ability to identify and track individual markers appearing in multiple two dimensional camera images. This is partly achieved by avoiding the necessity and limitations associated with tracking and identifying two dimensional camera images. Present identification and tracking procedures rely on identification of two dimensional camera coordinates and are restricted by the number of markers appearing in each camera image and the complexity of movement. Both can lead to significant increases in difficulty and time required to produce three dimensional coordinate data. The automated reproduction and tracking of three dimensional coordinates therefore can increase the accuracy and complexity currently attainable in human movement analysis. This approach will allow a greater number of markers to be placed on each body segment, thereby increasing the accuracy of rigid body location and enabling more complex movements to be analysed.

Presented in this chapter is a possible approach to the automated three dimensional tracking from two dimensional camera image data. This approach is reliant on the development of techniques for the automated reproduction of three dimensional coordinates and the implementation of these techniques in a tracking algorithm. The aim of the present research project is to establish imaging techniques for the automated reproduction of three dimensional coordinates as well as implementating these techniques in the analysis of human motion. The viability of the approach will be established as well as any limitations and practical problems associated with the techniques developed. The research carried out will result in an algorithm for the automated reproduction of three dimensional coordinates and form the basis of further research and development of an automated three dimensional tracking of two dimensional image data.

2.0 METHODOLOGY

2.1 Assumptions.

It is inevitable that digitised image coordinates will contain a combination of measurement and processing error and therefore conjugate imaging techniques will not always behave as the ideal case. In the application of conjugate imaging techniques to the automated identification of conjugate image points several assumption are made to account for digitisation error:

(i) a conjugate image point may lie at some finite distance from a conjugate epipolar line;
(ii) a conjugate image point may not necessarily be the closest point to the epipolar line; and
(iii) an image point and its respective collinear line may be coincident with more than one set of multiple collinear lines and their respective image points.

The third assumption states that even though a set of collinear lines intersect, this does not mean that all, or in fact any, of the collinear lines and their respective image points are correct. As an unrelated set of image points and respective collinear lines may coincide by chance to form an object point. The chance convergence of a set of collinear lines is even more likely when the object points and camera perspective centres lie in approximately the same plane.

2.2 Passpoint criteria.

In order to determine the validity of an object point reconstructed from any number of camera image points there needs to be a range of criteria against which the validity of the object point can be measured. Four criteria are necessary to account for the varied and uncontrolled nature of the problem. The criteria for testing the validity of conjugate image points were:

(i) Conjugate Point Error (CPE): the perpendicular distance between a conjugate image point and the conjugate epipolar line (Figure 8). As the photo scale may change from one camera to another the CPE is specific to the camera image in which it is measured.

Figure 8. Conjugate Point Error.

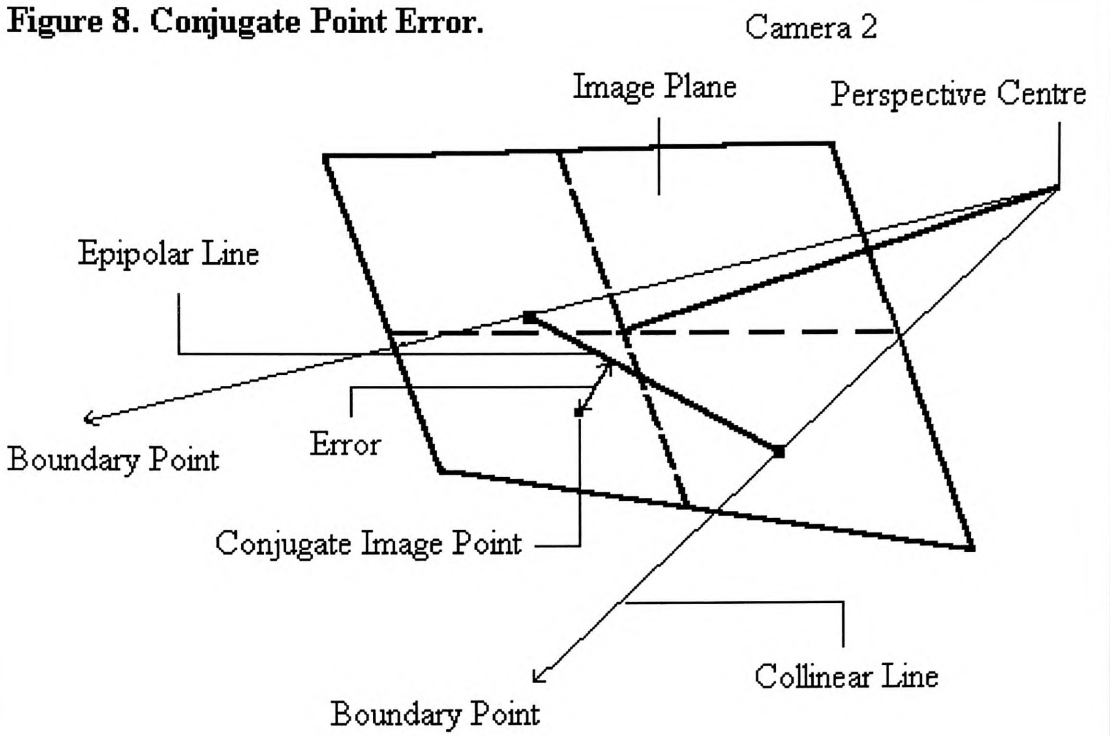

(ii) Lab Point Standard Error (LPSE): the standard error of the mean as calculated from the least squares laboratory point and the laboratory points derived from all paired conjugate image points (Figure 9). The LPSE can only be calculated for a point appearing in at least three cameras.

$$LPSE = \frac{\sigma}{\sqrt{N}} \qquad (2.2.1)$$

where:

$$\sigma^2 = \frac{1}{N-1} \cdot \sum_{1}^{n} (\hat{x}i - \bar{x})^2$$

N = number of paired conjugate image points.

$\hat{x}_i$ = laboratory point calculated from paired conjugate image points.

$\bar{x}_i$ = laboratory point calculated from all conjugate image points.

(iii) Lab Point Error (LPE): the maximum radius over which a laboratory point may vary.

Figure 9. Paired conjugate image points.

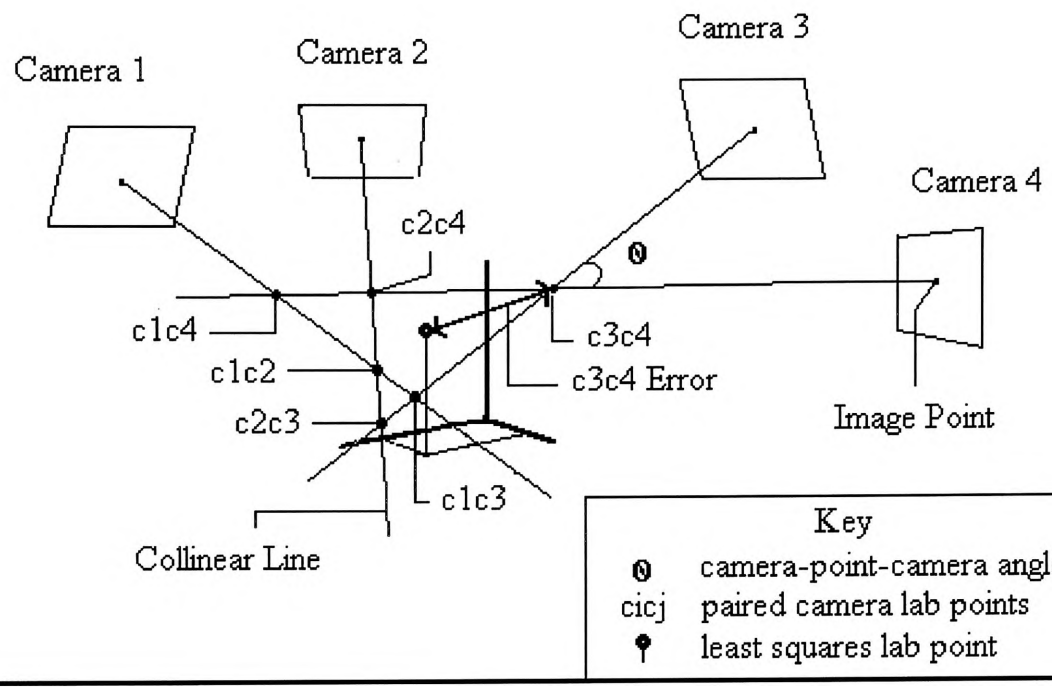

(iv) Lab Point Paired Error (LPPE): the maximum distance between calculated laboratory points formed from paired conjugate image points. The LPPE can only be calculated for a point appearing in at least three cameras (Figure 9).

2.2.1 Maximum criterion values.

The maximum acceptable value for each criterion was established as part of the normal calibration procedure. As stated in Chapter 1, camera calibration involved identification of six or more laboratory points with known spatial coordinates in all the cameras

present. With known laboratory points, respective collinear lines and image point coordinates, the mean and standard deviation of the four criteria measures were established. The maximum acceptable value of the four criterion measures were calculated as the mean plus three standard deviations. For two or more image points to be considered as a valid laboratory point they would have to satisfy the four criterion measures and be within the maximum acceptable value of all four criteria.

2.2.2 Laboratory point reduction.

A valid laboratory point is formed from two or more camera image points that satisfy the four criteria. In excess of one hundred valid laboratory points may be produced in collecting all valid laboratory points for an experimental set up involving fifty marker points and four cameras. However each camera image point is associated with only one laboratory point and therefore many laboratory points are either incorrect or are incorporating erroneous image points. Laboratory point reduction involves the elimination, separation or combination of valid laboratory points sharing common camera image points or which lie within the Lab Point Error of one another. The outcome of the processes of elimination, separation or combination of valid laboratory points is dependent on the values of the four criteria measures of the concerned laboratory points. Decisions to eliminate, separate or combine valid laboratory points were based on:

(i) the distances from the epipolar lines;
(ii) the magnitude of the respective Lab Point Standard Errors;
(iii) the magnitude of the Lab Point Paired Errors;
(iv) the distance between laboratory points and the Lab Point Standard Error;
(v) the number of unique and common image points associated with a laboratory point;
(vi) the total number of image points associated with a laboratory point.

When a valid laboratory point was reduced so that no camera image points were in common with any other laboratory point, then the associated image points could be regarded as the conjugate image points.

2.3 Mathematical procedures

In presenting the calculation of test data (Section 2.4) and the algorithm for the automated three dimensional reproduction of image points (Section 2.5) various mathematical procedures are referred to. The following is a description of the important mathematical procedures as they relate to these methods.

2.3.1 Least squares solution.

A least squares mathematical problem regularly results in an attempt to improve on an answer by incorporating more equations or observations into the problem than were required by the number of variables to be solved. In the present methodology the least squares approach has been adopted to solve the following problems:

(i) Calculation of DLT parameters.

The DLT equations (1.5.1.6) and (1.5.1.7) can be written in the following form:

$$x_i.(X_i.L_9 + Y_i.L_{10} + Z_i.L_{11} + 1) = X_i.L_1 + Y_i.L_2 + Z_i.L_3 + L_4 \qquad (2.3.1.1)$$

$$y_i.(X_i.L_9 + Y_i.L_{10} + Z_i.L_{11} + 1) = X_i.L_5 + Y_i.L_6 + Z_i.L_7 + L_8 \qquad (2.3.1.2)$$

where:

x_i, y_i = camera image coordinates of point i.
X_i, Y_i, Z_i = laboratory space coordinates of point i.
$L_1 ... L_{11}$ = DLT parameters.

If at least six camera image points of known three dimensional coordinates for a given camera configuration are identified then the eleven camera calibration coefficients can be calculated. Rearranging equations (2.3.1.1) and (2.3.1.2):

$$X_i.L_1 + Y_i.L_2 + Z_i.L_3 + L_4 - x_i.X_i.L_9 - x_i.Y_i.L_{10} - x_i.Z_i.L_{11} = x_i \qquad (2.3.1.3)$$

$$X_i.L_5 + Y_i.L_6 + Z_i.L_7 + L_8 - y_i.X_i.L_9 - y_i.Y_i.L_{10} - y_i.Z_i.L_{11} = y_i \qquad (2.3.1.4)$$

and expressing in matrix form:

$$\begin{bmatrix} X_1 & Y_1 & Z_1 & 1 & 0 & 0 & 0 & 0 & -x_1X_1 & -x_1Y_1 & -x_1Z_1 \\ 0 & 0 & 0 & 0 & X_1 & Y_1 & Z_1 & 1 & -y_1X_1 & -y_1Y_1 & -y_1Z_1 \\ X_2 & Y_2 & Z_2 & 1 & 0 & 0 & 0 & 0 & -x_2X_2 & -x_2Y_2 & -x_2Z_2 \\ 0 & 0 & 0 & 0 & X_2 & Y_2 & Z_2 & 1 & -y_2X_2 & -y_2Y_2 & -y_2Z_2 \\ \vdots & \vdots & \vdots & \vdots & \vdots & \vdots & \vdots & \vdots & \vdots & \vdots & \vdots \\ \vdots & \vdots & \vdots & \vdots & \vdots & \vdots & \vdots & \vdots & \vdots & \vdots & \vdots \\ X_n & Y_n & Z_n & 1 & 0 & 0 & 0 & 0 & -x_nX_n & -x_nY_n & -x_nZ_n \\ 0 & 0 & 0 & 0 & X_n & Y_n & Z_n & 1 & -y_nX_n & -y_nY_n & -y_nZ_n \end{bmatrix} \begin{bmatrix} L_1 \\ \vdots \\ \vdots \\ \vdots \\ L_{11} \end{bmatrix} = \begin{bmatrix} x_1 \\ y_1 \\ x_2 \\ y_2 \\ \vdots \\ \vdots \\ x_n \\ y_n \end{bmatrix} \qquad (2.3.1.5)$$

where

n = number of camera image points ($n \geq 6$).

(ii) Calculation of laboratory space coordinates.

If known DLT parameters and identified conjugate image points exist in two or more cameras then the respective laboratory space coordinate can be calculated. Rearranging equations (2.3.1.1) and (2.3.1.2):

$$X_i.(L_1 - x_i.L_9) + Y_i.(L_2 - x_i.L_{10}) + Z_i.(L_3 - x_i.L_{11}) = x_i - L_4 \qquad (2.3.1.6)$$

$$X_i.(L_5 - y_i.L_9) + Y_i.(L_6 - y_i.L_{10}) + Z_i.(L_7 - y_i.L_{11}) = y_i - L_8 \qquad (2.3.1.7)$$

and expressing in matrix form:

$$\begin{bmatrix} L_1 - x_1.L_9 & L_2 - x_1.L_{10} & L_3 - x_1.L_{11} \\ L_5 - y_1.L_9 & L_6 - y_1.L_{10} & L_7 - y_1.L_{11} \\ L_1 - x_2.L_9 & L_2 - x_2.L_{10} & L_3 - x_2.L_{11} \\ L_5 - y_2.L_9 & L_6 - y_2.L_{10} & L_7 - y_2.L_{11} \\ \vdots & \vdots & \vdots \\ \vdots & \vdots & \vdots \\ L_1 - x_n.L_9 & L_2 - x_n.L_{10} & L_3 - x_n.L_{11} \\ L_5 - y_n.L_9 & L_6 - y_n.L_{10} & L_7 - y_n.L_{11} \end{bmatrix} \begin{bmatrix} X \\ Y \\ Z \end{bmatrix} = \begin{bmatrix} x_1 - L_4 \\ y_1 - L_8 \\ x_2 - L_4 \\ y_2 - L_8 \\ \vdots \\ \vdots \\ x_n - L_4 \\ y_n - L_8 \end{bmatrix} \qquad (2.3.1.8)$$

where

n = the number of conjugate image points ($n \geq 2$).

(iii) Calculation of camera perspective centre.

For a given camera configuration, known DLT parameters and a defined laboratory space boundary, the respective camera perspective centre can be calculated. First, from the laboratory space boundary a number of dispersed points in three dimensional laboratory space are arbitrarily defined. Eight have been used in this study. With the use of the DLT equations (2.3.1.1) and (2.3.1.2) and with known DLT parameters, camera image points can be directly calculated for each respective laboratory point. Using conjugate imaging techniques (see Section 1.2.3) two points on the laboratory space boundary can be derived for each camera image point. These two points are the intersection of each respective collinear line with the laboratory space boundary. From the condition of collinearity, each collinear line passes through the camera perspective centre, the image point and the respective pair of laboratory points. In the ideal case the camera perspective centre is a common point of intersection of all collinear lines. From the mathematical vector cross product (Figure 10):

$$\bar{a} \times \bar{b} = 0 \qquad (2.3.1.9)$$

therefore:

$(x-px_i, y-py_i, z-pz_i)$ **x** $(dx_i-px_i, dy_i-py_i, dz_i-pz_i) = 0$

where

px_i,py_i,pz_i = laboratory coordinates of first intercept of collinear line i with laboratory boundary.

dx_i,dy_i,dz_i = laboratory coordinates of the second intercept of collinear line i with laboratory boundary.

x,y,z = camera perspective centre, a common point to all collinear lines.

let:

$$mx_i = dx_i-px_i \qquad (2.3.1.10)$$

$$my_i = dy_i-py_i \qquad (2.3.1.11)$$

$$mz_i = dz_i-pz_i \qquad (2.3.1.12)$$

By substitution and rearranging equations (2.3.1.10), (2.3.1.11) and (2.3.1.12) one obtains:

$$y.mz_i - py_i.mz_i - z.my_i + pz_i.my_i = 0 \qquad (2.3.1.13)$$

$$z.mx_i - pz_i.mx_i - x.mz_i + px_i.mz_i = 0 \qquad (2.3.1.14)$$

$$x.my_i - px_i.my_i - y.mx_i + py_i.mx_i = 0 \qquad (2.3.1.15)$$

writing in matrix form:

$$\begin{bmatrix} 0 & mz_1 & -my_1 \\ -mz_1 & 0 & mx_1 \\ my_1 & -mx_1 & 0 \\ 0 & mz_2 & -my_2 \\ -mz_2 & 0 & mx_2 \\ my_2 & -mx_2 & 0 \\ \vdots & \vdots & \vdots \\ \vdots & \vdots & \vdots \\ 0 & mz_n & -my_n \\ -mz_n & 0 & mx_n \\ my_n & -mx_n & 0 \end{bmatrix} \begin{bmatrix} x \\ y \\ z \end{bmatrix} = \begin{bmatrix} py_1.mz_1 - pz_1.my_1 \\ pz_1.mx_1 - px_1.mz_1 \\ px_1.my_1 - py_1.mx_1 \\ py_2.mz_2 - pz_2.my_2 \\ pz_2.mx_2 - px_2.mz_2 \\ px_2.my_2 - py_2.mx_2 \\ \vdots \\ \vdots \\ py_n.mz_n - pz_n.my_n \\ pz_n.mx_n - px_n.mz_n \\ px_n.my_n - py_n.mx_n \end{bmatrix} \quad (2.3.1.16)$$

where

n = the number of arbitrary laboratory points and collinear lines ($n \geq 2$).

Figure 10. Camera perspective centre.

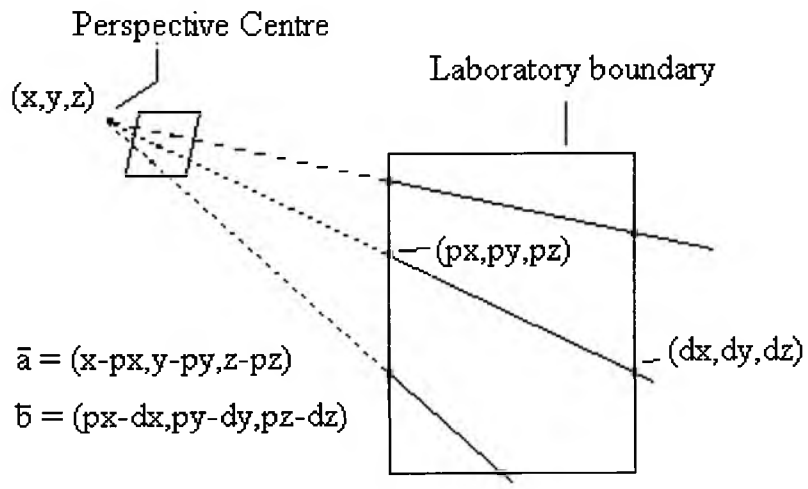

The least squares solution to the simultaneous equations (2.3.1.5), (2.3.1.8) and (2.3.1.16) was achieved by firstly pre-multiplying by the transpose of the coefficient matrix, then triangular (LU) decomposition of the resultant square matrix, followed by forward and back substitution to obtain an initial answer. An improvement on this answer was achieved via an analysis of residuals. In matrix form:

$$\mathbf{A}_{ij}.\mathbf{X}_{j1} = \mathbf{B}_{i1} \qquad (2.3.1.17)$$

where:

$\mathbf{A}_{ij}$ = coefficient matrix; i rows, j columns;

$\mathbf{X}_{i1}$ = variable matrix; j rows, 1 column;

$\mathbf{B}_{i1}$ = right hand side (RHS) matrix; i rows, 1 column.

Equation (2.3.1.17) is pre-multiplied by the transpose of the coefficient matrix to obtain:

$$\mathbf{A}_{ji}.\mathbf{A}_{ij}.\mathbf{X}_{j1} = \mathbf{A}_{ji}.\mathbf{B}_{i1} \qquad (2.3.1.18)$$

$$\mathbf{A}^T\mathbf{A}_{jj}.\mathbf{X}_{j1} = \mathbf{A}^T\mathbf{B}_{j1} \qquad (2.3.1.19)$$

where

$\mathbf{A}^T\mathbf{A}_{jj}$ = resultant matrix of **A** transpose multiplied by **A**; j rows, j columns;

$\mathbf{A}^T\mathbf{B}_{j1}$ = resultant matrix of **A** transpose multiplied by **B**; j rows, 1 column.

The square matrix $\mathbf{A}^T\mathbf{A}$ is then decomposed into an upper and lower triangular matrix:

$$\mathbf{A}^T\mathbf{A} = \mathbf{L}.\mathbf{U} \qquad (2.3.1.20)$$

where

$$\mathbf{L} = \begin{bmatrix} l_{11} & 0 & 0 & \cdots & 0 \\ l_{21} & l_{22} & 0 & \cdots & 0 \\ \vdots & \vdots & \vdots & \cdots & \vdots \\ l_{n1} & l_{n2} & l_{n3} & \cdots & l_{nn} \end{bmatrix} \qquad (2.3.1.21)$$

$$\mathbf{U} = \begin{bmatrix} u_{11} & u_{12} & \cdots & u_{1n} \\ 0 & u_{22} & \cdots & u_{2n} \\ \vdots & \vdots & \cdots & \vdots \\ 0 & 0 & \cdots & u_{nn} \end{bmatrix} \qquad (2.3.1.22)$$

The decomposition of matrix $\mathbf{A}^T\mathbf{A}$ into matrices **L** and **U** can be preformed so that the diagonals of matrix **L** are unity:

$l_{11} = l_{22} = \ldots = l_{nn} = 1.$

Calculation of the elements of **L** and **U** can be achieved via sequential calculations and the product **L.U** is given by:

$$\mathbf{A}^T\mathbf{A} = \mathbf{L}.\mathbf{U} = \begin{bmatrix} u_{11} & u_{12} & u_{13} & \ldots\ldots \\ l_{21}.u_{11} & l_{21}.u_{12} + u_{22} & l_{21}.u_{13} + u_{23} & \ldots\ldots \\ l_{31}.u_{11} & l_{31}.u_{12} + l_{32}.u_{22} & l_{31}.u_{13} + l_{32}.u_{23} + u_{33} & \ldots\ldots \\ \ldots\ldots & \ldots\ldots\ldots & \ldots\ldots\ldots & \ldots\ldots \end{bmatrix} \quad (2.3.1.23)$$

General formulae for the calculation of **L** and **U** can be derived by equating individual elements in equation (2.3.1.23). In the formulae, quantities required for the derivation of each element have been calculated in the previous step (Noble, 1969):

$$u_{pj} = a_{pj} - \sum_{k=1}^{p-1} l_{pk}.u_{kj} \qquad j = p, p+1, \ldots, n \qquad (2.3.1.24)$$

$$l_{iq} = \frac{a_{iq} - \sum_{k=1}^{q-1} l_{ik}.u_{kq}}{u_{qq}} \qquad i = q+1, \ldots, n \qquad (2.3.1.25)$$

where

a = elements of matrix **A**.

Applying the decomposition in equation (2.3.1.20) to the equation (2.3.1.19):

$$\mathbf{L}.\mathbf{U}.\mathbf{X} = \mathbf{A}^T\mathbf{B} \qquad (2.3.1.26)$$

If one introduces:

$$\mathbf{Y} = \mathbf{U}.\mathbf{X} \qquad (2.3.1.27)$$

which gives:

$$\mathbf{L}.\mathbf{Y} = \mathbf{A}^T\mathbf{B} \qquad (2.3.1.28)$$

The solution to equation (2.3.1.19) is found by first solving for matrix **Y** in equation (2.3.1.28) by forward substitution:

$$\begin{aligned} l_{11}.y_1 &= b_1 \\ l_{21}.y_1 + l_{22}.y_2 &= b_2 \\ \vdots \quad \vdots & \quad \vdots \\ l_{n1}.y_1 + l_{n2}.y_2 + \ldots\ldots + l_{nn}.y_n &= b_n \end{aligned} \qquad (2.3.1.29)$$

where:

$y_1 \ldots y_n$ = elements of matrix **Y**.

$b_1 \ldots b_n$ = elements of matrix $\mathbf{A}^T\mathbf{B}$.

With known matrix **Y** the variable matrix **X** in equation (2.3.1.27) can be solved by back substitution:

$$\begin{aligned} u_{11}.x_1 + u_{12}.x_2 + \ldots\ldots + u_{1n}.x_n &= y_n \\ u_{21}.x_1 + u_{22}.x_2 &= y_2 \\ \vdots \quad \vdots & \quad \vdots \\ u_{n1}.x_n &= y_1 \end{aligned} \qquad (2.3.1.30)$$

where:

$x_1 \ldots x_n$ = elements of matrix **X**.

An improvement on the variable matrix **X** can be obtained by analysis of residuals:

$$\mathbf{A}^T\mathbf{A}.\mathbf{X} - \mathbf{A}^T\mathbf{B} = \xi\mathbf{X}. \qquad (2.3.1.31)$$

where:

$\xi\mathbf{X}$ = errors in current values of matrix **X**.

Equation (2.3.1.26) is solved for the error term $\xi\mathbf{X}$ as the right hand side matrix to give a correction for matrix **X**. To gain this solution the same procedure is followed utilising the previously calculated triangular matrices **L** and **U** in equations (2.3.1.27) and (2.3.1.28) with forward and back substitution (equations 2.3.1.29 and 2.3.1.30).

$$\mathbf{L.U.}\Delta\mathbf{X} = \xi\mathbf{X} \qquad (2.3.1.31)$$

The new values for **X** are then obtained:

$$\mathbf{X} = \mathbf{X} - \Delta\mathbf{X}. \qquad (2.3.1.32)$$

2.3.2 Conjugate imagery in human motion analysis.

Conjugate imagery has been used in aerial photogrammetry to aid in the correlation of camera images (Keating, 1975). When used in this role it was sufficient to define two horizontal planes which vertically bound object space (see Section 1.2.3). In the close range photogrammetry of human motion analysis, multiple cameras may be positioned around the subject, usually at a slightly higher elevation than that of the subject. In the analysis of human motion it is therefore necessary to define a cube in three dimensional space which completely bounds the object space.

When defining a conjugate epipolar line on a second camera's image plane, the problem is to find two points of intersection of a collinear line with a three dimensional cube bounding the experimental region (Figure 11). This can be readily solved by systematically calculating the intersection of a collinear line with each plane in object space. Assume the limits in the horizontal Z plane are z1 and z2, and starting with the plane defined by z1, the DLT equations (2.3.1.1) and (2.3.1.2) can be written as:

$$X.(L_1 - x.L_9) + Y.(L_2 - x.L_{10}) = x - L_4 - z1.(L_3 - x.L_{11}) \quad (2.3.2.1)$$

$$X.(L_5 - y.L_9) + Y.(L_6 - y.L_{10}) = y - L_8 - z1.(L_7 - y.L_{11}) \quad (2.3.2.2)$$

where:

X, Y = laboratory space coordinates;

x, y = image coordinates;

L_1 .. L_{11} = eleven DLT coefficients;

z1 = point on Z axis defining horizontal plane.

Figure 11. Laboratory Boundary.

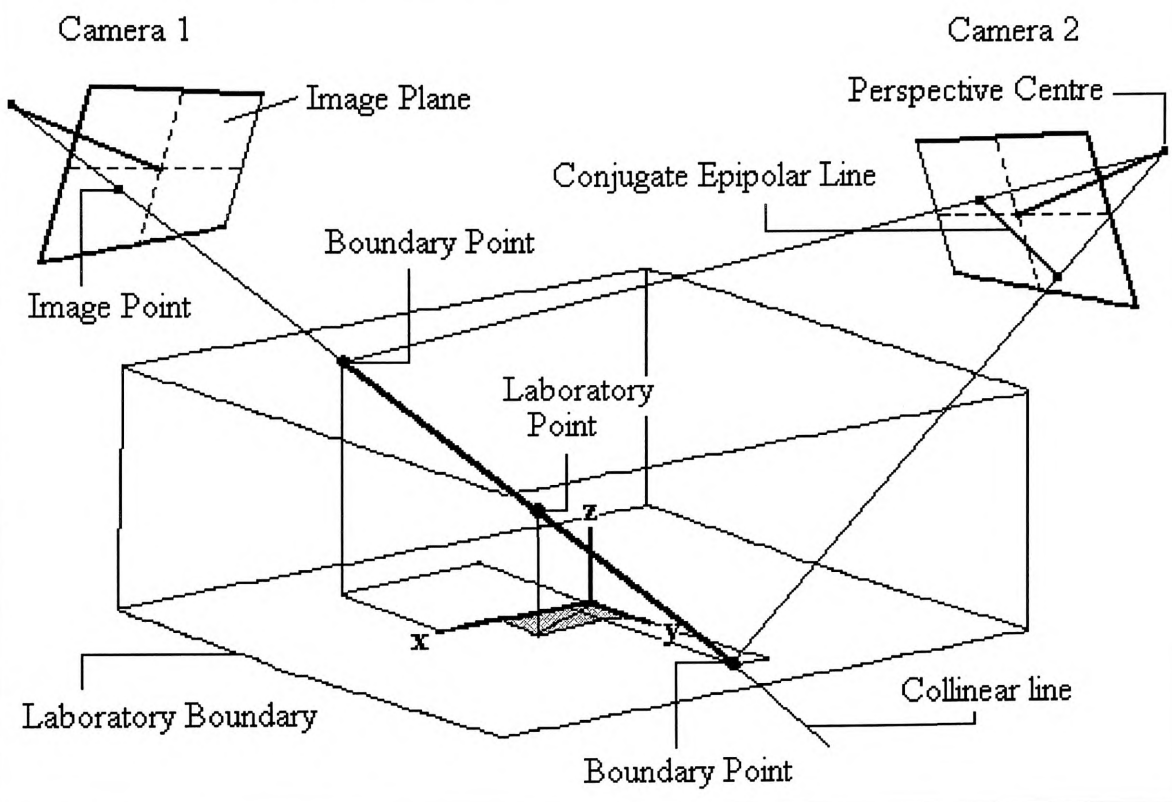

A solution is readily obtained to the matrix problem by the application of Cramer's rule to equations (2.3.2.1) and (2.3.2.2). Let:

$a_{11} = L_1 - x.L_9$,

$a_{12} = L_2 - x.L_{10}$,

$a_{21} = L_5 - y.L_9$,

$a_{22} = L_6 - y.L_{10}$,

$b_1 = x - L_4 - z1.(L_3 - x.L_{11})$, and

$b_2 = y - L_8 - z1.(L_7 - y.L_{11})$.

then:

$$X = (b_1.a_{22} - b_2.a_{12})/(a_{11}.a_{22} - a_{21}.a_{12}). \qquad (2.3.2.3)$$

$$Y = (a_{11}.b_2 - a_{21}.b_1)/(a_{11}.a_{22} - a_{21}.a_{12}). \qquad (2.3.2.4)$$

Similarly, a point in laboratory space can be calculated for z2. If either of these points are outside the laboratory boundary then the procedure can be repeated for the vertical planes defined by the X axis and, if required, by the Y axis. These two points in three dimensional space are then mapped onto the image plane of the second camera (see Section 1.2.3). With two points on the image plane defining the epipolar line, the perpendicular distance to this line and the point of intersection in relation to the length of the line can be obtained. Using the cosine rule and from Figure (12) one can write:

$$\bar{a}.\bar{b} = 0 \qquad (2.3.2.5)$$

with

$$\bar{a} = (dx - px, dy - py, dz - pz) \qquad (2.3.2.6)$$

and

$$\bar{b} = (x - \alpha\,(dx - px) - px, y - \alpha\,(dy - py) - py, z - \alpha\,(dz - pz) - pz) \qquad (2.3.2.7)$$

Figure 12. Image point to epipolar line.

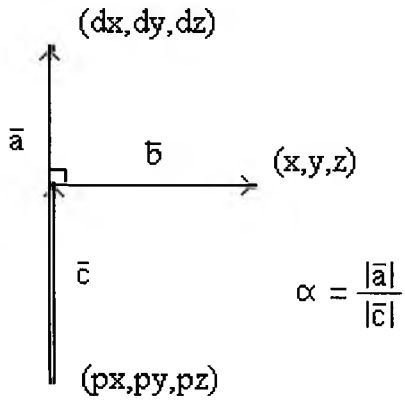

By substitution of (2.3.2.6) and (2.3.2.7) into (2.3.2.5) and on rearranging:

$$(x - px)(dx - px) - \alpha(dx - px)^2 + (y - py)(dy - py) - \alpha(dy - py)^2 + (z - pz)(dx - pz) - \alpha(dx - px)^2 = 0 \qquad (2.3.2.8)$$

hence:

$$\alpha = \frac{(x - px)(dx - px) + (y - py)(dy - py) + (z - pz)(dz - pz)}{(dx - px)^2 + (dy - py)^2 + (dz - pz)^2} \qquad (2.3.2.9)$$

$$(\text{distance})^2 = (x - px - \alpha(dx-px))^2 + (x - px - \alpha(dx-px))^2 + (x - px - \alpha(dx-px))^2 \qquad (2.3.2.10)$$

2.3.3 Paired image point normalisation.

The error in the calculation of laboratory points from paired image points was dependent on the accuracy of the photogrammetric system and on the angle formed between the first camera's perspective centre, the actual laboratory point and the second camera's perspective centre. For a given photogrammetric configuration, the relationship between error and angle can be approximated by a second degree polynomial with a minimum at an angle of ninety degrees and approaching positive

infinity as the angles approaches zero and 180 degrees (see Results, Figure 16 and Figure 17). The minimum of the polynomial is proportional to the accuracy of the photogrammetric system. In practical terms, this polynomial represents the maximum error expected in laboratory points produced from paired image points for various camera-laboratory point-camera angles from zero to 180 degrees.

To enable the criterion values of Lab Point Standard Error (LPSE) and Lab Point Paired Error (LPPE) to be compared between different laboratory points in a given photogrammetric configuration, all distances calculated from paired image points were normalised to 90 degrees. In this way the LPSE and LPPE are also normalised. Normalisation is achieved in the following manner:

Assume that the relationship between error and angle (see Results, Figure 17) is represented by the following second degree polynomial:

$$\xi D = a_0 + a_1.\theta + a_2.\theta^2 \qquad (2.3.3.1)$$

where:

ξD = maximum expected error in a laboratory point produced from paired image points;

a_0, a_1, a_2 = coefficients of second degree polynomial;

θ = camera-laboratory point-camera angle ($0 < \theta < 180$).

Assume the minimum value of this polynomial (at 90 degrees) is ξD_{90}. For a laboratory point composed of n image points ($n > 3$), a least squares solution to the DLT equations (Section 2.3.1) will give the mean laboratory point (X,Y,Z). If any two image points are taken at a time, the distances between the mean laboratory point and paired image points are calculated:

$$\Delta Dij = \sqrt{(X - Xij)^2 + (Y - Yij)^2 + (Z - Zij)^2} \qquad (2.3.3.2)$$

where:

ΔDij = distance between mean laboratory point and laboratory point formed from cameras i and j;

Xij, Yij, Zij = coordinates of laboratory point formed from cameras i and j.

The included angle for the camera pair is calculated:

$$\cos(\theta ij) = \frac{(cXi - X)(cXj - X) + (cYi - Y)(cYj - Y) + (cZi - Z)(cZj - Z)}{\sqrt{(cXi - X)^2 + (cYi - Y)^2 + (cZi - Z)^2 \,.\, (cXj - X)^2 + (cYj - Y)^2 \,(cZj - Z)^2}} \qquad (2.3.3.3)$$

where:

θij = included angle between camera centre i, mean laboratory point, and camera j;

cXi, cYi, cZi = location of perspective centre of camera i;

cXj, cYj, cZj = location of perspective centre of camera j.

The maximum expected difference for this camera pair is then calculated:

$$\xi Dij = a_0 + a_1.\theta ij + a_2.\theta ij^2 \qquad (2.3.3.4)$$

where:

ξDij = maximum expected error in a laboratory point produced from camera i and camera j.

The measured camera pair error is then normalised to 90 degrees:

$$nDij = \xi D_{90} \frac{\Delta Dij}{\xi Dij} \qquad (2.3.3.5)$$

The coordinates of the laboratory point reproduced from the paired cameras is also normalised to be at a distance of nDij from the mean laboratory point:

$$nXij = X + R.(Xij - X), \qquad (2.3.3.6)$$

$$nYij = Y + R.(Yij - Y), \qquad (2.3.3.7)$$

$$nZij = Z + R.(Zij - Z). \qquad (2.3.3.8)$$

where:

$R = nDij/\Delta Dij.$

From equation (2.2.1) the Lab Point Standard Error (LPSE) is calculated for a laboratory point identified in n cameras with N different camera pairs:

$$LPSE = \sqrt{\frac{1}{N-1}\ \Sigma(nDij)^2} \qquad \begin{matrix} i = 1, 2 \ldots n\text{-}1. \\ j = i, i+1, \ldots n. \end{matrix} \qquad (2.3.3.9)$$

Lab Point Paired Error (LPPE) is the maximum difference in normalised laboratory points calculated from each pair of image points:

$$LPPE = (\text{maximum})\sqrt{(nXij - nXrs)^2 + (nXij - nXrs)^2 + (nXij - nXrs)^2} \qquad (2.3.3.10)$$

$$\begin{matrix} i = 1, 2 \ldots n\text{-}1. \\ j = i+1, i+2, \ldots n \\ r = i+1, i+2, \ldots n\text{-}1. \\ s = r+1, r+2, \ldots n. \end{matrix}$$

The normalisation of LPSE and LPPE by the above method allows for the comparison of the LPSE and LPPE between laboratory points. As the magnitude of calculated LPSE and LPPE is dependent on both the error in the image coordinates and on angle between each paired image point, the measured criterion values do not truely reflect the accuracy of reproduced laboratory points. The normalisation procedure accounts for differences in camera-laboratory point-camera angle in pair image points and allows the comparison of the LPSE and LPPE in determining the laboratory point in greatest error.

2.4 Test data.

For the purposes of investigating the use of conjugate imagery in the automated reproduction of three dimensional coordinates, it was necessary to produce camera coordinate data with known error inherent in it. This was achieved by first producing camera coordinate data of zero error and then introducing small random errors of appropriate magnitude to all camera image coordinate data. The test data were produced mathemtically by first defining camera perspective centres, principal axis and principal distances, as well as laboratory points. Then image planes and respective image points could be calculated as described below. The zero error test data are presented in Appendix II. Test data were then produced with an introduced error of 0.18%, 0.35%, 0.53% and 0.7% respectively. In this study all percentage errors in camera image data have been expressed as a percentage of the maximum diagonal distance across the camera image. This means that if a camera image scale measured 100 units from bottom right to top left, then the size of the 0.18% introduced error would be 0.18 of a unit. The test data produced will have known introduced error, known laboratory points and known respective conjugate image points.

The experimental configuration consisted of eight cameras encircling the test area (see Appendix II, Figure 20). One walking trial was video-taped with the subject having 55 marker points attached to various limb segements as follows: five markers on the pelvis, eight on each thigh and shank, four on each foot, two on each knee and six additional markers on the upper extremities. The markers on the pelvis were right and left greater trochanter, right and left superior anterior iliac spines and posterior saccrum. The markers on the knee were medial and lateral condyles of the femur and markers on the ankle were the medial and lateral malleolus. The markers on the foot were placed over the 1st and 5th metatarsal/phalangeal joint. Markers on the upper extremity were placed at the shoulder, elbow and wrist joints. The remaining 32 markers were placed on the thigh and shank with three anterior, two lateral and three posterior to each segment. In the construction of the test data a global axes system and a test area were defined, in which eight arbitrary points were chosen for the location of each camera perspective centre. For convenience, the principal axes of all cameras were directed at the same

central point in the test area. An arbitary camera principal distance was chosen, in this case 10 cm. Each camera's image plane was then defined by a unit vector along the camera principal axis and a point located on the principal axis at the principal distance from the camera perspective centre.

$$uXi = \frac{(cXi - oX)}{\sqrt{(cXi - oX)^2 + (cYi - oY)^2 + (cZi - oZ)^2}} \qquad (2.4.1)$$

$$uYi = \frac{(cYi - oY)}{\sqrt{(cXi - oX)^2 + (cYi - oY)^2 + (cZi - oZ)^2}} \qquad (2.4.2)$$

$$uZi = \frac{(cZi - oZ)}{\sqrt{(cXi - oX)^2 + (cYi - oY)^2 + (cZi - oZ)^2}} \qquad (2.4.3)$$

where:

uXi, uYi, uZi = unit vector along principle axis of camera i;
oX, oY, oZ = coordinates of central point in test area;
cXi, cYi, cZi = coordinates of perspective centre of camera i.

The coordinates of the principal point on the image plane is give by:

$$pXi = cXi + f.uXi, \qquad (2.4.4)$$

$$pYi = cYi + f.uYi, \qquad (2.4.5)$$

$$pZi = cZi + f.uZi. \qquad (2.4.6)$$

where:

pXi, pYi, pZi = coordinates of principle point on image plane of camera i;
f = principal distance of camera i.

The camera image coordinates of the eight arbitrary points located in laboratory space can now be calculated as the intersection of a line with a plane. This line is the collinear

line for each laboratory point, all of which pass through the perspective centre of each respective camera. The parametric equation of each collinear line is:

$$X = cXi + t.uXij, \qquad (2.4.7)$$

$$Y = cYi + t.uYij, \qquad (2.4.8)$$

$$Z = cZi + t.uZij. \qquad (2.4.9)$$

where:

t = parameter determining a point on line;
X, Y, Z = coordinates of a point on line;
uXij, uYij, uZij = unit vector from camera perspective centre i to arbitrary laboratory point j.

The equation of each camera image plane is:

$$uXi.(X - pXi) + uYi.(Y - pYi) + uZi.(Z - pZi) = 0. \qquad (2.4.10)$$

By substitution of equations (2.4.7), (2.4.8) and (2.4.9) into (2.4.10) and on rearranging gives:

$$t_{ij} = \frac{uXi.pXi - uXi.cXi + uYi.pYi - uYi.cYi + uZi.pZi - uZi.cZi}{uXi.uXij + uYi.uYij + uZi.uZij} \qquad (2.4.11)$$

For a given camera image plane (i) with known coordinates of the principal point and perspective centre a value of t_{ij} can be calculated for a given point in laboratory space (X_j, Y_j, Z_j). By placing the calculated parameter t_{ij} for each respective point (j) and camera (i) in the equations (2.4.7), (2.4.8) and (2.4.9) for the respective collinear lines, the laboratory point coordinates for that image point were calculated. These coordinates were relative to the laboratory axis and were transformed to the image plane axis by a coordinate transformation. For this transformation the axes of the camera image plane needed to be calculated (Figure 13). The image plane $\bar{r}$ axis is directed along the

camera principal axis and is therefore already defined. It is assumed that one rotation was required about the image plane $\bar{s}$ axis to bring the image plane $\bar{r}$ axis from the horizontal laboratory plane into alignment with the principal axes of the camera (Figure 12). By this definition the $\bar{s}$ axis was perpendicular to both the vertical laboratory $\bar{k}$ axis and the image plane $\bar{r}$ axis, with $\bar{r}$, $\bar{s}$ and $\bar{t}$ axes given by:

$$\bar{r}_i = (uXi, uYi, uZi). \qquad (2.4.12)$$

$$\begin{aligned} \bar{s}_i &= \bar{k} \times \bar{r}_i, \\ &= (0, 0, 1) \times (uXi, uYi, uZi), \\ &= (-uYi, uXi, 0). \end{aligned} \qquad (2.4.13)$$

$$\begin{aligned} \bar{t}_i &= \bar{r}_i \times \bar{s}_i, \\ &= (uXi, uYi, uZi) \times (-uYi, uXi, 0), \\ &= (-uZi.uXi, -uZi.uYi, uXi^2 + uYi^2). \end{aligned} \qquad (2.4.14)$$

where:

x = vector cross product.

$\bar{r}_i$, $\bar{s}_i$, $\bar{t}_i$ = axis system of camera plane i.

Figure 13. Camera image plane axes.

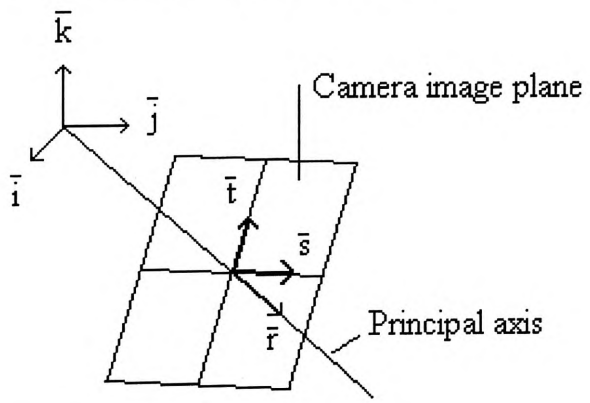

Key

$\bar{i}, \bar{j}, \bar{k}$ = laboratory axes

$\bar{r}, \bar{s}, \bar{t}$ = image plane axes

With the image plane axes origin located at the principal point of the image plane, the location of the laboratory axis origin relative to the image plane coordinate system is given by:

$$\begin{bmatrix} oRi \\ oSi \\ oTi \end{bmatrix} = \begin{bmatrix} r_{1i} & r_{2i} & r_{3i} \\ s_{1i} & s_{2i} & s_{3i} \\ t_{1i} & t_{2i} & t_{3i} \end{bmatrix} \begin{bmatrix} -pXi \\ -pYi \\ -pZi \end{bmatrix} \qquad (2.4.15)$$

where:

oRi, oSi, oTi = origin of laboratory axes relative to image coordinates of camera i.

r_{1i}, r_{2i}, r_{3i} = vector components of image plane axis $\bar{r}_i$ of camera i.

s_{1i}, s_{2i}, s_{3i} = vector components of image plane axis $\bar{s}_i$ of camera i.

t_{1i}, t_{2i}, t_{3i} = vector components of image plane axis $\bar{t}_i$ of camera i.

The transformation from laboratory coordinates to image plane coordinates of camera (i) is:

$$\begin{bmatrix} Ri \\ Si \\ Ti \end{bmatrix} = \begin{bmatrix} oRi & r_{1i} & r_{2i} & r_{3i} \\ oSi & s_{1i} & s_{2i} & s_{3i} \\ oTi & t_{1i} & t_{2i} & t_{3i} \end{bmatrix} \begin{bmatrix} 1 \\ X \\ Y \\ Z \end{bmatrix} \qquad (2.4.16)$$

The laboratory space coordinates giving the intersection of the collinear lines with camera image plane, equations (2.4.11), (2.4.7) (2.4.8) and (2.4.9) can now be transformed into respective image plane coordinates, as given in equation (2.4.16).

The eight arbitrary points previously defined in laboratory space form the camera calibration points. From the image coordinates obtained for the respective calibration points the DLT parameters were calculated for each camera (see Section 2.3.1). Laboratory space coordinate data were then directly transformed to camera image data via the DLT equations. The accuracy of the calculated data for the eight cameras can be

measured by the LPE, LPSE and CPE. The maximum error in reproducing three dimensional coordinates (LPE) from two camera image points was 0.000069 m. at a camera-point-camera angle of 2.96 radians. The greatest conjugate point distance error (CPE) was 0.000229 units in a camera view of 50 units x 50 units. The maximum lab point standard error (LPSE) was 0.000003 m. The zero error test data are presented in Appendix II.

2.5 Three dimensional reproduction algorithm.

The approach to automated reproduction of three dimensional points from multiple camera images can be split into three main stages. They cover the generation of three dimensional points and the processes of establishing conjugate image points from the all the valid image points collected. A schematic out line of the algorithm is presented in Appendix III.

2.5.1 Three dimensional point generation.

This involved the generation of all possible valid laboratory points based on the criterion measures by systematically selecting and comparing camera image points. The process constructs laboratory points of multiple camera image points with the aim being to ensure that the actual laboratory points are amongst those laboratory points generated. No attempt was made at this stage to overcome the problems of excessive numbers of valid laboratory points and laboratory points sharing common image points.

The algorithm iterated through the camera coordinate data of the camera (arbitarily assigned as the "main camera") and used conjugate imaging techniques to match image points in successive search cameras. The cameras searched for a given main camera were those that lay within an arc of 120 degrees of the main camera and had not previously been used as a main camera. On the first iteration a camera which had been previously used as a search camera was not repeated as a main camera. The algorithm iterated through the cameras a second time, this time only cameras that had been previously used as a search camera were used as a main camera and only points in those

cameras which had not been matched with other camera image points were used. The search cameras on the second pass were again those cameras which lay within an arc of 120 degrees of the main camera and had not previously been used as a main camera. The algorithm continued until no more main cameras could be defined.

For any given main camera and image point in the search process, all camera images that were within the CPE of their respective search cameras points were returned. When each new camera image point was collected for a main image point it could be combined with an image point already collected from a previous camera search if the normalised distance between respective laboratory points was less than LPE and the resultant multi-image point satisfied the LPSE and LPPE. If the collected image point satisfied the criteria for more than one set of previously collected image points then it was combined with the set that would produce the lowest LPSE and LPPE. After the search of all possible cameras a given image point in the main camera may be associated with any number of laboratory points. If for a given main image point there was at least one laboratory point which had been formed from three or greater camera image points, then all laboratory points formed from two camera image points were automatically deleted.

When each main camera has collected all valid laboratory points for its respective image points, these were combined with those collected from previous main cameras. Each laboratory point was compared in turn with those previously collected and if the normalised distance was less than CPE, there were no uncommon image points and the criteria LPSE and LPPE were met, then the image points were combined. In this way multiple camera laboratory points were built up.

At the completion of three dimensional point generation a large proportion of the valid laboratory points collected were in error due to the large numbers of common image points shared amongst the generated laboratory points. It was also evident that the majority of laboratory points were of two camera image points and progressively fewer were of three or more camera image points. The greater number of laboratory points generated from two camera images was also due to the lower likelihood of the

coincidental alignment of unrelated image points in greater numbers of cameras that also meet the criterion values.

2.5.2 Three dimensional point reduction : amongst object points of multiple image points.

Multiple image point reduction resolved errors due to image points being shared amongst laboratory points associated with three or more camera image points. Laboratory points associated with greater than two camera image points had all four criteria measures available and therefore decisions as to the validity of conjugate image points could be made with more certainty.

The algorithm searched only laboratory points consisting of three or more image points for image points that were in common. If only one image point was in common and the distance between the laboratory points was greater than the LPE then they were separated. If one point was in common and the distance was less than the LPE, or there was more than one image point in common, then they were combined. The process of separating or combining laboratory points first assumed that certain image points were correct. These were either single and uncommon image points in laboratory point separation or common image points in laboratory point combination. An iterative process then proceeded to determine the validity of all remaining image points. In combining laboratory points, all image points in doubt were added sequentially. If the combined laboratory point met the LPSE and LPPE criteria then the image point was kept, otherwise it was removed. In separating laboratory points, all image points in doubt were compared against both laboratory points. The image point remained with the laboratory point in which the lowest LPSE and LPPE values were produced.

At the completion of this stage of laboratory point reduction, all laboratory points consisting of greater than three image points should have had no image points in common with any other laboratory point of greater than three image points. The image points associated with laboratory points consisting of greater than three image points could therefore be considered conjugate image points.

2.5.3 Three dimensional point reduction : amongst object points of paired image points.

Paired image point reduction involved laboratory point reduction amongst laboratory points consisting of two camera image points. In laboratory points associated with only two camera image points, the LPSE and LPPE were not available, which greatly reduced the ability to determine the validity conjugate image points. The generation process also tended to produce a larger number of erroneous laboratory points of paired camera image points due to the increased chance of two unrelated collinear lines intersecting as opposed to three or more unrelated collinear lines. This stage had two steps: firstly the elimination of all laboratory points associated with two image points that had an image point in common with a laboratory point consisting of three or more conjugate image points; the second step was laboratory point reduction amongst laboratory points associated with two camera image points.

The algorithm for the reduction amongst laboratory points consisting of two image points relied on comparing the links between the laboratory points and on individual epipolar line errors. To enable an epipolar line error to be compared across different cameras each measure was normalised. Normalisation was done by subtracting the mean CPE from the measured value and dividing by the standard deviation of the CPE for the respective camera. The means and standard deviations of the CPE were established as part of the camera calibration procedure as required for the calculation of the criterion CPE for each camera.

2.5.4 Algorithm summary.

The automated reproduction of three dimensional coordinate from multiple camera images was achieved by the systematic generation of all valid laboratory points followed by the systematic reduction of erroneous image points to arrive at the set of laboratory points. The outcome of the process relied on evaluation of four criteria measures (CPE, LPSE, LPPE and LPE) to establish controls in the generation of

laboratory points and to enable comparisons to be made between laboratory points to eliminate erroneous image points. The results of the automated reproduction of three dimensional coordinates was a set of laboratory points with matched conjugate image points generated from two dimensional image coordinate data taken from each camera.

3.0 RESULTS

3.1 Lab Point Error

The Lab Point Error (LPE) for three dimensional coordinates reproduced from various camera combinations ranging from three to eight camera images are presented in Tables 5 - 8. Each table represents a different magnitude of error introduced to the camera image coordinates. These errors were 0.18%, 0.35%, 0.53% and 0.7% respectively.

Table 5. Lab Point Error, with 0.18% introduced error in camera image data.

Cameras	N	Mean (m)	Std.Dev. (m)	Minimum (m)	Maximum (m)
3	128	.001441	.000675	.000311	.003309
4	128	.001252	.000605	.000132	.002849
5	80	.001037	.000409	.000182	.002142
6	80	.000904	.000344	.000143	.001632
7	40	.000754	.000258	.000253	.001275
8	8	.000705	.000223	.000362	.000928

Table 6. Lab Point Error with 0.35% introduced error in camera image data.

Cameras	N	Mean (m)	Std.Dev. (m)	Minimum (m)	Maximum (m)
3	128	.003708	.001689	.000770	.007379
4	128	.003522	.001640	.000417	.007043
5	80	.002513	.001238	.000852	.005930
6	80	.001914	.000821	.000365	.004229
7	40	.001976	.000839	.000468	.003843
8	8	.001369	.000815	.000330	.002646

Table 7. Lab Point Error with 0.53% introduced error in camera image data.

Cameras	N	Mean (m)	Std.Dev. (m)	Minimum (m)	Maximum (m)
3	128	.006986	.003008	.001173	.019506
4	128	.005613	.002702	.001723	.014262
5	80	.004790	.002103	.001030	.011038
6	80	.004287	.002003	.000712	.009283
7	40	.003964	.001658	.000744	.008112
8	8	.003663	.001946	.000441	.006391

Table 8. Lab Point Error with 0.70% introduced error in camera image data.

Cameras	N	Mean (m)	Std.Dev. (m)	Minimum (m)	Maximum (m)
3	128	.008365	.003219	.001889	.018254
4	128	.007360	.002971	.000955	.014368
5	80	.006747	.002634	.001102	.014085
6	80	.006286	.002115	.002240	.011203
7	40	.005783	.001996	.001902	.008994
8	8	.005563	.001811	.002817	.008351

Several trends can be seen in the relationship between LPE, the number of cameras and the accuracy of image data. A reduction in the mean, standard deviation and maximum LPE was observed over the four image coordinate error levels when the number of cameras was systematically increased from three to eight cameras. This trend of continued improvement in LPE was still present in eight cameras at the 0.18 % image coordinate error level. The significance of the improvement in laboratory point accuracy depended on the number of cameras used. When increasing the number of cameras from three to four the mean LPE did not decrease significantly in any of the four image coordinate error levels at the 95% confidence level (Table 9). However the use of five or more cameras saw a significant ($p < 0.05$) improvement

in LPE over the use of three cameras. Similarly, the use of six or more cameras saw a significant ($p < 0.05$) improvement in LPE over the use of four cameras for the 0.18%, 0.35% and 0.53% image coordinate error levels. There were no significant improvements in LPE beyond the use of five cameras in any of the four image coordinate error levels.

Table 9. Lab Point Error analysis of variance between cameras.

Introduced Error	F-value	P-value	Homogeneous Subsets * (camera combinations)
0.18%	18.2384	0.0000	(8-7-6-5)(5-4)(4-3)
0.35%	27.6223	0.0000	(8-7-6-5)(4-3)
0.53%	17.8971	0.0000	(8-7-6-5)(5-4)(4-3)
0.7%	9.4296	0.0000	(8-7-6-5)(7-6-5-4)(5-4-3)

* Analysis of variance was done with $\alpha = 0.05$. Post-hoc analysis of individual differences was with a Bonferroni adjustment for α. In each subset the highest and lowest means were not significantly different. The number of cameras used to reproduce a laboratory point are listed from lowest to highest LPE.

The rate of change of the mean LPE generally decreased when the number cameras was systematically increased from three to eight cameras in each of the four error levels. The expected diminishing improvements in mean LPE was clearly demonstrated in the 0.53% image error data, with mean LPE improving by 1.373 mm, 0.823 mm, 0.503 mm, 0.323 mm and 0.301 mm respectively as camera numbers were sequentially increased from three to eight. The general trend, as opposed to a significant change, towards a decreasing rate of change of mean LPE with increasing camera numbers may have been due to the small and non-significant decreases in mean LPE when introducing just one additional camera.

A doubling of the introduced error from 0.18% to 0.35% saw an increase in the mean LPE by a factor of 2.53. A further doubling of the introduced error from 0.35% to 0.70% again saw a similar (factor of 2.54) increase in the mean LPE. Further partialling of this result showed an increase in LPE by a factor of 1.89 when introduced error was increased by fifty percent from 0.35% to 0.53%. These proportionally larger increases in mean LPE were not maintained with the remaining one third increase in introduced error from 0.53% to 0.70%, which resulted in a similar factor of 1.34 (one third) increase in mean LPE.

The trends of the maximum LPE mirrored those of the mean LPE in terms of rate of decrease with increasing camera numbers and proportional increases with respect to increasing magnitude of introduced error. For comparison, the corresponding decreases in maximum LPE for the 0.53% error level were 5.244 mm, 3.224 mm, 1.755 mm 1.171 mm and 1.721 mm as camera numbers increased from three through to eight respectively whereas the proportional increases in maximum LPE between the 0.18%, 0.35%, 0.53% and 0.70% error levels were 2.53, 2.211 and 1.082 respectively.

3.1.1 Lab Point Error and two camera image points.

The Lab Point Error (LPE) for three dimensional coordinates reproduced from two camera images for the image coordinate error level of 0.35% is presented in Table 10. Relatively large variations occurred in the accuracy of two camera laboratory points (mean = 0.007507 m ± 0.007461 m, Table 10) as opposed to the LPE for laboratory points consisting of three or more camera image points (see Table 6). An important relationship between LPE and camera configuration became apparent when analysing the variation between the LPE of different paired camera combinations (Tables 10 and Table 11). With eight cameras, use of the four diagonally opposite camera pairs (c3c7, c2c6, c4c8, c1c5) resulted in a significantly larger LPE than all other camera combinations. One obtuse camera angle combination (c1c6) had a significantly larger LPE than all camera pairs positioned at

90°. Conversely, one acute camera angle combination (c3c4) had a significantly larger LPE than all but one right angle camera combination. The remaining significant differences were produced by four acute/obtuse camera angle combinations (c3c4, c3c6, c2c7, c6c7, c1c8) which had significantly higher LPE than only the more accurate right angle camera combinations. The eighteen lowest LPE camera combinations were not significantly different and the trend was for the right angle camera combinations to have the lowest LPE while only two acute/obtuse camera angle combinations (c4c7, c1c2) had a lower LPE than any right angle camera combination (c6c8, c2c8, c5c7, c3c5, c2c4, c4c6, c1c3, c1c7).

Table 10. Lab Point Error for laboratory points reproduced from paired camera image points, with 0.35% introduced error in camera image data.

Cameras*	N	Mean (m)	Std.Dev. (m)	Minimum (m)	Maximum (m)
c1-c2	160	.004655	.002021	.000693	.009603
c1-c3	168	.004706	.001730	.001235	.009366
c1-c4	128	.005544	.002462	.001014	.012785
c1-c5	160	.014930	.008140	.001103	.034685
c1-c6	136	.008055	.005573	.000952	.018706
c1-c7	160	.005034	.001654	.000556	.008918
c1-c8	144	.006074	.003421	.000996	.013990
c2-c3	160	.005644	.002362	.000598	.010612
c2-c4	136	.004406	.001818	.000714	.008618
c2-c5	144	.005633	.002879	.000677	.011439
c2-c6	168	.019582	.014749	.000543	.049288
c2-c7	112	.006515	.003180	.002023	.014349
c2-c8	144	.003758	.001421	.000276	.007069
c3-c4	152	.007184	.003510	.001494	.014898
c3-c5	192	.004381	.001460	.001078	.007480
c3-c6	160	.006548	.003625	.000465	.014885
c3-c7	168	.025356	.014831	.000487	.053091
c3-c8	128	.005404	.001639	.000268	.011570
c4-c5	152	.005677	.002905	.001340	.012390
c4-c6	152	.004613	.002161	.000835	.008648
c4-c7	112	.004543	.001340	.001270	.007881
c4-c8	152	.017982	.004714	.006174	.028716
c5-c6	176	.005584	.002021	.001533	.010947
c5-c7	152	.003810	.001261	.000423	.007083

Table 10. cont.

Cameras*	N	Mean (m)	Std.Dev. (m)	Minimum (m)	Maximum (m)
c5-c8	144	.005227	.002081	.000742	.011387
c6-c7	136	.006079	.002241	.001344	.011966
c6-c8	160	.003745	.002220	.000143	.008742
c7-c8	160	.005544	.002715	.000504	.012150
all pairs	4261	.007507	.007461	.000143	.053091

* See Appendix II for camera configuration and numbering.

Table 11. Lab Point Error analysis of variance between camera pairs with 0.35% introduced error in camera image data.

Homogeneous Subsets * (F-value 175.1836, P-value 0.0000)
(c6c8,c2c8,c5c7,c3c5,c2c4,c4c7,c4c6,c1c2,c1c3,c1c7,c5c8,c3c8,c1c4,c7c8,c5c6,c2c5,c2c3,c4c5)
(c5c7,c3c5,c2c4,c4c7,c4c6,c1c2,c1c3,c1c7,c5c8,c3c8,c1c4,c7c8,c5c6,c2c5,c2c3,c4c5,c1c8,c6c7)
(c3c5,c2c4,c4c7,c4c6,c1c2,c1c3,c1c7,c5c8,c3c8,c1c4,c7c8,c5c6,c2c5,c2c3,c4c5,c1c8,c6c7,c2c7)
(c2c4,c4c7,c4c6,c1c2,c1c3,c1c7,c5c8,c3c8,c1c4,c7c8,c5c6,c2c5,c2c3,c4c5,c1c8,c6c7,c2c7,c3c6)
(c1c7,c5c8,c3c8,c1c4,c7c8,c5c6,c2c5,c2c3,c4c5,c1c8,c6c7,c2c7,c3c6,c3c4)
(c1c8,c6c7,c2c7,c3c6,c3c4,c1c6)
(c1c5)
(c4c8,c2c6)
(c3,c7)

* Analysis of variance was done with $\alpha = 0.05$. Post-hoc analysis of individual differences was with a Bonferroni adjustment for α. In each subset the highest and lowest means were not significantly different. Camera pairs used to reproduce a laboratory point are listed from lowest to highest LPE. See Appendix II for camera configuration and numbering.

3.1.2 Lab Point Error and camera to laboratory point angle.

The Lab Point Error (LPE) in three dimensional coordinates for varying camera-laboratory point-camera angles reproduced from two camera images are presented graphically in Figure 14. The figure represents four different magnitudes of

Figure 14) Paired conjugate image points; angle and Lab Point Error.

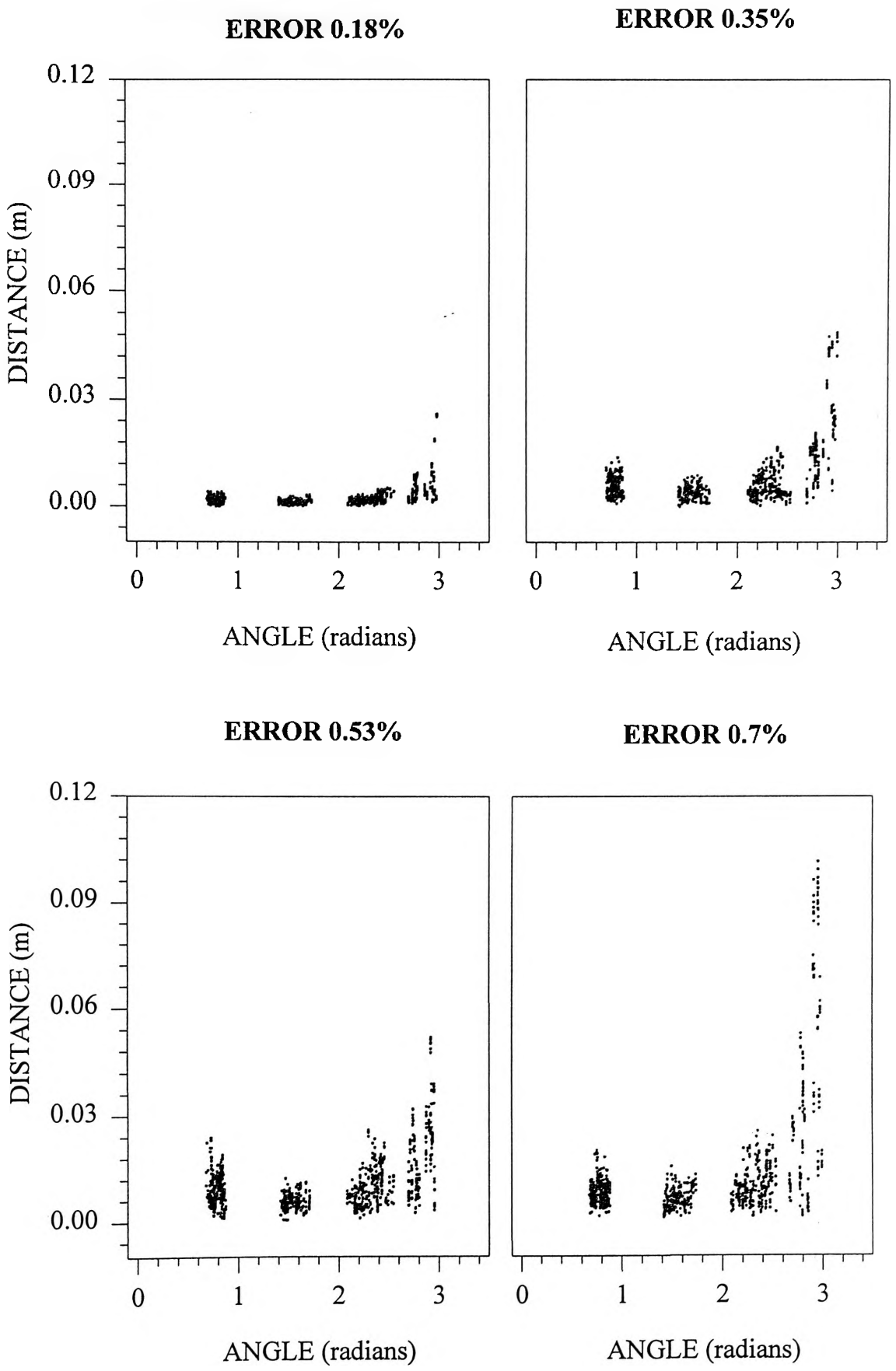

error (0.18%, 0.35%, 0.53% and 0.7% respectively) introduced into the camera image coordinates. The accuracy of reproducing three dimensional coordinates from two cameras was clearly dependent on the camera-laboratory point-camera angle. The relationship between LPE and camera-laboratory point-camera angle can be crudely represented by a second degree polynomial with a minimum at 90^{o} and approaching $+\infty$ as the camera-laboratory point-camera angle approaches 0^{o} and 180^{o} (Figure 15). The minimum of the polynomial increased in direct proportion to the error of camera image data: 0.004 m, 0.008 m, 0.012 m and 0.016 m for the 0.18%, 0.35%, 0.53% and 0.70% error levels respectively. With small changes in the camera angle from 90^{o} the error in three dimensional coordinates increased more rapidly with increasing error in camera image data. A normalisation process adjusted all laboratory points reproduced from paired camera image points so that the LPE was equivalent to a 90^{o} camera-laboratory point-camera angle. The normalised Lab Point Error (LPE) for three dimensional coordinates for varying camera-laboratory point-camera angles, reproduced from paired cameras, are presented in graphically in Figure 16. The diagram represented the four different magnitudes of error (0.18%, 0.35%, 0.53% and 0.7% respectively) introduced to the camera image coordinates.

3.2 Lab Point Standard Error.

The non-normalised Lab Point Standard Error (LPSE) for three dimensional coordinates reproduced from three to eight camera images are presented in Tables 12 - 15. The normalised LPSE for three dimensional coordinates reproduced from three to eight camera images are presented in Tables 17 - 20. Each table in the non-normalised and normalised LPSE data represents a different magnitude of error (0.18%, 0.35%, 0.53% and 0.7% respectively) introduced to the image coordinates. The trends observed in the relationship between LPSE the number of cameras and the accuracy of image data are similar to those previously mentioned for LPE.

Figure 15) Normalisation curve; angle and Lab Point Error.

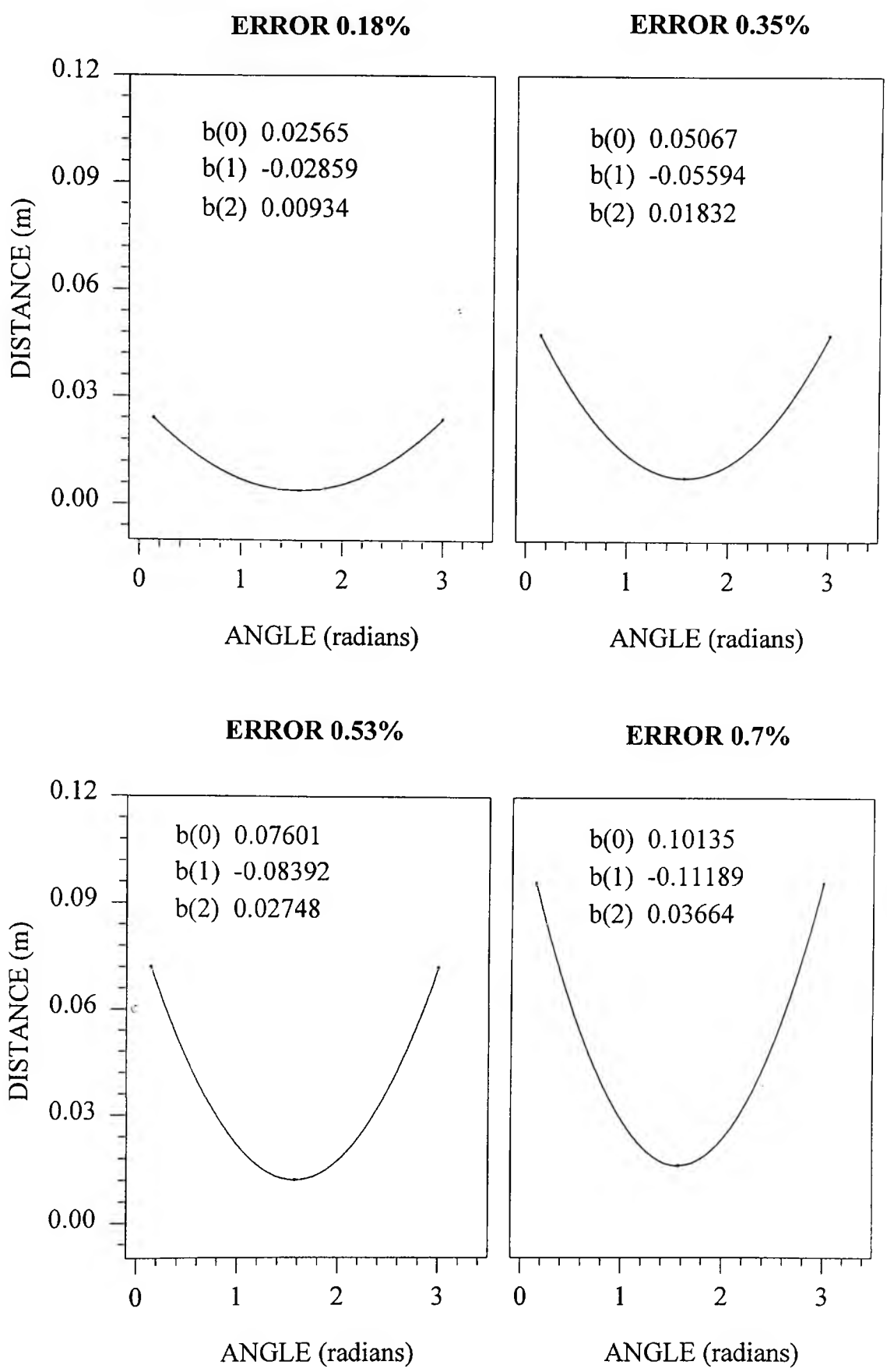

Figure 16) Paired conjugate image points; angle and Normalised Lab Point Error.

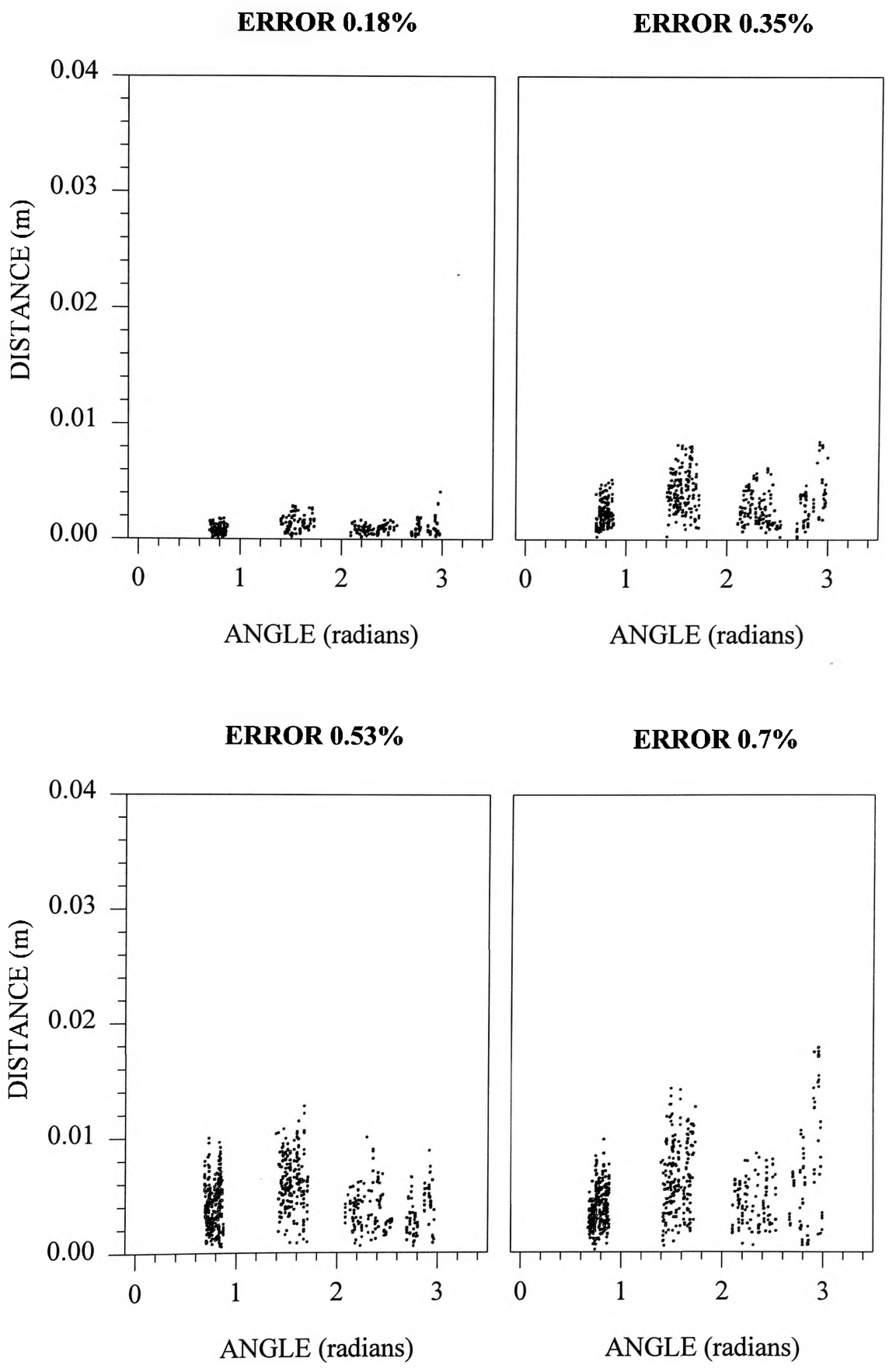

Table 12. Non-normalised Lab Point Standard Error with 0.18% introduced error in camera image data.

Cameras	N	Mean (m)	Std.Dev. (m)	Minimum(m)	Maximum(m)
3	128	.001705	.001642	.000214	.010745
4	128	.001378	.000784	.000308	.004894
5	80	.001129	.000523	.000556	.002964
6	80	.000956	.000384	.000548	.002050
7	40	.000794	.000247	.000548	.001436
8	8	.000679	.000211	.000536	.001123

Table 13. Non-normalised Lab Point Standard Error with 0.35% introduced error in camera image data.

Cameras	N	Mean (m)	Std.Dev. (m)	Minimum(m)	Maximum(m)
3	128	.004874	.004117	.000465	.020562
4	128	.004106	.002389	.000834	.010358
5	80	.003283	.001401	.001279	.007347
6	80	.002792	.000952	.001465	.005333
7	40	.002234	.000703	.001192	.003868
8	8	.001959	.000596	.001261	.003038

Table 14. Non-normalised Lab Point Standard Error with 0.53% introduced error in camera image data.

Cameras	N	Mean (m)	Std.Dev. (m)	Minimum(m)	Maximum(m)
3	128	.005946	.003979	.000618	.020848
4	128	.004782	.001720	.001515	.010667
5	80	.003987	.000943	.002006	.006409
6	80	.003314	.000560	.002200	.004701
7	40	.002748	.000380	.002034	.003452
8	8	.002380	.000246	.002004	.002753

Table 15. Non-normalised Lab Point Standard Error with 0.70% introduced error in camera image data.

Cameras	N	Mean (m)	Std.Dev. (m)	Minimum(m)	Maximum(m)
3	128	.008542	.008175	.001164	.042649
4	128	.007350	.005106	.001506	.021458
5	80	.006080	.002975	.001806	.012792
6	80	.005098	.002040	.001847	.009422
7	40	.004207	.001548	.001455	.006489
8	8	.003622	.001321	.002086	.005389

In both the normalised and non-normalised LPSE, a reduction in the mean, standard deviation and maximum LPSE occurred over the four image coordinate error levels when systematically increasing the number of cameras from three to eight. This trend in the improvement in LPSE was still present in eight cameras at the 0.18% image coordinate error level. The significance of the improvement in laboratory point accuracy depended on the number of cameras used (Tables 16 and 21). These findings are in agreement with those observed for the LPE. In the non-normalised LPSE an increase the number of cameras from three to four did not significantly decrease the mean LPSE at the 0.05 confidence level, for the 0.18%, 0.35% and 0.70% image coordinate error levels (Table 17). In the non-normalised LPSE, five or six cameras were generally needed to produce a significant decrease in mean LPSE. By comparison, for the normalised LPSE an increase in the number of cameras from three to four produced a significant decrease in mean LPSE for all image coordinate error levels. While comparing the improvements for four cameras, the non-normalised LPSE required the use of six to seven cameras to produce a significant decrease in mean LPE in the four image coordinate error levels. For the normalised LPSE an increase in the number of cameras from four to six produced a significant decrease in mean LPSE in the four image coordinate error levels. For both the normalised and non-normalised LPSE no significant improvement in mean LPE was

achieved beyond the use of five cameras to reproduce a three dimensional coordinate in all but one of the four levels of introduced image coordinate error. The one exception to this trend was at the 0.53% error level of the normalised LPSE which saw a decrease in mean LPSE between five to eight cameras.

Table 16. Non-normalised Lab Point Standard Error analysis of variance between cameras.

Introduced Error	F-value	P-value	Homogeneous Subsets * (camera combinations)
0.18%	9.4106	0.0000	(8-7-6-5)(6-5-4)(5-4-3)
0.35%	11.3254	0.0000	(8-7-6-5)(5-4)(4-3)
0.53%	21.0087	0.0000	(8-7-6-5)(5-4)(3)
0.7%	7.4255	0.0000	(8-7-6-5)(6-5-4)(5-4-3)

* Analysis of variance was done with $\alpha = 0.05$. Post-hoc analysis of individual differences was with a Bonferroni adjustment for α. In each subset the highest and lowest means were not significantly different. The number of cameras used to reproduce a laboratory point are listed from lowest to highest LPSE.

Table 17. Normalised Lab Point Standard Error with 0.18% introduced error in camera image data.

Cameras	N	Mean (m)	Std.Dev. (m)	Minimum(m)	Maximum(m)
3	128	.000676	.000341	.000144	.001906
4	128	.000466	.000172	.000131	.000978
5	80	.000392	.000098	.000214	.000649
6	80	.000328	.000063	.000203	.000452
7	40	.000280	.000047	.000198	.000370
8	8	.000241	.000038	.000182	.000291

Table 18. Normalised Lab Point Standard Error with 0.35% introduced error in camera image data.

Cameras	N	Mean (m)	Std.Dev. (m)	Minimum(m)	Maximum(m)
3	128	.002008	.001069	.000212	.004952
4	128	.001364	.000541	.000504	.003012
5	80	.001203	.000367	.000527	.001956
6	80	.001007	.000225	.000485	.001429
7	40	.000840	.000171	.000541	.001129
8	8	.000742	.000153	.000579	.000947

Table 19. Normalised Lab Point Standard Error with 0.53% introduced error in camera image data.

Cameras	N	Mean (m)	Std.Dev. (m)	Minimum(m)	Maximum(m)
3	128	.002613	.001262	.000391	.005873
4	128	.001958	.000587	.000786	.004011
5	80	.001721	.000361	.000987	.002526
6	80	.001396	.000213	.000902	.001917
7	40	.001195	.000157	.000934	.001529
8	8	.001057	.000121	.000869	.001228

Table 20. Normalised Lab Point Standard Error with 0.70% introduced error in camera image data

Cameras	N	Mean (m)	Std.Dev. (m)	Minimum(m)	Maximum(m)
3	128	.003310	.001718	.000714	.009144
4	128	.002263	.000963	.000685	.005783
5	80	.001951	.000634	.000765	.003653
6	80	.001633	.000441	.000781	.002559
7	40	.001361	.000369	.000654	.001933
8	8	.001207	.000322	.000792	.001570

Table 21. Normalised Lab Point Standard Error analysis of variance between cameras.

Introduced Error	F-value	P-value	Homogeneous Subsets * (camera combinations)
0.18%	43.7630	0.0000	(8-7-6-5)(5-4)(3)
0.35%	36.5057	0.0000	(8-7-6-5)(5-4)(3)
0.53%	39.9139	0.0000	(8-7-6)(6-5)(5-4)(3)
0.7%	37.0754	0.0000	(8-7-6-5)(5-4)(3)

* Analysis of variance was done with $\alpha = 0.05$. Post-hoc analysis of individual differences was with a Bonferroni adjustment for α. In each subset the highest and lowest means were not significantly different. The number of cameras used to reproduce a laboratory point are listed from lowest to highest normalised LPSE.

The rate of change of the mean LPSE for both the normalised and non-normalised LPSE generally decreased with increasing camera numbers from three to eight cameras in each of the four error levels. The expected diminishing improvements in mean LPSE were demonstrated more clearly than that observed in the LPE. The improvements in the 0.53% image error level for the non-normalised mean LPE were 1.164 mm, 0.795 mm, 0.673 mm, 0.566 mm and 0.368 mm respectively as camera numbers increased from three to eight. The corresponding improvements in normalised mean LPSE were 0.655 mm, 0.237 mm, 0.325 mm, 0.201 mm and 0.138 mm respectively as camera numbers increased from three to eight. As mentioned with regard to LPE, variations in the rate of change of the mean LPSE indicated a general trend towards improvement as camera numbers were increased due to the small and generally non-significant decreases in mean LPSE when introducing just one additional camera.

A doubling of the introduced error from 0.18% to 0.35% saw relatively greater increases in both non-normalised and normalised mean LPSE by factors of 2.91 and 2.99 respectively. A further doubling of the introduced error from 0.35% to 0.70%, saw a similar 1.81 increase in the non-normalised mean LPSE, but a slightly reduced

1.64 increase in the normalised mean LPSE. A one half increase in introduced error from 0.35% to 0.53%, saw a smaller increase of 1.20 for the non-normalised mean LPSE and a similar 1.39 increase for the normalised mean LPSE. The remaining increase in introduced error from 0.53% to 0.70%, resulted in a slightly greater (1.51) increase in non-normalised mean LPSE and a similar (1.18) increase in normalised mean LPSE. These data show that, apart from the initial similar increases in non-normalised and normalised mean LPSE, the normalised mean LPSE followed the relative increases in image point error more closely than the non-normalised mean LPSE.

With regard to rate of decrease with increasing camera numbers and proportional increases with respect to increasing magnitude of introduced error the trends in the normalised and non-normalised maximum LPSE mirrored those of the respective mean LPSE. By way of comparison, the corresponding decreases at the 0.53% error level of the non-normalised maximum LPSE were 10.181 mm, 4.258 mm, 1.708 mm 1.249 mm and 0.699 mm respectively as camera numbers increased from three to eight and for the normalised maximum LPSE were 1.862 mm, 1.485 mm, 0.609 mm, 0.388 mm and 0.301 mm respectively. The proportional increases between the 0.18%, 0.35%, 0.53% and 0.70% error levels for the non-normalised maximum LPE were 2.27, 0.96 and 2.00 and for the normalised maximum LPE were 2.95, 1.29 and 1.44 respectively.

3.3 Conjugate Point Error.

The Conjugate Point Error (CPE) for two dimensional image coordinates in each of the eight cameras are presented in Tables 22 - 25. Each table represents an error of 0.18%, 0.35%, 0.53% and 0.7% respectively introduced to the image coordinates. Several trends can be seen in the relationship between CPE, the number of cameras and the accuracy of image data.

Table 22. Conjugate Point Error with 0.18% introduced error in camera image data.

Camera	N	Mean (m)	Std.Dev. (m)	Minimum(m)	Maximum(m)
1	56	.014121	.013535	.000600	.050100
2	56	.021375	.010425	.002700	.051200
3	56	.016100	.014972	.000000	.066900
4	56	.018745	.015628	.000200	.055000
5	56	.027189	.019587	.001400	.064300
6	56	.024854	.015644	.000200	.060300
7	56	.032196	.016544	.002100	.057000
8	56	.016188	.014161	.000000	.045600

Table 23. Conjugate Point Error with 0.35% introduced error in camera image data.

Camera	N	Mean (m)	Std.Dev. (m)	Minimum(m)	Maximum(m)
1	56	.033621	.023783	.000600	.088800
2	56	.041130	.027116	.000000	.105000
3	56	.031939	.021116	.000900	.084200
4	56	.032380	.024810	.000700	.097200
5	56	.039198	.022835	.003800	.081800
6	56	.043641	.027657	.000800	.108300
7	56	.042623	.028851	.000000	.094000
8	56	.047234	.027886	.002000	.103800

Table 24. Conjugate Point Error with 0.53% introduced error in camera image data.

Camera	N	Mean (m)	Std.Dev. (m)	Minimum(m)	Maximum(m)
1	56	.043511	.032569	.000100	.123900
2	56	.059543	.044056	.002700	.197900
3	56	.053836	.043229	.001700	.156800
4	56	.068680	.047621	.000100	.179100
5	56	.058638	.041589	.002300	.154500
6	56	.095366	.050134	.000600	.207900
7	56	.053654	.038400	.000600	.165800
8	56	.070236	.044977	.001800	.160500

Table 25. Conjugate Point Error with 0.70% introduced error in camera image data.

Camera	N	Mean (m)	Std.Dev. (m)	Minimum(m)	Maximum(m)
1	56	.075414	.055584	.002100	.238200
2	56	.094943	.080181	.002200	.285600
3	56	.091462	.072049	.005700	.256200
4	56	.088412	.055980	.002400	.227600
5	56	.091120	.057526	.000000	.211000
6	56	.086011	.059332	.002700	.242700
7	56	.084339	.063518	.000000	.210700
8	56	.081995	.060281	.002200	.211900

At the largest introduced error of 0.70% there were no significant ($p < 0.05$) differences in the mean CPE among all eight cameras. However as the introduced image point error decreased to 0.18%, the trend was for increasing differentiation in the mean CPE of the different cameras (Table 26). Cameras 1, 3, 4 and 2 were always associated with the smallest mean CPE at the 0.18%, 0.35% and 0.53% error

levels, while camera six was always associated with the largest mean CPE for the 0.18%, 0.35% and 0.53% error levels.

Table 26. Conjugate Point Error; analysis of variance between cameras.

Introduced Error	F-value	P-value	Homogeneous Subsets * (camera combinations)
0.18%	9.5257	0.0000	(1-3-8-4-2)(3-8-4-2-6)(4-2-6-5)(6-5-7)
0.35%	2.7948	0.0074	(3-4-1-5-2-7-6)(4-1-5-2-7-6-8)
0.53%	7.3740	0.0000	(1-7-3-5-2-4)(7-3-5-2-4-8)(8-6)
0.7%	0.5316	0.8107	(1-8-7-6-4-5-3-2)

* Analysis of variance was done with $\alpha = 0.05$. Post-hoc analysis of individual differences was with a Bonferroni adjustment for α. In each subset the highest and lowest means were not significantly different. Each subset contained camera numbers listed from lowest to highest CPE.

A significant ($p < 0.05$) negative correlation was found between CPE and the distance of the camera's perspective centre from the mid laboratory position for the 0.18% and 0.53% error levels (Table 27). The mid laboratory position being the central point relative to the laboratory boundary. The correlation for the 0.35% error level was significant at the 0.058 significance level. An inverse correlation would suggest that some of the differences seen in camera CPE at the 0.18%, 0.35% and 0.53% errors were due to the cameras closer to the central object point having slightly larger CPE or equivalently the cameras further away had slightly reduced CPE. However the small magnitude of the correlation would only sugest a very small explained variance (1%-8%). The relationship between the CPE for two dimensional image coordinates and the camera-laboratory point distance is presented graphically in Figure 17. From Figure 17 the maximum CPE values of the 0.18%, 0.35% and 0.53% error levels also suggest an inverse relationship between maximum CPE and camera distance for these levels of introduced camera image point error.

An increase in the magnitude of the introduced error saw a similar increase in the mean CPE. A doubling of the introduced error from 0.18% to 0.35% saw an increase

Figure 17) Conjugate Point Error and camera distance.

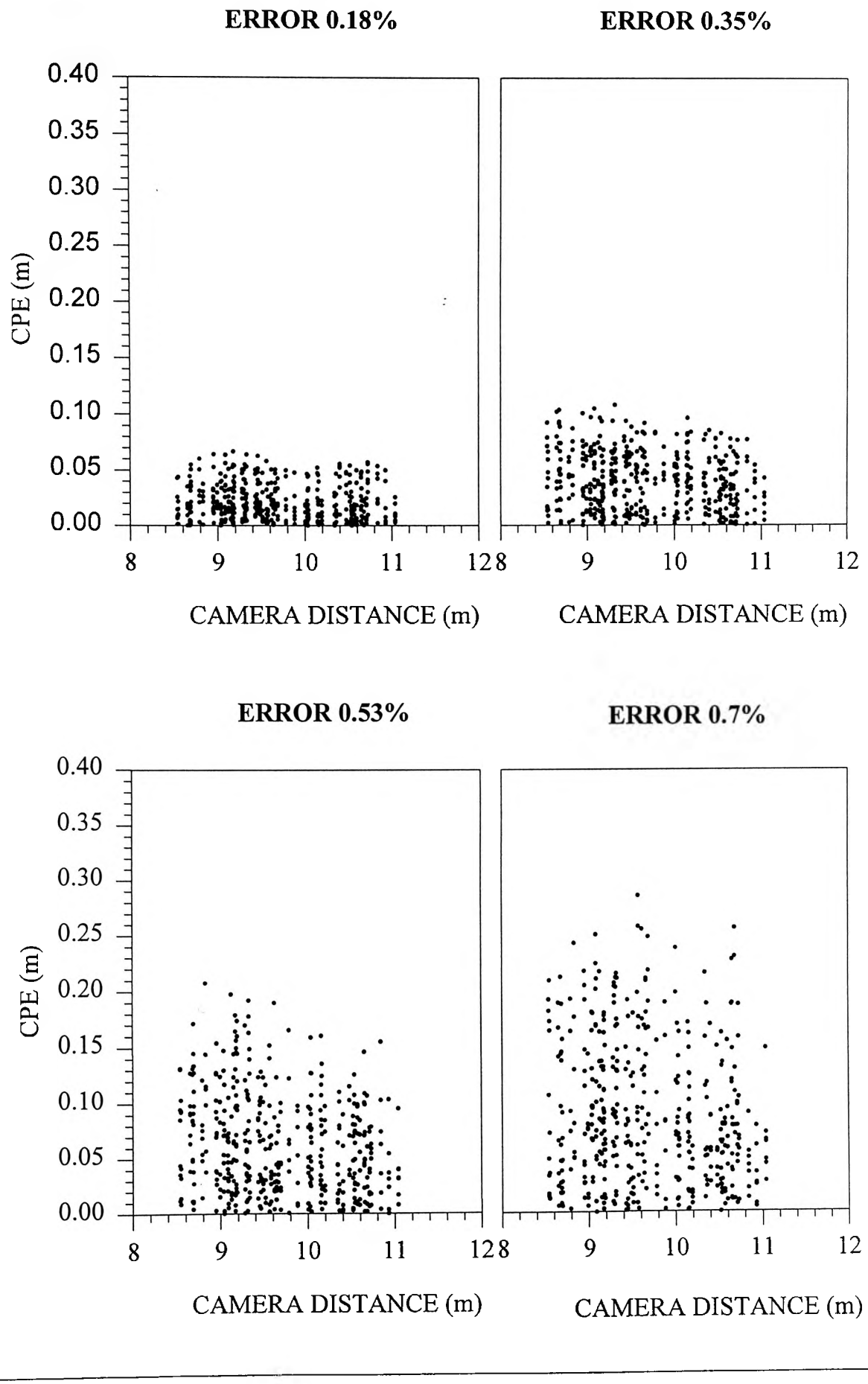

in the mean CPE by a factor of 1.83. A further doubling of the introduced error from 0.35% to 0.70% saw a similar 2.22 increase in the mean CPE. When the introduced error was increased from 0.35% to 0.53 %, the CPE increased by a factor of 1.61. The remaining increase in introduced error from 0.53% to 0.70% resulted in an increase in mean CPE by a factor of 1.37.

Table 27. Conjugate Point Error - distance from camera perspective centre to midpoint in laboratory space.

Camera	Distance*(m)	CPE rank from smallest to largest				
		0.18%	0.35%	0.53%	0.70%	overall
camera 1	10.52	1	3	1	1	1
camera 7	10.11	8	6	2	3	= 4
camera 3	9.83	2	1	3	7	2
camera 4	9.56	4	2	6	5	3
camera 8	9.56	3	8	7	2	= 4
camera 5	9.39	7	4	4	6	6
camera 2	9.37	5	5	5	8	7
camera 6	8.78	6	7	8	4	8
Correlation** (r) Significance level (P)		-.096 (0.042)	-.090 (0.058)	-.284 (0.000)	-.051 (0.284)	

* Distance from camera perspective centre to mid point in laboratory space.
** Correlation between camera distance and CPE, n = 448.

The CPE for two dimensional image coordinates for varying camera-laboratory point-camera angles are presented in graphically in Figure 18. The diagram represents different magnitudes of error introduced to the camera image coordinates, 0.18%, 0.35%, 0.53% and 0.7% respectively. The CPE was not dependent on camera-laboratory point-camera angle.

Figure 18) Conjugate Point Error and angle.

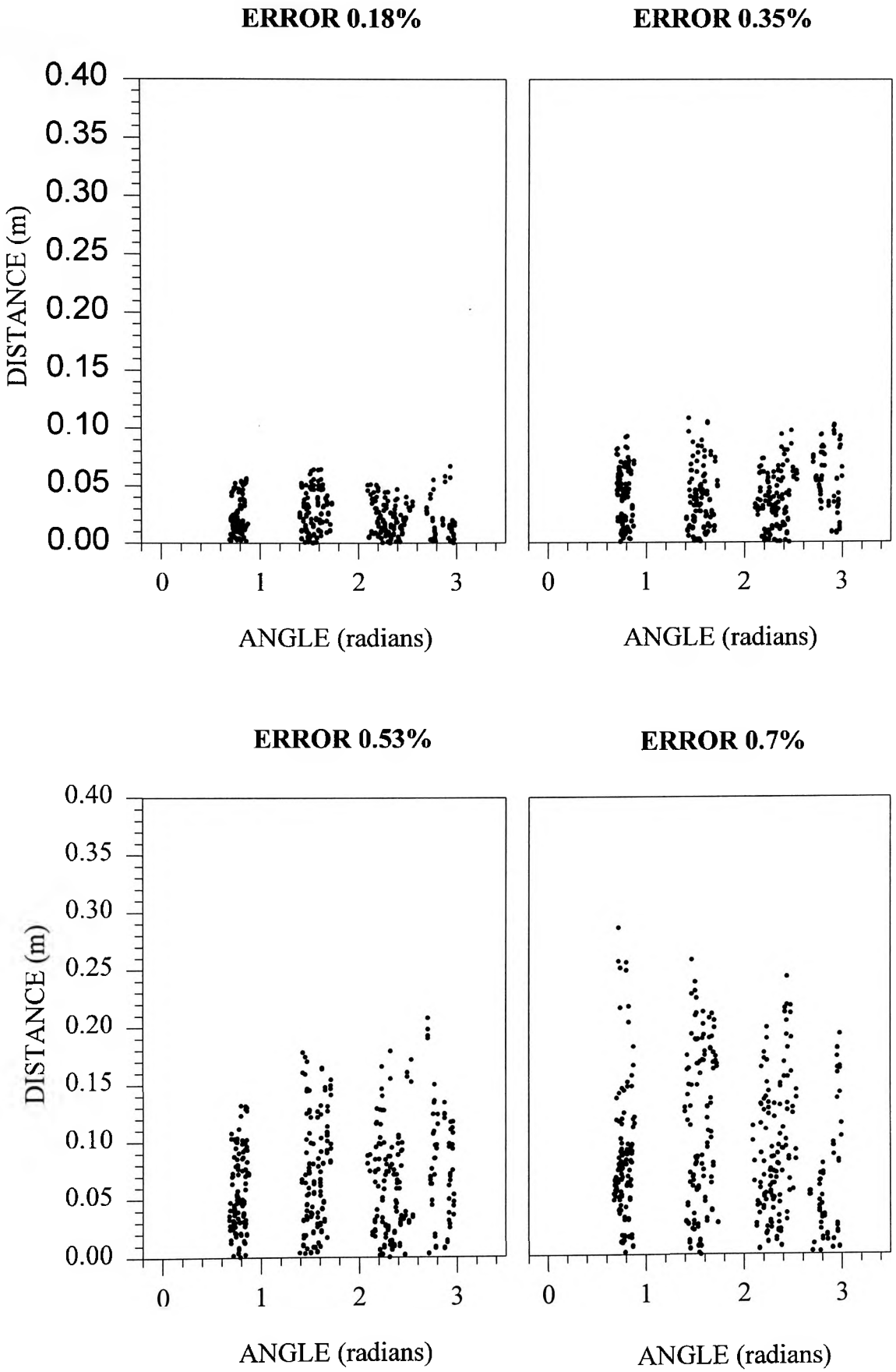

3.4 Reproduction of three dimensional coordinates.

The digitised video data was obtained via the Motion Analysis System's (Motion Analysis Corporation, Santa Rosa, USA) automated video recording and digitisation hardware and software. The digitised coordinate data were then used in the presently presented algorithm for camera calibration and automated three dimensional coordinate reproduction.

The results of the video camera calibration, including DLT parameters, CPE and LPE and presented in Appendix IV. The accuracy of the video test data, as measured by the CPE, non-normalised LPSE and normalised LPSE, are presented in Tables 28 and 29 respectively. In comparison with the test data of 0.18%, 0.35%, 0.53% and 0.70% introduced error levels, the video test data could be considered as having an equivalent accuracy of a 0.2% random error introduced to camera image data. The normalisation of both the LPSE and CPE were carried out using the 0.35% error curve presented in Figure 17. However normalisation by the 0.18% curve produced identical results.

The algorithm was successfull in reproducing the three dimensional coordinates, and respective conjugate image points, of a 55 point marker system viewed in the four cameras. The input into the algorithm being the calibration information (DLT parameters, CPE for each camera, LPSE, LPPE and LPE), and the digitised image coordinate data from a single frame of video data from each of the four cameras. The digitised image data for a single frame is presented in Table 49 in Appendix IV. The output of the algorithm, for this frame of data, is presented in Table 50. Table 50 shows the laboratory points reproduced, the number of image points associated with the respective laboratory point and the number of the image point in each camera. The actual image coordinate and the image point can be found in Table 49, Appendix IV, under the appropriate camera and image point number.

Table 28. Video Camera Conjugate Point Error.

	Image Scale (units)*	Conjugate Point Error	
		mean	Std. Deviation
Camera 1	30 x 40	0.0256	0.0202
Camera 2	30 x 40	0.0291	0.0106
Camera 3	30 x 40	0.0311	0.0130
Camera 4	30 x 40	0.0240	0.0099

* Scale adjusted from 240 x 240 pixels, as presented in Appendix IV, to 30 x 40 units so as to match 0.18%, 0.35%, 0.53% and 0.70% test data.

Table 29. Video Camera Lab Point Standard Error.

Cameras *	Lab Point Standard Error (m)			
	non-normalised		normalised**	
	mean	Std.Deviation	mean	Std.Deviation
3 (1-2-3)	0.0028	0.0010	0.0009	0.0005
3 (1-2-4)	0.0072	0.0083	0.0013	0.0007
3 (1-3-4)	0.0026	0.0017	0.0009	0.0006
3 (2-3-4)	0.0068	0.0083	0.0012	0.0008
4 (1-2-3-4)	0.0036	0.0035	0.0009	0.0003

* Lab Point Standard Error calculated for combinations of three cameras and all four cameras.

** Normalisation using 0.18% and 0.35% normalisation curves for identical results.

4.0 DISCUSSION

The previous chapters have presented a theoretical background to the reproduction of three dimensional image points, the concept and application of conjugate imagery to these procedures and experimental treatment of a data set with systematically introduced error levels. Therefore, the discussion of results will cover four areas:

(i) the general accuracy of a photogrammetric system in relation to the number of cameras, accuracy of image data and stereoscopic configuration;
(ii) the performance of the criterion measures with respect to image point error and the number of cameras and camera configuration;
(iii) the performance of the three dimensional reproduction algorithm; and
(iv) problems and future research.

4.1 Accuracy of three dimensional coordinate reproduction.

The observed reduction in mean, standard deviation and maximum Lab Point Error (LPE) was expected with a systematic increase in the number of cameras from three to eight in each of the four image coordinate error levels. The reduced LPE was due to the fact that each image point contained error and the additional image points improved the least squares approximation of the three dimensional coordinate. Also as expected, the reduction in LPE occurred regardless of the error level or the number of cameras used. However the significance of the improvement in LPE was dependent on the number of cameras used to reproduce the three dimensional coordinate. The advantage of the least squares solution at these error levels was apparent when compared to the large errors due to external camera configuration when reproducing a laboratory point from only two cameras. This will be discussed in more detail in a later section.

The use of three cameras produced a significant improvement in accuracy over the use of two cameras at all four error levels. The present study has shown that to gain a

significant improvement on the use of three cameras in the error range 0.18% to 0.70%, the laboratory point would need to be visible in least five cameras. No significant improvement would be expected with more cameras. The limitation of ensuring that laboratory points were visible in five cameras for maximum accuracy at the current error levels is either impractical or impossible in most cases. Based on an approximate image point error level of 0.18% and the present accuracy of film and video analysis systems, the motion recording protocol should ensure that laboratory points are visible in three cameras for greatest accuracy in the reproduction of three dimensional coordinates. The least squares solution from three camera image points will avoid the inaccuracies associated with reproducing a three dimensional coordinate from two camera images. For highly accurate photogrammetric systems (for example those using metric cameras) it would be expected that no significant improvement in accuracy would be gained beyond the used of two cameras to reproduce a three dimensional coordinate. Also the errors in reproducing a three dimensional point would be comparable to that of three non-metric camera images except in the situation when the two cameras perspective centres and laboratory point are nearly collinear.

A deceasing rate of improvement in both the mean and maximum LPE was expected with increasing numbers of cameras. The decreasing LPE was a result of the error in reproducing a laboratory point tending towards zero as the error in image coordinates approaches zero or the number of cameras approaches infinity. The decreasing LPE was only seen as a trend in the LPE data over the four error levels tested due to the small and non-significant changes in LPE between successive laboratory points reproduced from increasing numbers of cameras.

The use of two image points to reproduce a three dimensional point resulted in large variations in LPE which were dependent on the error of image coordinates and the camera-laboratory point-camera angle. This same dependency on camera angle was expressed by the general formula developed for determining the laboratory point accuracy as a function of image point accuracy, overlap angle and convergence angle

(see Section 1.2.2). Indeterminacy in the calculation of laboratory points from two image points was found to occur in two situations: the first was when the camera-laboratory point-camera angle approached 180^{o} and the two camera perspective centers and the laboratory point lay on the same straight line. The second point of indeterminacy will not occur in practice, but can be approached as the camera-laboratory point-camera angle approaches 0^{o}. The stereometric configuration must therefore avoid points of indeterminacy in the DLT equations caused by the relative positions of laboratory points and cameras.

For a given error in image coordinates the accuracy of reproduced laboratory points improves as the stereoscopic configuration moves further away from points of indeterminacy. The maximum accuracy of reproducing a three dimensional coordinate from two image points was attained at a camera-laboratory point-camera angle of 90^{o}. The experimentally found optimum angle for two cameras was in agreement with the general formulae for stereoscopic configuration and laboratory point accuracy developed in Section 1.2.2. The accuracy attainable at an angle of 90^{o}, and the tolerance of the accuracy to small changes in camera-laboratory point-camera angle, was found to be directly related to the accuracy of digitised image points. Therefore to maintain the level of accuracy in three dimensional coordinates at angles other than 90^{o}, a high level of accuracy of image data is essential.

Based on the results of the present study, the accuracy in reproducing three dimensional coordinates from two non-metric cameras is dependent on maintaining an included angle of approximately 90^{o} between cameras and laboratory points and ensuring the maximum possible accuracy of digitised image data. It should also be noted that the accuracy of photogrammetry with metric cameras is significantly greater than that of video or cinematographic digitisation (see Table 3) and that the magnitude of image errors, LPE and influence of stereometric configuration will be greatly reduced.

The least squares approach of reproducing three dimensional coordinates with three or more cameras images may have produced the comparable rises in both the camera image errors and mean and maximum LPE between the 0.53% and 0.70% error levels. The rise in LPE is in comparison to the relatively greater increases in mean and maximum LPE between the 0.18%, 0.35% and 0.53% error levels. However it would be expected that the error in digitised image data would not approach the 0.70% error level in normal video or cinematographic analysis of motion. For practical purposes, an error in the order of 0.18% in film and video image data would be expected, and the increases in LPE can be considered greater (2 : 2.5) than that of the increases in image data error. The nature of the rise in LPE between zero and 0.35% image error is unclear at this stage, but based on the changes between 0.18% and 0.35% and between 0.35% and 0.53%, errors may be exponential in nature.

4.2 Performance of passpoint criteria.

The Lab Point Standard Error (LPSE), Conjugate Point Error (CPE) and Lab Point Paired Error (LPPE) are discussed in the following sections. The LPE has been discussed in the previous section as part of the accuracy of photogrammetric system and therefore will not be repeated in this section. A valid laboratory point and respective valid image points mean that the image points meet the four criterion measures of the CPE, LPSE, LPPE and LPE. If these valid image points are unique (in that they are not associated with any other laboratory points) then they are considered to be the conjugate image points for the respective laboratory point.

4.2.1 Lab Point Standard Error.

The reduction in the Lab Point Standard Error (LPSE) over the four image coordinate error levels was expected with the systematic increase in number of cameras from three to eight. This reduction occurred for the same reason as noted with the LPE. As was found with the LPE, a reduction in LPSE occurred regardless of the error level or the number of cameras.

The major reason for normalising the LPSE was to improve the ability of the algorithm to evaluate the validity of image points amongst laboratory points which contain the same number of image points. The problem existed because a valid set of three conjugate image points may produce a larger LPSE than an invalid set which shared a common image point. In such a situation, the camera image point in question would be passed to the invalid set based on the non-normalised criteria because the valid set contained a disadvantageous camera-laboratory point-camera angle relative to the invalid set. This situation was seen in the algorithm in the generation of three dimensional points where the valid set may not be collected or may lose an image point to an invalid set in image point reduction. Normalising all paired LPE to 90^{o} in the calculation of the normalised LPSE helped overcome the dependency between angle and reproduced laboratory point and increased the ability to determine the validity of image points. Normalising the LPSE also had the effect of producing greater differentiation between increasing numbers of cameras by removing the extreme errors which resulted from paired image points. The net result of the normalisation was to reduced the magnitude and variability of the normalised LPSE to the effect that there was a significant difference in the normalised LPSE between laboratory points calculated from three and four camera image points. The criterion values of the normalised LPSE, in this case the maximum value the LPSE may take, were calculated for each number of cameras from three up to the maximum number of cameras. These additional criterion measures allowed for the comparison of normalised LPSE between laboratory points calculated from varying numbers of camera image points.

The normalised LPSE was the strongest predictor of conjugate image points between laboratory points calculated from three or more cameras. Since calculation of the LPSE requires that at least three valid image points be identified, a laboratory point formed from just two image points will not have

a LPSE, LPPE or LPE but will have met the CPE criterion. It is therefore advantageous in terms of both accuracy and the determination of conjugate image points, to have the laboratory points visible in at least three or four cameras. If four cameras are used in the analysis of human motion an advantageous configuration can be achieved by placing four cameras on one side of the subject. As discussed later in the case of four cameras placed around the subject, the algorithm can successfully reconstruct the three dimensional coordinates from digitised video data. The success of accurately reproducing three dimensional coordinates ultimately depends on the LPE and marker separation. The more cameras in which a laboratory point is visible, the greater will be the ability to construct valid laboratory points and determine conjugate image points due to the availability of the LPSE.

The normalised LPSE can be considered to be a measure of the accuracy of the photogrammetric system. It shares the same properties as the LPE with respect to the number of cameras used to reproduce a three dimensional point and the accuracy of camera image coordinates. An advantage of the normalised LPSE, over the LPE, is that it is less variable and better at differentiating between laboratory points reconstructed from varing numbers of cameras.

4.2.2 Conjugate Point Error.

The inverse relationship between camera distance and Conjugate Point Error (CPE) resulted from errors produced in the calculation of an epipolar line with changing photo scale of the camera. The errors in the epipolar line in a secondary camera image were a function of the errors in image coordinates of the primary camera, the photo scale of the two cameras and errors in the DLT parameters. For a given point in the first camera image a collinear line can be established in three dimensional space by two boundary laboratory points. The epipolar line is then established in the second camera image plane from

these two laboratory points. The magnitude of the error produced in the epipolar line of the second camera will be dependent on the accuracy of the calculated laboratory boundary points and on the photo scale of the second camera. The further the second camera is positioned from the central laboratory point the smaller will be the photo scale and the smaller will be the errors in producing image coordinates relative to the errors in the three dimensional coordinates of the boundary points. Hence, as the second camera is positioned further from the central laboratory point, the errors in defining the epipolar line from laboratory boundary points decrease. This was due to small errors in laboratory boundary points producing smaller errors in calculated image plane coordinates at the larger object distances. The accuracy of the laboratory boundary points will be dependent on the accuracy of the image data of the first camera and its photo scale. The closer the first camera is to the central laboratory point, the larger will be the photo scale and measurement error in the original image point will result in relatively smaller parallax errors in defining the boundary points on the collinear line in laboratory space. The errors transferred to the collinear lines which define the epipolar line of the second camera are only the components of parallax of the first collinear line which are perpendicular to both collinear lines. Parallax error of the first collinear line in the direction parallel to the second collinear line will not result in error of the second collinear line and vice versa (Figure 19). It can be seen that if the two collinear lines are at 90^{o} to each other, and hence a camera-laboratory point-camera angle of 90^{o}, then the error of the image point of the second camera will be limited to a line on the camera image plane perpendicular to both collinear lines. The negative relationship between CPE and object distance of the second camera resulted from the greater in error in reproducing the epipolar line in the second camera. This was likely due to an increase in photo scale of this same camera rather than greater laboratory point error arising from decreasing photo scale of the first camera.

Figure 19. Image point error and reproduction error.

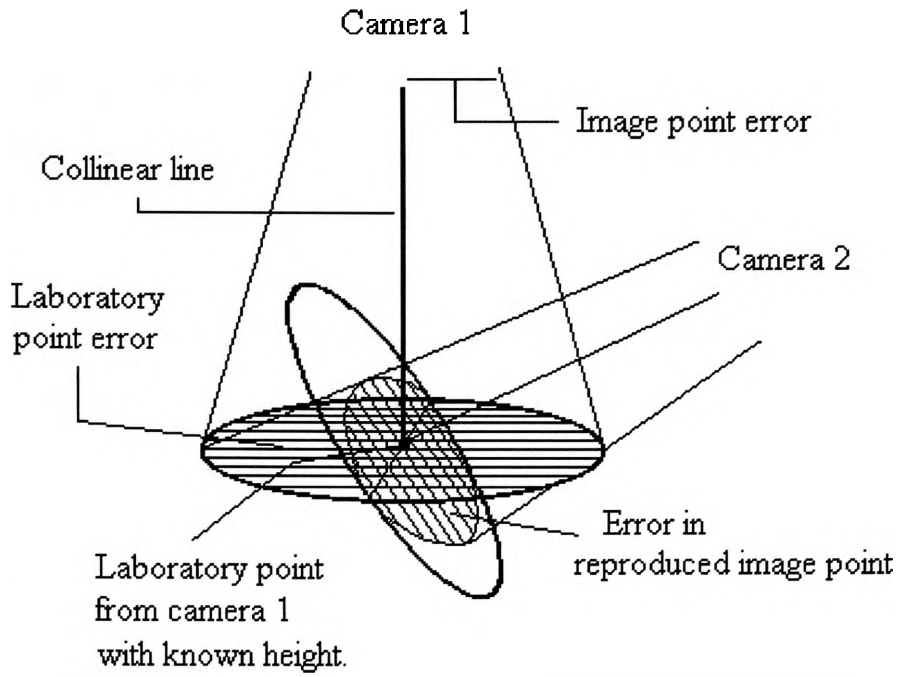

The CPE was not normalised for the distance between cameras and the individual laboratory points despite a negative relationship existing between the magnitude of the CPE and the distance to the laboratory points. Variations in photo scale between cameras could account for some of the differences seen in the magnitude of the CPE between different cameras. Therefore in the initial stage of collecting valid image points, separate criterion CPE values were calculated for each camera to account for the variations in mean photo scale. In the collection of valid laboratory points it was not necessary to compare the CPE between different cameras and therefore it did not prove necessary to normalise each object distance for each laboratory point in the calculation of CPE. The mean photo scale was calculated as the principal distance of the camera divided by the distance between the camera and the central laboratory point. In the final stage of the algorithm, when deleting image points amongst laboratory points associated with just two camera images, it was necessary to compare CPE between image points of different cameras. To enable comparison of the CPE between cameras in this situation

each CPE was normalised by subtracting the CPE from the mean CPE for that camera and dividing by the respective standard deviation.

The primary use of the CPE was in the first stage of creating valid laboratory points where all image points lying with the criteria CPE were collected. By chance alone, the geometric arrangement of laboratory points may result in an incorrect image point lying closer to the epipolar line than the conjugate image point, irrespective of the magnitude of error involved. Measurement error will effect the position of image points and also the calculation of the epipolar line. By calculating the mean and standard deviation of known distances between conjugate image points and epipolar lines in the calibration procedure, the criterion CPE established would be of sufficient magnitude to include all conjugate image points for that camera. As previously mentioned, CPE calculated for each camera has proved sufficient in collecting all valid image points. Once the valid laboratory points are constructed it is the normalised LPSE that plays the major role in determining the validity of common image points shared amongst the generated laboratory points.

The calculation of the criterion CPE for a single camera uses image points in all other cameras to construct epipolar lines. Therefore the criterion CPE is not only dependent on the image coordinate errors of its own image points but also the image coordinate errors of all other cameras. The errors of image points in respective camera images will be functions of comparator film deformation and distortion, comparator photo scale, perception, as well as factors relating to the individual cameras such as stability of interior orientation, camera photo scale and film deformation and distortion in the camera image plane. Further errors in the analytical process result from the errors in the DLT parameters arising from accuracy to which marker points are known in laboratory space in the camera calibration procedure.

4.2.3 Lab Point Paired Error.

The Lab Point Paired Error (LPPE) acted as an additional check to the LPSE by comparing the individual differences in laboratory points reproduced from paired image points. Like the LPSE, the LPPE could only be calculated for laboratory points associated with three or more cameras and the LPPE was normalised for camera-laboratory point-camera angle. The normalisation of LPPE was carried out by first calculating the distances between the mean laboratory point and the laboratory points produced from each pair of image points. These distances were then normalised to a camera-laboratory point-camera angle of 90°. A respective normalised laboratory point was then calculated for each pair of camera image points. A normalised laboratory point would lie at this normalised distance from the mean laboratory point in the same direction as the actual laboratory point produced from the paired image point. The normalised LPPE was then the maximum distance between all normalised paired laboratory points derived from all image points associated with a mean laboratory point. If the normalised LPPE was greater than the criterion value, the image point associated with the LPPE that was furthest from the mean laboratory point was deleted from the set of image points. The rationale behind the use of the LPPE was to prevent the inclusion of one wayward image point which, by virtue of the closeness of the other image points, still meet the criterion LPSE value. The actual importance of the LPPE in the reproduction of three dimensional points is unknown but has been included as an additional value in the calculation of LPSE and used as an additional check on the validity of conjugate image points.

4.2.4 Coincidence with another set of collinear lines.

It is possible that a collinear line will coincide with an unrelated set of collinear lines and meet the criterion measures of this set better than the set to which it belongs. The likelihood of this situation happening will depend on

the accuracy of the photogrammetric system and the number and closeness of body markers. In such a situation the algorithm would conclude that the set with the lowest criterion values were correct and assign the image points accordingly. This situation is also theoretically possible if two body markers and a camera perspective should all lie on the same line, regardless of photogrammetric error. In such a circumstance, the laboratory point to which the image point was assigned would be dependent on the error of the other laboratory points which determine the LPPE and LPPE. In terms of the outcome of an image point being assigned to an incorrect laboratory point, the laboratory point coordinates reproduced with the additional image point will not have changed significantly as the set of image points will have met the four criterion measures. The laboratory point which "lost" the image point would also not have changed significantly and may possibly be better off for having "lost" an image point with large errors. However, a problem will arise if the laboratory point that loses an image point was only visible in two camera images. In this situation the loss of an image point would cause the laboratory point to disappear.

4.3 Three dimensional reproduction algorithm.

The present algorithm to reproduce three dimensional coordinates did not appear to be limited by the number of body markers or the number of cameras. What did appear to determine the limits of the algorithm was the relationship between the accuracy of the photogrammetric system, the closeness of body markers and the number of markers appearing in just two cameras. It would be expected that if the LPE, the radius over which a laboratory point may vary, was of the same order as the minimum separation of body markers then considerable difficulties would result in the determination of valid conjugate image points. Clearly the separation of body markers needs to be considerably larger than the LPE to avoid separate laboratory markers from being combined and to prevent collinear lines and their respective image points from being freely interchanged between laboratory points.

The algorithm successfully reproduced three dimensional coordinates from video data of a 55 point marker system viewed in four cameras. The results of the video camera calibration procedure (DLT parameters, LPE and LSPE) and reproduced calibration and marker coordinates are presented in Appendix IV. The error was approximately 0.2% in image data. The minimum body marker separation was approximately 5 cm and the LPE for two cameras was approximately 0.5 cm. However the LPE for two camera points was dependent on camera configuration angle and could have reached 1.5 cm for cameras that had a camera-laboratory point-camera angle nearer to 70 degrees. In these data, 31 of the 55 markers were visible in just two cameras. An improvement in the ability of the algorithm to reproduce three dimensional coordinates was made by increasing the number of cameras. Increasing the number of cameras had three main effects on the algorithm. Firstly, it increased the accuracy of the photogrammetric system by increasing the number of cameras in which a laboratory point was visible. Secondly, an increase in the number of conjugate image points also increased the ability of the algorithm to establish the validity of laboratory points. With more laboratory points visible in three or more cameras, greater use of the LPSE and LPPE could be made in establishing the validity of conjugate image points. Thirdly, the influence of chance alignment of collinear lines was decreased. With more markers being associated with more camera images, and the magnitude of the normalised LPSE decreasing, the likelihood that this number of collinear lines would intersect by chance as well as meeting the criterion measures also decreased.

The algorithm also successfully reproduced experimental data of a 55 point marker set viewed by eight cameras with approximately 0.35% error in image data. The minimum body marker separation was 5 cm and the LPE for three cameras was 0.7 cm. The relationship between the separation of body markers, the number of two camera laboratory points, the LPE and the performance of the algorithm in reproducing three dimensional coordinates has yet to be fully investigated. At present it can be said that provided the markers are sufficiently separated with respect to this

accuracy of the photogrammetric system, then the algorithm can systematically work through a large array of image points in as many cameras that are required to reproduce three dimensional coordinates.

From the view point of accuracy we have seen that there is little improvement in increasing the number of cameras beyond three to reproduce a three dimensional coordinate. However in establishing the validity of conjugate image points in the automated reproduction of three dimensional coordinates, definite improvements are made if the markers are visible in three or four cameras. Markers which are visible in greater than two cameras enables the use of the strongest predictive criterion, the LPSE, to be used in testing the validity of conjugate image points. In practice no more than four cameras are likely to be present and if whole body motion is analysed the cameras would normally be distributed evenly around the test area. The result of this configuration is that the majority of body markers will be visible in only two cameras with only a few visible in three cameras. The ability to establish the validity of markers visible in only two cameras is considered as the major limitation of the present algorithm which stems from the inability to determine the validity of laboratory points derived from just two camera image points. However in the two camera situation, the present algorithm can successfully reproduce the three dimensional coordinates given sufficient accuracy of the photogrammetric system relative to the separation of markers. The algorithm was successfully tested with 31 two camera image points, 22 three camera image points and 2 four camera image points of a 55 body marker set. The error in image coordinates was approximately 0.2% and the minimum marker separation was 5 cm. As mentioned above, the success of the algorithm in accurately reproducing three dimensional coordinates is dependent on the photogrammetric accuracy, the minimum separation of body markers, and the number of two camera image points.

The accuracy of the photogrammetric system in reproducing three dimensional coordinates is essential to the performance of the algorithm. The more accurate the photogrammetric system the greater its ability to determine conjugate image points

and the closer markers can be placed to one another. Every effort therefore needs to taken to ensure maximum accuracy of the photogrammetric system. Steps include:

(i) Optimal camera configuration, which involves the use of the convergent case, where the camera principal axes are directed towards the central laboratory point at a convergence angle of 45^{o}. If cameras are to be placed around the test area, the cameras should not be placed at 180^{o} to one another and in the same plane as the laboratory markers. Raising the cameras above the test area will avoid indeterminacy in the photogrammetric equations produced when markers fall on the line joining each camera's perspective centre. Not placing the cameras in the same plane as the laboratory markers also reduces the likelihood of unrelated collinear lines intersecting and reduces the number of incorrect laboratory points initially generated by the algorithm.

(ii) A large photo scale, which can be achieved by a small object distance or large principle distance, will minimise the error in reproducing three dimensional coordinates by reducing the influence of digitisation error in the comparator plane. A large photoscale could be achieved by placing the cameras close to the object space. However, an improved accuracy may well be achieved with a larger object distance to reduce parallax with the use of a large focal length lens system and/or camera format. In practice the object distance is usually determined by the focal length of the camera, the image size and required camera field of view.

(iii) A large image format will reduce errors in the measurement of comparator coordinates, however the image format is usually predetermined by the available camera - lens configuration.

(iv) Accurate measurement of three dimensional coordinates of control points during calibration of camera configuration.

The advantages of the present algorithm lie in accommodating protocols that involve large marker sets in the laboratory space and, if it should occur, large numbers of cameras. Less complex analyses involving limited marker sets in a predominantly sagittal plane motion, for example lifting with markers placed on one side of the ankle, knee, hip, shoulder, elbow and hand respectively, can be efficiently handled with existing tracking and identification procedures. However, these procedures become difficult and time consuming when the total number of markers and the complexity of the task increases. With existing systems the difficulties encountered with more complex analyses have lead to limitations in the number of three dimensional segments, the markers per segment and the complexity of movement analysed with existing systems. The algorithm presented in this thesis has attempted to overcome these limitations by increasing the ability to reproduce three dimensional coordinates. The algorithm is largely independent of the number of markers and its accuracy improves with increasing numbers of cameras. The implementation of the algorithm will facilitate an increase in the accuracy and complexity of human movement suitable for biomechanical analysis.

4.4 Future research.

The work presented represents an investigation into the use of conjugate imaging techniques in the automated reproduction of three dimensional coordinates. Techniques and procedures have been developed and practical problems identified in applying the algorithm to the analysis of human motion. Considerable work still remains in the refinement and improvement of the algorithm. It is anticipated most of the development will now come through use of the algorithm and analysing its behaviour in different situations. The result will be further improvements in accuracy and efficiency. Areas of possible future research are listed below:

(i) There is scope in improving the current criteria or creating new criterion measures for determining the validity of conjugate image points. The

criterion measures are fundamental to the approach adopted and to the success of the algorithm in reproducing three dimensional coordinates. The most apparent area of future development is in assessing the validity of two camera laboratory points.

(ii) The use of twelve DLT parameters, instead of the usual eleven, needs further investigation in the area of video and film photogrammetry and may provide a significant improvement in the accuracy of reproducing three dimensional coordinates. The inclusion of a non-linear component of film deformation and distortion in the DLT photogrammetric model may have a greater effect than that found with stereometric cameras due to the larger errors in comparator coordinates derived from film and video.

(iii) Further investigation is needed into the accuracy of video and cinematographic analysis systems to provide a clear understanding of the accuracy of three dimensional coordinates reproduced. Often movement analysis is carried out without a sound knowledge of the accuracy of the positional data obtained.

(iv) The relationship between the accuracy of the photogrammetric system (LPE and LPSE), the minimum separation of body markers and the ability of the algorithm to determine conjugate image points needs to be defined and is essential to the application of the algorithm. With knowledge of the LPSE or LPE of a photogrammetric system, a suitable separation of body markers should be readily attainable that will ensure accurate reproduction of three dimensional coordinates. This relationship of performance to the minimum separation of markers will hopefully improve with improvements that are made in the functioning of the algorithm.

(v) The relationship between the total number of body markers, the number of body markers appearing in just two camera images and the ability of the algorithm to reproduce three dimensional coordinates will improve the application of the algorithm. If this relationship is known, an experimental set up in which the algorithm is not successful in accurately reproducing three dimensional coordinates, may be reconfigured in such a manner so as to improve the performance of the algorithm. Improved results of the algorithm would be achieved either by increasing the number of cameras, or re-positioning the current cameras to increase the number of markers which were visible in three or more cameras. The effect would be to increase the accuracy of the photogrammetric system as well as increase the ability of the algorithm to determine conjugate image points.

(vi) Although normalisation of CPE was not carried out for every image point in the present algorithm, it warrants further investigation as it may prove useful in reducing the number of laboratory points collected. One form of normalisation may be to calculate the criterion CPE for each camera pair instead of having one criterion LPE for each camera. Normalisation may be required for each laboratory point in a situation where the object distance of the camera is relatively small compared to the distance between laboratory points in the direction of the camera principal axis. The relatively large changes in object distance will result in relatively large changes in photo scale from one laboratory point to another.

The algorithm presented for automated reproduction of three dimensional coordinates is intended as a starting point in the development of a more accurate three dimensional tracking algorithm. The successful implementation of such an algorithm will require answers to many of the questions posed above to produce a robust algorithm with known tolerances and performance.

The use of conjugate imaging techniques as well as some of the procedures developed in this study, such as the criterion measures, may be implemented into a three dimensional tracking algorithm. As such the development of a three dimensional tracking algorithm is a further investigation in itself, requiring the identification of limitations and practical problems associated with the use of conjugate imaging techniques and the development of procedures for its application to the analysis of human motion.

5.0 SUMMARY AND CONCLUSION

The three dimensional quantitative analysis of human motion requires the reproduction of three dimensional coordinates from multiple camera images. In current photogrammetric systems the ability to identify and track individual camera image points imposes limitations on the accuracy and complexity of human motion analysis. Current human motion analysis systems are limited in the number of cameras, three dimensional segments, markers per segment and the complexity of movement due to increased difficulty and time required to reproduce three dimensional coordinates. Reduced external marker sets and the restriction of analyses to planar motions are often used to overcome these limitations.

The aim of the present study was to investigate the use of conjugate imaging techniques in the automated reproduction of thee dimensional coordinates from multiple camera images. The investigation involved, firstly, identifying limitations and practical problems associated with the use of conjugate imagery when applied to the reproduction of three dimensional coordinates in the analysis of human motion and secondly, identifying procedures which will enable the application of conjugate imaging techniques to the analysis of human motion. The purpose of the study was to increase the accuracy and complexity currently attainable in the analysis of human motion.

An important concept of conjugate imagery and epipolar geometry is the fact that conjugate image points will always lie on conjugate epipolar lines regardless of camera orientation. With error present in digitised camera image coordinates several assumptions need to be made:

(i) a conjugate image point will lie at some finite distance from the conjugate epipolar line;

(ii) a conjugate image point may not necessarily be the closest image point to the conjugate epipolar line; and

(iii) an image point and its collinear line may be coincident with more than one set of image points and their respective collinear lines.

With these assumption, four criteria were established for testing the validity of conjugate image points. The four criteria were:

(i) Conjugate Point Error (CPE), the perpendicular distance between a conjugate image point and its respective conjugate epipolar line;

(ii) Lab Point Standard Error (LPSE), the standard error between the least squares laboratory point and laboratory points reproduced from paired conjugate image points;

(iii) Lab Point Paired Error (LPPE) the maximum distance between laboratory points reproduced from paired conjugate image points; and

(iv) Lab Point Error (LPE), the maximum radius over which a laboratory point may vary.

The maximum value for each criterion could readily be obtained as part of the standard camera calibration procedure. Each criterion value provided a means by which laboratory points and respective image points could be compared and the validity of conjugate image points determined.

The errors in calculating laboratory points from paired conjugate image points were found to be dependent on the angle formed between the two cameras' perspective centres and the resulting laboratory point. This error was minimal at an angle of 90°, but approached infinity as the angle approached either 0° or 180°. To avoid the possibility of an incorrect set of image points having a lower LPSE or LPPE than a set of conjugate image points due to the fact that the correct set were at a disadvantageous angle, it was necessary to normalise all laboratory points reproduced from paired image points. Normalisation was achieved by adjusting the reproduced

coordinates of all paired laboratory points so as to have an equivalent error of 90° in the calculation of the normalised LPSE and LPPE. Normalisation allowed the comparison of LPSE and LPPE between all laboratory points in the determination of the validity of individual image points. The CPE was found to be inversely related to the distance of each camera from the central laboratory point. However it was sufficient to calculate a CPE for each camera to account for individual changes in photo scale between cameras.

This study has shown the applicability of conjugate imaging techniques in the automated reproduction of three dimensional coordinates in the analysis of human motion. The algorithm developed was able to accurately reproduce three dimensional coordinates and conjugate image points for video data of a 55 point marker system viewed by four cameras with a digitisation error of approximately 0.2% and a minimum marker distance of 5 cm. The capacity of the present system to accurately reproduce three dimensional coordinates was dependent on the accuracy of the photogrammetric system, the minimum distance between body markers and the number of markers appearing in just two cameras. When there was increased error in the digitised image data or a decrease in the marker separation, improved results could be obtained by increasing the number of cameras. Additional cameras effectively increased the number of cameras in which a laboratory point would appear, thereby increasing the accuracy of the photogrammetric system and increasing the ability of the algorithm to determine the validity of conjugate image points.

This study has shown the viability of conjugate imagery, in the automated reproduction of three dimensional coordinates as a means of achieving an increase in accuracy and complexity of human movement analysis. Automated three dimensional coordinate reproduction will allow analyses to include an increased number of segments, an increased the number of markers per segment and greater complexity of movement with a reduction in the time and difficulties currently

limiting the reproduction of three dimensional coordinates, than current practices allow.

6.0 REFERENCES

Abdel-Aziz, Y.I. & Karara, H.M. (1974) Photogrammetric potentials of non-metric cameras: Civil Engineering Studies, Photogrammetry Series no. 36. Virginia: National Technical Information Service.

Cappozzo, A. (1985) Experimental techniques, data acquisition and reduction. In N. Berme, A.E. Engin & K.M. Correia da Silva, (Eds.) Biomechanics of Normal and Pathological Human Articulating Joints. Boston: Martinus Nijhoff Publishers.

Chao, E.Y.S. (1980) Justification of triaxial goniometer for the measurement of joint rotation. Journal of Biomechanics, 13(12), 989-1006.

Grood, E.S. & Suntay, W.J. (1983) A joint coordinate system for the clinical description of three dimensional motions: application to the knee. Journal of Biomechanical Engineering, 105(May), 136-144.

Hatze, H. (1980) A mathematical model for the computational determination of parameter values of anthropometric segments. Journal of Biomechanics, 13(10), 833-844.

Hussain, M. (1977) Measurement of Spatial Motion Using Analytical Photogrammetric System. Michigan: University Microfilms.

Karara, H.M. (1980) Non-topographic photogrammetry. In C.C. Slama, C. Theurer & S.W. Henriksen (Eds.) Manual of Photogrammetry, 4th Ed. Virginia: American Society of Photogrammetry, 785-882.

Keating, T.J. (1977) Analytical Photogrammetry from Digitized Image Densities. Michigan: University Microfilms.

Marzan, G.T. (1977) Rational Design for Close-Range Photogrammetry. Michigan: University Microfilms.

McGee, R.J., Koozeekanani, S.H., Weimer, F.C. & Rahmani, S. (1979) Dynamic modelling of human locomotion. In Proceedings of Joint Automated Control Conference. New York: American Institute of Mechanical Engineers.

Miller, N.R., Shapiro, R.S. & McLaughlin, T.M. (1980) A technique for obtaining spatial kinematic parameters of segments of biomechanical system from cinematographic data. Journal of Biomechanics, 13(7), 535-548.

Noble, B. (1969) Applied Linear Algebra. New Jersey: Prentice-Hall.

Seireg, A. & Arvikar, R.J. (1989) Biomechanical Analysis of the Musculoskeletal Structure for Medicine and Sports. New York: Hemisphere Publishing Corporation.

Shapiro, R.S. (1978) The direct linear transformation method for three-dimensional cinematography. Research Quarterly, 49(2), 197-205.

Shapiro, R.S. (1979) Three-dimensional kinetic analysis of the baseball swing. Unpublished doctoral dissertation, University of Illinois.

Small, C.F., Bryant, J.T. & Pichora, D.R. (1982) Rationalisation of kinetic descriptions for three dimensional hand and finger motions. Journal of Biomedical Engineering, 14(March), 133-141.

Spoor, C.W. & Veldpaus, F.E. (1980) Rigid body motion calculated from spatial co-ordinates of markers. Journal of Biomechanics, 13, 391-393.

Wong, K.W. (1980) Basic Mathematics of Photogrammetry. In C.C. Slama, C. Theurer & S.W. Henriksen (Eds.) Manual of Photogrammetry, 4th Ed. Virginia, U.S.A: American Society of Photogrammetry, 37-101.

APPENDIX I

ERROR FACTOR IN STEREOSCOPIC CONFIGURATION

In section (1.2.2) formulae were presented (equation 1.2.2.31) for calculating the expected positional error of a three dimensional point given the standard error of the image points and the photogrammetric configuration. The formulae were:

$$m_T = \frac{D}{\sqrt{2}.C} .m.(\text{Error Factor})$$

$$\text{Error Factor} = \sqrt{\frac{1}{(\cos\phi - {}^1/_2.\tan\theta.\sin\phi)^2} + 1 + \frac{1}{(\sin\phi + {}^1/_2\tan\theta.\cos\phi)^2}}$$

Where:

m_T = positional error of three dimensional point.

m = standard error of image coordinates.

ϕ = convergence of camera axes (symmetrical).

θ = overlap angle.

C = camera principal distance.

D = object distance.

C/D = photo scale.

Following are tabulated results of the error factor for every degree of convergence and overlap from 0° to 90° respectively. Each column represents varying degrees of convergence for a fixed overlap angle. The special case of photography when the camera axes are directed towards the central point in object space occurs when the overlap is equal to zero (column 1). Each row represents varying degrees of overlap for a fixed angle of convergence. The normal case of photography is when the convergence is equal to zero (row 1).

Table 30. Error factor

θ / ϕ	0	1	2	3	4	5	6	7	8
0	999.999	114.5887	57.28996	38.18847	28.63627	22.90381	19.08121	16.34997	14.30084
1	57.31614	38.2253	28.67988	22.95193	19.13253	16.40365	14.35632	12.76335	11.48843
2	28.68861	22.96798	19.15481	16.43105	14.38791	12.79841	11.52638	10.48521	9.61717
3	19.15966	16.44066	14.40207	12.81669	11.54833	10.51039	9.6452	8.91284	8.28481
4	14.40534	12.82336	11.55843	10.52377	9.66163	8.93208	8.30663	7.7644	7.28976
5	11.56087	10.52881	9.66937	8.94248	8.31958	7.77977	7.30739	6.8905	6.5198
6	9.67131	8.9465	8.32579	7.78819	7.31797	6.90317	6.53447	6.20454	5.90754
7	8.32739	7.79151	7.32313	6.9102	6.54335	6.21525	5.92001	5.65289	5.41003
8	7.3245	6.91303	6.54775	6.22125	5.92763	5.66211	5.42082	5.20054	4.99862
9	6.54893	6.22371	5.93145	5.66734	5.42747	5.20861	5.00809	4.82367	4.65347
10	5.9325	5.66951	5.43084	5.21323	5.01398	4.83083	4.66189	4.50553	4.36039
11	5.43178	5.21517	5.01699	4.83496	4.66715	4.51194	4.36795	4.23397	4.10898
12	5.01784	4.83671	4.66987	4.51567	4.37271	4.23977	4.11583	3.99998	3.89144
13	4.67065	4.51728	4.37519	4.24317	4.12016	4.00527	3.89769	3.79673	3.7018
14	4.3759	4.24464	4.12244	4.00839	3.90167	3.80159	3.70754	3.61897	3.53542
15	4.12311	4.00975	3.90377	3.80447	3.71121	3.62346	3.54072	3.46257	3.38863
16	3.90439	3.80574	3.71317	3.62613	3.54413	3.46673	3.39355	3.32424	3.25851
17	3.71375	3.62732	3.54596	3.46923	3.39674	3.32813	3.2631	3.20137	3.14268
18	3.54651	3.47035	3.39846	3.33047	3.26609	3.20501	3.14699	3.0918	3.03923
19	3.39897	3.33153	3.26771	3.20722	3.1498	3.09522	3.04328	2.99377	2.94654
20	3.2682	3.20822	3.15133	3.09731	3.04593	2.99701	2.95036	2.90584	2.86329
21	3.1518	3.09826	3.04739	2.99899	2.95288	2.90891	2.86692	2.82678	2.78838
22	3.04783	2.99989	2.95427	2.91079	2.86931	2.8297	2.79183	2.75558	2.72087
23	2.95469	2.91166	2.87064	2.8315	2.79411	2.75836	2.72415	2.69138	2.65996
24	2.87105	2.83233	2.79538	2.76009	2.72634	2.69404	2.6631	2.63343	2.60498
25	2.79577	2.76088	2.72756	2.69569	2.66519	2.63598	2.60798	2.58112	2.55535
26	2.72793	2.69646	2.66636	2.63757	2.60999	2.58357	2.55823	2.53391	2.51057
27	2.66673	2.63831	2.61113	2.5851	2.56017	2.53627	2.51334	2.49134	2.47021
28	2.61148	2.58582	2.56126	2.53775	2.51521	2.49361	2.47289	2.453	2.43391
29	2.56161	2.53845	2.51628	2.49504	2.4747	2.4552	2.4365	2.41856	2.40135
30	2.51661	2.49572	2.47573	2.45659	2.43825	2.42069	2.40385	2.38771	2.37224
31	2.47606	2.45725	2.43926	2.42204	2.40556	2.38978	2.37467	2.36021	2.34636
32	2.43958	2.42268	2.40653	2.39109	2.37633	2.36221	2.34872	2.33582	2.32349
33	2.40685	2.39173	2.37729	2.3635	2.35034	2.33777	2.32579	2.31436	2.30346
34	2.37759	2.36412	2.35127	2.33903	2.32737	2.31627	2.3057	2.29566	2.28612
35	2.35157	2.33964	2.32829	2.3175	2.30725	2.29752	2.28831	2.27958	2.27134
36	2.32858	2.31809	2.30815	2.29873	2.28982	2.28141	2.27348	2.26601	2.25901
37	2.30844	2.29932	2.29071	2.28259	2.27496	2.2678	2.2611	2.25485	2.24904
38	2.29099	2.28317	2.27584	2.26897	2.26257	2.25661	2.2511	2.24602	2.24137
39	2.27612	2.26954	2.26342	2.25776	2.25254	2.24775	2.24339	2.23946	2.23594
40	2.26371	2.25832	2.25339	2.24888	2.24481	2.24116	2.23793	2.23511	2.23271
41	2.25367	2.24944	2.24565	2.24228	2.23933	2.2368	2.23467	2.23296	2.23167
42	2.24593	2.24284	2.24016	2.23791	2.23606	2.23463	2.2336	2.23299	2.2328
43	2.24044	2.23845	2.23688	2.23573	2.23498	2.23464	2.23471	2.2352	2.23611
44	2.23716	2.23627	2.2358	2.23573	2.23607	2.23683	2.238	2.2396	2.24163
45	2.23607	2.23627	2.23689	2.23791	2.23935	2.24121	2.2435	2.24622	2.24939
46	2.23716	2.23846	2.24017	2.24229	2.24484	2.24782	2.25124	2.25511	2.25944
47	2.24044	2.24284	2.24565	2.2489	2.25258	2.25671	2.26129	2.26634	2.27187
48	2.24593	2.24944	2.25339	2.25778	2.26262	2.26792	2.2737	2.27997	2.28675

Table 30. Error factor (cont.)

θ / ϕ	0	1	2	3	4	5	6	7	8
42	2.24593	2.24284	2.24016	2.23791	2.23606	2.23463	2.2336	2.23299	2.2328
43	2.24044	2.23845	2.23688	2.23573	2.23498	2.23464	2.23471	2.2352	2.23611
44	2.23716	2.23627	2.2358	2.23573	2.23607	2.23683	2.238	2.2396	2.24163
45	2.23607	2.23627	2.23689	2.23791	2.23935	2.24121	2.2435	2.24622	2.24939
46	2.23716	2.23846	2.24017	2.24229	2.24484	2.24782	2.25124	2.25511	2.25944
47	2.24044	2.24284	2.24565	2.2489	2.25258	2.25671	2.26129	2.26634	2.27187
48	2.24593	2.24944	2.25339	2.25778	2.26262	2.26792	2.2737	2.27997	2.28675
49	2.25367	2.25833	2.26343	2.269	2.27503	2.28155	2.28857	2.29611	2.30419
50	2.26371	2.26954	2.27584	2.28263	2.2899	2.29769	2.30601	2.31488	2.32433
51	2.27612	2.28317	2.29072	2.29877	2.30734	2.31646	2.32614	2.33642	2.34731
52	2.29099	2.29932	2.30816	2.31754	2.32747	2.33799	2.34912	2.36089	2.37332
53	2.30844	2.31809	2.3283	2.33908	2.35046	2.36246	2.37512	2.38848	2.40256
54	2.32858	2.33964	2.35129	2.36355	2.37647	2.39006	2.40436	2.41941	2.43526
55	2.35157	2.36412	2.3773	2.39115	2.40571	2.421	2.43706	2.45395	2.47171
56	2.37759	2.39173	2.40655	2.42211	2.43842	2.45554	2.47352	2.4924	2.51223
57	2.40685	2.42269	2.43928	2.45666	2.47489	2.49399	2.51404	2.53509	2.5572
58	2.43958	2.45725	2.47575	2.49513	2.51542	2.5367	2.55901	2.58243	2.60703
59	2.47606	2.49573	2.5163	2.53784	2.5604	2.58404	2.60885	2.63488	2.66223
60	2.51661	2.53845	2.56129	2.5852	2.61025	2.63651	2.66405	2.69298	2.72339
61	2.56161	2.58583	2.61116	2.63768	2.66547	2.69462	2.72521	2.75736	2.79117
62	2.61148	2.63832	2.6664	2.69581	2.72665	2.75901	2.793	2.82875	2.86639
63	2.66673	2.69646	2.72759	2.76022	2.79446	2.83042	2.86822	2.90803	2.94998
64	2.72793	2.76089	2.79542	2.83165	2.8697	2.9097	2.95182	2.99621	3.04307
65	2.79577	2.83233	2.87069	2.91096	2.95331	2.9979	3.0449	3.09452	3.14698
66	2.87105	2.91166	2.95432	2.99918	3.04641	3.09621	3.1488	3.20441	3.26332
67	2.95469	2.9999	3.04745	3.09752	3.15034	3.20612	3.26513	3.32766	3.39405
68	3.04783	3.09827	3.1514	3.20746	3.26669	3.32938	3.39584	3.46642	3.54155
69	3.1518	3.20823	3.26778	3.33074	3.39741	3.46814	3.5433	3.62334	3.70877
70	3.2682	3.33154	3.39854	3.46953	3.5449	3.62505	3.71047	3.80172	3.89941
71	3.39897	3.47036	3.54606	3.62648	3.71208	3.8034	3.90105	4.0057	4.11815
72	3.54651	3.62733	3.71328	3.80486	3.90266	4.00735	4.11969	4.24058	4.37103
73	3.71375	3.80575	3.9039	4.00884	4.12131	4.24218	4.37243	4.51323	4.66593
74	3.90439	4.00977	4.12259	4.24369	4.37403	4.51475	4.66714	4.83274	5.01338
75	4.12311	4.24466	4.37535	4.51628	4.66871	4.83413	5.01431	5.21135	5.42775
76	4.3759	4.5173	4.67007	4.83567	5.01582	5.21255	5.42828	5.66596	5.92914
77	4.67065	4.83674	5.01722	5.21408	5.42968	5.66687	5.92911	6.22063	6.54666
78	5.01784	5.2152	5.43112	5.66837	5.93033	6.2211	6.54579	6.91072	7.32396
79	5.43178	5.66955	5.93179	6.22252	6.54671	6.91053	7.32181	7.79053	8.32972
80	5.9325	6.22376	6.54817	6.91179	7.32224	7.78928	8.32556	8.9478	9.67858
81	6.54894	6.91309	7.32367	7.79024	8.32518	8.94481	9.67108	10.53425	11.57722
82	7.3245	7.79159	8.32649	8.94523	9.6693	10.52825	11.5638	12.83687	14.44001
83	8.32739	8.9466	9.67033	10.52763	11.55941	12.82518	14.41498	16.47184	19.2375
84	9.67131	10.52896	11.55982	12.82247	14.40528	16.44803	19.18574	23.04645	28.90044
85	11.56087	12.82358	14.40425	16.44063	19.16349	22.99097	28.76743	38.49184	58.31696
86	14.40535	16.44102	19.15869	22.97076	28.70605	38.31287	57.7129	117.466	999.999
87	19.15967	22.96869	28.68862	38.24084	57.42123	115.5949	999.999	111.4642	56.07732
88	28.68863	38.22727	57.32494	114.7989	999.999	113.4105	56.76925	37.82586	28.34129
89	57.31622	114.6064	999.999	114.3269	57.14175	38.07036	28.53179	22.80705	18.98944
90	999.999	114.5883	57.28989	38.18843	28.63626	22.90379	19.0812	16.34996	14.30083

Table 30. Error factor (cont.)

θ / ϕ	9	10	11	12	13	14	15	16	17
0	12.70645	11.43039	10.38584	9.51494	8.77763	8.14527	7.59689	7.11676	6.69282
1	10.44481	9.57467	8.83798	8.20615	7.65821	7.17844	6.75481	6.37797	6.04054
2	8.88228	8.25201	7.70543	7.22685	6.80428	6.42837	6.09176	5.78857	5.51402
3	7.74023	7.26345	6.84247	6.46801	6.13271	5.8307	5.55721	5.30838	5.08097
4	6.87075	6.49807	6.16442	5.86391	5.59181	5.34425	5.11801	4.91044	4.7193
5	6.18798	5.88919	5.61868	5.3726	5.14774	4.94145	4.7515	4.57601	4.41335
6	5.63873	5.39424	5.17089	4.96602	4.7774	4.60316	4.44168	4.29161	4.15175
7	5.18823	4.98484	4.79763	4.62472	4.46451	4.31564	4.17692	4.04734	3.92601
8	4.81283	4.64128	4.48239	4.33477	4.19725	4.06881	3.94857	3.83576	3.72969
9	4.49587	4.34951	4.2132	4.08594	3.96682	3.85509	3.75007	3.65114	3.5578
10	4.22528	4.09917	3.98119	3.87055	3.76658	3.66868	3.57633	3.48905	3.40643
11	3.9921	3.88253	3.77961	3.68273	3.59137	3.50505	3.42337	3.34595	3.27245
12	3.78953	3.69365	3.60326	3.5179	3.43715	3.36063	3.28802	3.21902	3.15336
13	3.61235	3.52792	3.44807	3.37245	3.30072	3.23257	3.16774	3.10599	3.0471
14	3.45645	3.38169	3.3108	3.2435	3.17949	3.11855	3.06045	3.00499	2.952
15	3.31856	3.25205	3.18885	3.12869	3.07137	3.01667	2.96443	2.91448	2.86666
16	3.19606	3.13666	3.08008	3.02613	2.97462	2.92539	2.87828	2.83316	2.78991
17	3.08682	3.03358	2.98277	2.93424	2.88782	2.84339	2.80081	2.75998	2.72078
18	2.98909	2.94123	2.89547	2.8517	2.80978	2.76959	2.73103	2.69401	2.65843
19	2.90142	2.85828	2.81698	2.77742	2.73948	2.70307	2.6681	2.63449	2.60216
20	2.8226	2.78363	2.74629	2.71047	2.67609	2.64306	2.61131	2.58076	2.55136
21	2.75161	2.71636	2.68254	2.65007	2.61888	2.58889	2.56004	2.53227	2.50552
22	2.68759	2.65566	2.62501	2.59555	2.56723	2.53999	2.51377	2.48852	2.46419
23	2.62982	2.60087	2.57307	2.54634	2.52062	2.49588	2.47205	2.44911	2.427
24	2.57766	2.55142	2.52619	2.50194	2.4786	2.45613	2.4345	2.41367	2.39359
25	2.53059	2.5068	2.48392	2.46193	2.44076	2.42038	2.40077	2.38189	2.3637
26	2.48814	2.46659	2.44587	2.42594	2.40677	2.38833	2.37058	2.3535	2.33707
27	2.44992	2.43042	2.41168	2.39366	2.37634	2.35969	2.34368	2.32828	2.31349
28	2.41558	2.39798	2.38107	2.36482	2.34922	2.33423	2.31984	2.30603	2.29277
29	2.38483	2.36898	2.35377	2.33918	2.32518	2.31176	2.29889	2.28656	2.27476
30	2.35741	2.3432	2.32958	2.31653	2.30404	2.29209	2.28066	2.26974	2.25932
31	2.33311	2.32043	2.3083	2.29671	2.28564	2.27508	2.26501	2.25544	2.24633
32	2.31172	2.30048	2.28976	2.27955	2.26984	2.2606	2.25184	2.24355	2.23572
33	2.29309	2.28322	2.27384	2.26494	2.25652	2.24856	2.24105	2.234	2.22739
34	2.27707	2.26851	2.26041	2.25277	2.24559	2.23885	2.23256	2.22671	2.2213
35	2.26356	2.25624	2.24938	2.24295	2.23697	2.23142	2.22631	2.22164	2.21739
36	2.25245	2.24634	2.24066	2.23542	2.2306	2.22622	2.22226	2.21874	2.21565
37	2.24367	2.23872	2.2342	2.23011	2.22644	2.2232	2.22039	2.21801	2.21606
38	2.23714	2.23334	2.22996	2.227	2.22446	2.22235	2.22067	2.21943	2.21863
39	2.23284	2.23016	2.2279	2.22606	2.22465	2.22366	2.22311	2.22301	2.22337
40	2.23073	2.22916	2.22801	2.22729	2.22699	2.22714	2.22773	2.22878	2.23031
41	2.23079	2.23033	2.23029	2.23069	2.23153	2.23281	2.23456	2.23679	2.2395
42	2.23302	2.23368	2.23476	2.23629	2.23827	2.24072	2.24365	2.24707	2.25102
43	2.23745	2.23923	2.24145	2.24413	2.24728	2.25091	2.25505	2.25972	2.26493
44	2.2441	2.24702	2.2504	2.25425	2.25861	2.26347	2.26886	2.27481	2.28134
45	2.25301	2.2571	2.26167	2.26675	2.27234	2.27847	2.28517	2.29246	2.30037
46	2.26425	2.26955	2.27535	2.28169	2.28857	2.29603	2.3041	2.3128	2.32216
47	2.2779	2.28445	2.29154	2.29919	2.30743	2.31628	2.32579	2.33598	2.34689
48	2.29406	2.30191	2.31035	2.31938	2.32905	2.33938	2.35041	2.36218	2.37474

Table 30. Error factor (cont.)

θ / ϕ	9	10	11	12	13	14	15	16	17
42	2.23302	2.23368	2.23476	2.23629	2.23827	2.24072	2.24365	2.24707	2.25102
43	2.23745	2.23923	2.24145	2.24413	2.24728	2.25091	2.25505	2.25972	2.26493
44	2.2441	2.24702	2.2504	2.25425	2.25861	2.26347	2.26886	2.27481	2.28134
45	2.25301	2.2571	2.26167	2.26675	2.27234	2.27847	2.28517	2.29246	2.30037
46	2.26425	2.26955	2.27535	2.28169	2.28857	2.29603	2.3041	2.3128	2.32216
47	2.2779	2.28445	2.29154	2.29919	2.30743	2.31628	2.32579	2.33598	2.34689
48	2.29406	2.30191	2.31035	2.31938	2.32905	2.33938	2.35041	2.36218	2.37474
49	2.31284	2.32207	2.33192	2.34242	2.35359	2.36549	2.37815	2.39162	2.40594
50	2.33438	2.34507	2.35642	2.36847	2.38126	2.39483	2.40924	2.42453	2.44076
51	2.35886	2.37109	2.38404	2.39775	2.41227	2.42765	2.44394	2.4612	2.47949
52	2.38646	2.40034	2.41501	2.43051	2.44689	2.46422	2.48254	2.50195	2.5225
53	2.4174	2.43306	2.44958	2.46701	2.48541	2.50486	2.52541	2.54716	2.57018
54	2.45195	2.46953	2.48805	2.50758	2.52819	2.54995	2.57294	2.59726	2.623
55	2.4904	2.51006	2.53077	2.5526	2.57562	2.59992	2.6256	2.65276	2.68153
56	2.53309	2.55504	2.57814	2.60249	2.62817	2.65528	2.68394	2.71426	2.74638
57	2.58044	2.60488	2.63063	2.65776	2.68638	2.71661	2.74858	2.78243	2.81832
58	2.63289	2.6601	2.68877	2.71899	2.75089	2.78461	2.82029	2.8581	2.89823
59	2.691	2.72128	2.75319	2.78686	2.82243	2.86006	2.89992	2.94222	2.98716
60	2.75538	2.78909	2.82464	2.86218	2.90189	2.94393	2.98853	3.03592	3.08635
61	2.82679	2.86434	2.90398	2.9459	2.99028	3.03735	3.08735	3.14056	3.1973
62	2.90607	2.94796	2.99225	3.03913	3.08885	3.14166	3.19786	3.25779	3.32182
63	2.99427	3.04109	3.09066	3.14322	3.19906	3.25849	3.32187	3.38959	3.46212
64	3.09261	3.14506	3.20069	3.25979	3.32271	3.38981	3.46155	3.5384	3.62094
65	3.20254	3.26147	3.32411	3.3908	3.46196	3.53805	3.6196	3.70724	3.80166
66	3.32583	3.39229	3.46308	3.53864	3.61949	3.70618	3.7994	3.8999	4.00857
67	3.46465	3.5399	3.62027	3.7063	3.79863	3.89797	4.00516	4.12118	4.24717
68	3.62165	3.70727	3.79899	3.8975	4.00359	4.11818	4.24233	4.37731	4.5246
69	3.80014	3.89811	4.00343	4.11697	4.23974	4.37293	4.51793	4.6764	4.85032
70	4.00426	4.1171	4.2389	4.37078	4.51405	4.67028	4.84131	5.02937	5.23716
71	4.23933	4.37032	4.51235	4.66691	4.83575	5.02096	5.22506	5.45112	5.7029
72	4.51226	4.66566	4.83291	5.01599	5.21728	5.43967	5.68666	5.96263	6.27299
73	4.83213	5.01371	5.21295	5.43257	5.67591	5.94704	6.25106	6.59436	6.98512
74	5.21123	5.42889	5.66954	5.93704	6.23619	6.573	6.95511	7.39234	7.8976
75	5.66654	5.93144	6.227	6.55892	6.93439	7.36263	7.85568	8.42948	9.10573
76	6.22221	6.5506	6.92116	7.34262	7.82631	8.38717	9.04534	9.82864	10.77659
77	6.91378	7.33033	7.80708	8.35818	9.00256	9.76619	10.68565	11.81419	13.2324
78	7.79583	8.33984	8.974	9.72285	10.62068	11.71702	13.08605	14.84415	17.18488
79	8.95667	9.69478	10.57665	11.64892	12.98092	14.68023	16.92335	20.02143	24.57884
80	10.54916	11.60403	12.90885	14.56461	16.7352	19.70532	24.01702	30.84533	43.30318
81	12.86288	14.48737	16.60526	19.482	23.61508	30.05834	41.50167	67.45964	183.4537
82	16.52105	19.33153	23.33713	29.50697	40.24611	63.61954	153.7979	999.999	81.94846
83	23.15523	29.13531	39.38977	61.05435	137.0752	999.999	90.04716	48.95661	33.52296
84	38.83044	59.3713	127.0613	999.999	97.34995	51.42621	34.85682	26.31278	21.09981
85	121.0026	999.999	103.48	53.44272	35.94834	27.03904	21.63994	18.01765	15.41878
86	108.2008	54.9865	36.79589	27.61242	22.07325	18.3679	15.71479	13.72124	12.16835
87	37.41298	28.04149	22.40536	18.642	15.95068	13.93023	12.35744	11.09825	10.06728
88	22.64578	18.84635	16.13098	14.09339	12.5078	11.23869	10.19979	9.33358	8.60024
89	16.2617	14.21516	12.62279	11.34834	10.30514	9.43537	8.69903	8.06753	7.51993
90	12.70644	11.43038	10.38584	9.51494	8.77762	8.14527	7.59689	7.11676	6.69282

Table 30. Error factor (cont.)

θ / ϕ	18	19	20	21	22	23	24	25	26
0	6.31574	5.97811	5.67402	5.3987	5.14822	4.91937	4.70943	4.51615	4.33762
1	5.73662	5.46142	5.21104	4.98224	4.77233	4.57906	4.40051	4.23506	4.0813
2	5.26421	5.03592	4.82647	4.6336	4.4554	4.29025	4.13676	3.99373	3.86012
3	4.87232	4.68018	4.50264	4.3381	4.18516	4.04262	3.90946	3.78477	3.66777
4	4.54268	4.37899	4.22683	4.08502	3.95252	3.82845	3.71201	3.60251	3.49936
5	4.26216	4.12126	3.98961	3.86632	3.75062	3.64181	3.53929	3.44253	3.35106
6	4.02108	3.89872	3.78389	3.6759	3.57416	3.47812	3.38732	3.30134	3.21981
7	3.81215	3.70509	3.60422	3.50901	3.419	3.33376	3.25292	3.17615	3.10315
8	3.62977	3.53547	3.44632	3.36191	3.28185	3.20583	3.13353	3.06469	2.99907
9	3.46957	3.38604	3.30683	3.23161	3.16009	3.09199	3.02707	2.96511	2.90592
10	3.3281	3.25374	3.18303	3.11572	3.05155	2.99032	2.93183	2.87589	2.82235
11	3.20259	3.1361	3.07273	3.01226	2.9545	2.89927	2.8464	2.79576	2.74719
12	3.0908	3.03111	2.97411	2.91962	2.86747	2.81751	2.76961	2.72364	2.6795
13	2.99088	2.93713	2.88571	2.83646	2.78924	2.74395	2.70045	2.65865	2.61846
14	2.90132	2.85278	2.80627	2.76165	2.71882	2.67766	2.63809	2.60002	2.56337
15	2.82085	2.77692	2.73475	2.69425	2.65532	2.61787	2.58182	2.5471	2.51365
16	2.74842	2.70857	2.67028	2.63346	2.59802	2.5639	2.53103	2.49934	2.46878
17	2.68313	2.64693	2.61211	2.57859	2.5463	2.51519	2.48519	2.45626	2.42834
18	2.62422	2.5913	2.5596	2.52906	2.49963	2.47125	2.44387	2.41745	2.39194
19	2.57104	2.54108	2.5122	2.48437	2.45754	2.43164	2.40666	2.38254	2.35926
20	2.52304	2.49576	2.46946	2.4441	2.41963	2.39602	2.37324	2.35125	2.33002
21	2.47975	2.45491	2.43096	2.40786	2.38557	2.36407	2.34332	2.3233	2.30398
22	2.44075	2.41815	2.39635	2.37534	2.35506	2.33551	2.31664	2.29845	2.28092
23	2.40569	2.38515	2.36534	2.34625	2.32785	2.3101	2.293	2.27653	2.26066
24	2.37426	2.35562	2.33767	2.32037	2.3037	2.28765	2.2722	2.25734	2.24305
25	2.34619	2.32933	2.3131	2.29747	2.28244	2.26798	2.25409	2.24075	2.22796
26	2.32126	2.30606	2.29144	2.27739	2.2639	2.25095	2.23853	2.22664	2.21528
27	2.29928	2.28563	2.27253	2.25997	2.24793	2.23642	2.22541	2.21491	2.20491
28	2.28006	2.26788	2.25623	2.24508	2.23443	2.22428	2.21463	2.20546	2.19678
29	2.26347	2.25269	2.24241	2.23261	2.2233	2.21447	2.20611	2.19824	2.19085
30	2.24939	2.23994	2.23097	2.22248	2.21445	2.20689	2.1998	2.19319	2.18705
31	2.23771	2.22954	2.22184	2.2146	2.20782	2.20151	2.19566	2.19028	2.18538
32	2.22834	2.22142	2.21495	2.20894	2.20338	2.19828	2.19364	2.18948	2.18581
33	2.22123	2.21552	2.21025	2.20544	2.20108	2.19718	2.19375	2.1908	2.18835
34	2.21632	2.2118	2.20771	2.20408	2.20091	2.1982	2.19598	2.19424	2.19302
35	2.21359	2.21023	2.20731	2.20486	2.20287	2.20136	2.20034	2.19983	2.19985
36	2.213	2.2108	2.20906	2.20778	2.20697	2.20667	2.20687	2.2076	2.20888
37	2.21457	2.21353	2.21295	2.21285	2.21325	2.21416	2.21561	2.21761	2.22019
38	2.21829	2.21841	2.21902	2.22013	2.22175	2.2239	2.22662	2.22993	2.23385
39	2.22419	2.2255	2.22731	2.22964	2.23251	2.23595	2.23998	2.24464	2.24996
40	2.23232	2.23484	2.23788	2.24147	2.24563	2.2504	2.25579	2.26186	2.26863
41	2.24273	2.24649	2.2508	2.2557	2.2612	2.26735	2.27417	2.28171	2.29002
42	2.2555	2.26054	2.26617	2.27242	2.27933	2.28692	2.29524	2.30435	2.31428
43	2.27071	2.27709	2.2841	2.29177	2.30015	2.30927	2.31918	2.32995	2.34161
44	2.28848	2.29626	2.30471	2.31389	2.32382	2.33457	2.34617	2.35871	2.37223
45	2.30894	2.31819	2.32818	2.33895	2.35054	2.36301	2.37643	2.39087	2.4064
46	2.33224	2.34306	2.35468	2.36714	2.38051	2.39485	2.41022	2.42671	2.44441
47	2.35857	2.37106	2.38442	2.39871	2.41399	2.43033	2.44782	2.46655	2.48662
48	2.38813	2.40242	2.41766	2.43391	2.45126	2.46979	2.48959	2.51076	2.53342

Table 30. Error factor (cont.)

θ / ϕ	18	19	20	21	22	23	24	25	26
42	2.2555	2.26054	2.26617	2.27242	2.27933	2.28692	2.29524	2.30435	2.31428
43	2.27071	2.27709	2.2841	2.29177	2.30015	2.30927	2.31918	2.32995	2.34161
44	2.28848	2.29626	2.30471	2.31389	2.32382	2.33457	2.34617	2.35871	2.37223
45	2.30894	2.31819	2.32818	2.33895	2.35054	2.36301	2.37643	2.39087	2.4064
46	2.33224	2.34306	2.35468	2.36714	2.38051	2.39485	2.41022	2.42671	2.44441
47	2.35857	2.37106	2.38442	2.39871	2.41399	2.43033	2.44782	2.46655	2.48662
48	2.38813	2.40242	2.41766	2.43391	2.45126	2.46979	2.48959	2.51076	2.53342
49	2.42118	2.4374	2.45467	2.47306	2.49266	2.51357	2.5359	2.55975	2.58528
50	2.458	2.47632	2.49579	2.51652	2.53859	2.56211	2.58721	2.61404	2.64273
51	2.49891	2.51951	2.54141	2.56469	2.58947	2.61588	2.64407	2.67418	2.70641
52	2.54429	2.5674	2.59195	2.61806	2.64585	2.67546	2.70707	2.74087	2.77705
53	2.59458	2.62046	2.64795	2.67719	2.70831	2.74151	2.77696	2.81489	2.85554
54	2.65029	2.67924	2.71	2.74273	2.77759	2.8148	2.85458	2.89717	2.94289
55	2.71202	2.74439	2.7788	2.81544	2.85452	2.89626	2.94093	2.98884	3.04033
56	2.78046	2.81666	2.85519	2.89624	2.94008	2.98697	3.03723	3.09122	3.14935
57	2.85643	2.89696	2.94013	2.9862	3.03546	3.08823	3.14491	3.2059	3.27173
58	2.94089	2.98632	3.03478	3.08658	3.14206	3.20162	3.2657	3.33484	3.40964
59	3.035	3.08602	3.14055	3.19893	3.2616	3.32902	3.40175	3.48042	3.56578
60	3.14012	3.19758	3.2591	3.32512	3.39615	3.47276	3.55564	3.64558	3.74349
61	3.25791	3.32281	3.39247	3.46741	3.54825	3.63572	3.73064	3.83402	3.947
62	3.39038	3.46397	3.54317	3.62861	3.72109	3.82148	3.93085	4.05043	4.18173
63	3.54	3.62382	3.7143	3.81225	3.91864	4.0346	4.16148	4.30087	4.45472
64	3.70982	3.8058	3.90977	4.02276	4.146	4.28094	4.42933	4.59327	4.77532
65	3.90368	4.01427	4.13455	4.26584	4.40974	4.56815	4.74337	4.93822	5.15618
66	4.12647	4.25481	4.39505	4.54894	4.71856	4.90645	5.11572	5.35024	5.61487
67	4.38447	4.53469	4.69975	4.88195	5.08412	5.30974	5.56312	5.84972	6.17652
68	4.68598	4.86358	5.05998	5.27833	5.52255	5.79751	6.10941	6.46622	6.87839
69	5.04207	5.25455	5.49134	5.75684	6.05665	6.39787	6.78972	7.24435	7.77815
70	5.46796	5.72584	6.01587	6.34448	6.71992	7.15297	7.65802	8.25462	8.97014
71	5.98508	6.30354	6.66577	7.08148	7.56347	8.12898	8.80179	9.61561	10.61995
72	6.62465	7.02646	7.48999	8.03068	8.66955	9.43605	10.37267	11.54311	13.04738
73	7.43395	7.95486	8.56677	9.29584	10.17934	11.27215	12.65866	14.47568	16.96047
74	8.48816	9.18766	10.02937	11.06159	12.35734	14.03233	16.28166	19.46182	24.3013
75	9.91461	10.89947	12.12483	13.6911	15.76365	18.63537	22.87898	29.78604	43.01068
76	11.94731	13.42991	15.36827	18.0109	21.82703	27.82162	38.60537	63.73509	188.704
77	15.06842	17.53896	21.04196	26.39591	35.59513	55.10431	124.3507	999.999	78.97015
78	20.45572	25.34895	33.47048	49.589	96.97487	999.999	101.6561	49.65434	32.68222
79	31.94518	45.8756	82.19857	999.999	133.4725	57.06535	36.10819	26.31058	20.63316
80	73.23903	243.9123	179.4678	65.08543	39.55686	28.31123	21.98194	17.92329	15.09923
81	248.4354	73.49019	42.92273	30.2125	23.24865	18.85258	15.82507	13.6131	11.92625
82	46.09223	31.96419	24.40628	19.6998	16.48704	14.1542	12.38328	10.99306	9.87269
83	25.43275	20.4518	17.07639	14.63786	12.79358	11.34988	10.189	9.23523	8.43768
84	17.58742	15.05998	13.15401	11.6653	10.47028	9.48982	8.67086	7.97652	7.38036
85	13.46313	11.93808	10.71545	9.71332	8.87694	8.1683	7.56018	7.0326	6.57055
86	10.92445	9.90559	9.0557	8.33591	7.71845	7.18291	6.71399	6.29997	5.93174
87	9.20755	8.47963	7.8553	7.31388	6.83987	6.42138	6.04919	5.716	5.41599
88	7.97132	7.42596	6.94849	6.52696	6.15205	5.81642	5.51419	5.24059	4.99174
89	7.04048	6.61719	6.2407	5.90362	5.60007	5.32525	5.07526	4.84687	4.63739
90	6.31574	5.97811	5.67402	5.3987	5.14822	4.91937	4.70943	4.51615	4.33762

Table 30. Error factor (cont.)

θ / ϕ	27	28	29	30	31	32	33	34	35
0	4.17221	4.01852	3.87535	3.74166	3.61653	3.49918	3.38891	3.28511	3.18723
1	3.93804	3.80424	3.67899	3.5615	3.45107	3.34709	3.24901	3.15635	3.06869
2	3.73502	3.61766	3.50732	3.4034	3.30536	3.21272	3.12505	3.04196	2.96311
3	3.55775	3.45412	3.35633	3.2639	3.17642	3.09348	3.01476	2.93994	2.86876
4	3.402	3.30997	3.22284	3.14024	3.06181	2.98725	2.91629	2.84868	2.7842
5	3.26444	3.1823	3.10431	3.03015	2.95956	2.89229	2.82811	2.76683	2.70825
6	3.14237	3.06874	2.99864	2.93182	2.86806	2.80717	2.74895	2.69324	2.63989
7	3.03363	2.96737	2.90414	2.84373	2.78597	2.73069	2.67774	2.62698	2.57828
8	2.93644	2.87661	2.81939	2.76462	2.71215	2.66185	2.61358	2.56724	2.52271
9	2.84932	2.79513	2.74322	2.69344	2.64567	2.5998	2.55572	2.51334	2.47256
10	2.77104	2.72185	2.67464	2.6293	2.58573	2.54382	2.50351	2.46469	2.42731
11	2.70059	2.65583	2.61281	2.57144	2.53163	2.49331	2.45639	2.42081	2.38651
12	2.63708	2.59628	2.55702	2.51923	2.48281	2.44772	2.41388	2.38125	2.34977
13	2.57978	2.54254	2.50667	2.4721	2.43877	2.40661	2.37559	2.34565	2.31675
14	2.52807	2.49404	2.46124	2.4296	2.39906	2.3696	2.34115	2.31368	2.28716
15	2.4814	2.45029	2.42027	2.3913	2.36334	2.33633	2.31026	2.28507	2.26076
16	2.4393	2.41085	2.38339	2.35687	2.33127	2.30653	2.28265	2.25959	2.23732
17	2.40139	2.37538	2.35026	2.326	2.30257	2.27995	2.2581	2.23701	2.21666
18	2.36732	2.34355	2.32059	2.29842	2.27702	2.25635	2.23641	2.21717	2.19862
19	2.33679	2.31509	2.29413	2.27391	2.25439	2.23556	2.21741	2.19991	2.18306
20	2.30953	2.28976	2.27068	2.25227	2.23452	2.21742	2.20095	2.1851	2.16987
21	2.28534	2.26736	2.25004	2.23334	2.21726	2.20179	2.18692	2.17264	2.15896
22	2.26401	2.24773	2.23205	2.21696	2.20247	2.18855	2.1752	2.16243	2.15023
23	2.24538	2.2307	2.21658	2.20303	2.19004	2.1776	2.16573	2.1544	2.14364
24	2.22932	2.21614	2.20352	2.19143	2.17989	2.16888	2.15842	2.1485	2.13913
25	2.2157	2.20397	2.19277	2.18209	2.17194	2.16232	2.15323	2.14468	2.13668
26	2.20442	2.19408	2.18425	2.17494	2.16614	2.15786	2.15012	2.14291	2.13626
27	2.19541	2.18641	2.17791	2.16992	2.16244	2.15549	2.14907	2.14319	2.13788
28	2.1886	2.1809	2.1737	2.16701	2.16083	2.15518	2.15007	2.14552	2.14155
29	2.18394	2.17752	2.1716	2.16618	2.16129	2.15694	2.15313	2.14991	2.14728
30	2.1814	2.17624	2.17158	2.16744	2.16383	2.16077	2.15828	2.15639	2.15513
31	2.18096	2.17705	2.17365	2.17077	2.16845	2.1667	2.16554	2.16501	2.16514
32	2.18263	2.17996	2.17782	2.17622	2.1752	2.17477	2.17497	2.17583	2.17739
33	2.18641	2.18499	2.18412	2.18382	2.18412	2.18504	2.18663	2.18892	2.19196
34	2.19232	2.19217	2.19259	2.19361	2.19527	2.19759	2.20061	2.20439	2.20897
35	2.20042	2.20156	2.2033	2.20568	2.20873	2.21249	2.21701	2.22234	2.22854
36	2.21075	2.21321	2.21632	2.22011	2.22461	2.22987	2.23595	2.24291	2.25082
37	2.22338	2.22722	2.23175	2.23699	2.24301	2.24985	2.25758	2.26627	2.27598
38	2.23842	2.24369	2.24969	2.25647	2.26408	2.27259	2.28207	2.29259	2.30424
39	2.25597	2.26273	2.27028	2.27868	2.28798	2.29827	2.3096	2.32209	2.33582
40	2.27616	2.28449	2.29368	2.3038	2.3149	2.32708	2.34042	2.35502	2.371
41	2.29915	2.30915	2.32008	2.33203	2.34506	2.35928	2.37478	2.39167	2.4101
42	2.32511	2.33689	2.34969	2.36361	2.37872	2.39514	2.41298	2.43238	2.45348
43	2.35425	2.36794	2.38276	2.3988	2.41617	2.43499	2.45539	2.47752	2.50156
44	2.38683	2.40257	2.41957	2.43792	2.45775	2.47919	2.5024	2.52755	2.55484
45	2.42311	2.44109	2.46046	2.48134	2.50386	2.52818	2.55449	2.58299	2.6139
46	2.46342	2.48384	2.50581	2.52946	2.55495	2.58247	2.61222	2.64444	2.6794
47	2.50814	2.53124	2.55607	2.58278	2.61157	2.64263	2.67623	2.71262	2.75213
48	2.5577	2.58376	2.61175	2.64187	2.67432	2.70936	2.74727	2.78837	2.83304

Table 30. Error factor (cont.)

θ / ϕ	27	28	29	30	31	32	33	34	35
42	2.32511	2.33689	2.34969	2.36361	2.37872	2.39514	2.41298	2.43238	2.45348
43	2.35425	2.36794	2.38276	2.3988	2.41617	2.43499	2.45539	2.47752	2.50156
44	2.38683	2.40257	2.41957	2.43792	2.45775	2.47919	2.5024	2.52755	2.55484
45	2.42311	2.44109	2.46046	2.48134	2.50386	2.52818	2.55449	2.58299	2.6139
46	2.46342	2.48384	2.50581	2.52946	2.55495	2.58247	2.61222	2.64444	2.6794
47	2.50814	2.53124	2.55607	2.58278	2.61157	2.64263	2.67623	2.71262	2.75213
48	2.5577	2.58376	2.61175	2.64187	2.67432	2.70936	2.74727	2.78837	2.83304
49	2.61262	2.64195	2.67346	2.70738	2.74395	2.78346	2.82625	2.87268	2.92322
50	2.67347	2.70646	2.74192	2.7801	2.82131	2.86589	2.91421	2.96674	3.02401
51	2.74095	2.77804	2.81794	2.86095	2.90743	2.95777	3.01243	3.07197	3.13702
52	2.81587	2.85759	2.90252	2.95103	3.00351	3.06046	3.12244	3.19008	3.26418
53	2.89919	2.94616	2.99683	3.05162	3.11103	3.17562	3.24607	3.32318	3.40789
54	2.99204	3.04503	3.10229	3.16432	3.23173	3.30521	3.38559	3.47384	3.57113
55	3.0958	3.15571	3.22057	3.29103	3.36779	3.4517	3.5438	3.64528	3.75761
56	3.2121	3.28003	3.35377	3.43408	3.52185	3.61813	3.72419	3.84156	3.9721
57	3.34295	3.42025	3.50442	3.59637	3.69723	3.80831	3.93121	4.06788	4.22071
58	3.4908	3.57916	3.67568	3.78154	3.89812	4.02711	4.17055	4.33097	4.51151
59	3.6587	3.76021	3.87155	3.99418	4.12988	4.28082	4.44967	4.63978	4.85534
60	3.85047	3.96782	4.09712	4.24024	4.39949	4.57773	4.77853	5.00637	5.26706
61	4.07098	4.20763	4.35897	4.52747	4.7162	4.92898	5.17067	5.44751	5.76768
62	4.32653	4.487	4.66582	4.86629	5.09256	5.34988	5.64508	5.98707	6.38786
63	4.62538	4.81575	5.02942	5.2709	5.54598	5.86211	6.22916	6.6604	7.17416
64	4.97866	5.20721	5.46595	5.76125	6.10139	6.49735	6.964	7.52201	8.20094
65	5.4016	5.68	5.99846	6.36627	6.79578	7.30387	7.91414	8.6607	9.5947
66	5.91576	6.26091	6.6608	7.12953	7.68646	8.35897	9.18705	10.23149	11.58948
67	6.55259	6.98994	7.50485	8.11987	8.86724	9.79468	10.97597	12.53149	14.67201
68	7.35983	7.9296	8.61438	9.45282	10.50303	11.85661	13.66687	16.21125	20.04886
69	8.41375	9.18328	10.13399	11.33826	12.91293	15.05958	18.15842	23.02242	31.7578
70	9.84402	10.93531	12.33655	14.20145	16.80541	20.69567	27.13661	39.85687	76.75717
71	11.89052	13.54927	15.80595	19.05462	24.13287	33.19044	53.91249	149.5287	183.1054
72	15.05197	17.85611	22.05697	29.04337	42.9578	84.22943	999.999	85.25615	41.77368
73	20.56391	26.2605	36.61954	61.32672	197.2923	155.9859	55.1316	33.20031	23.606
74	32.55681	49.8168	108.477	999.999	76.03038	40.51901	27.44102	20.64243	16.47685
75	78.523	999.999	112.4731	49.96993	31.90322	23.31327	18.29346	15.00146	12.67656
76	189.6393	62.37588	37.0631	26.22954	20.21517	16.38979	13.74263	11.80227	10.3192
77	42.97394	29.36721	22.21642	17.80814	14.81874	12.65834	11.02429	9.74529	8.71713
78	24.26255	19.23194	15.88712	13.50247	11.71657	10.3292	9.22047	8.31422	7.55974
79	16.92854	14.32072	12.38551	10.8925	9.70576	8.73989	7.93858	7.26316	6.6862
80	13.02084	11.42727	10.16665	9.14456	8.2992	7.58846	6.98261	6.46009	6.00488
81	10.59738	9.52349	8.63766	7.89449	7.26214	6.71758	6.24377	5.8278	5.45975
82	8.95056	8.17834	7.52224	6.95794	6.46745	6.03722	5.65682	5.31811	5.01463
83	7.76087	7.17932	6.67426	6.23155	5.84034	5.49215	5.1803	4.8994	4.6451
84	6.86292	6.4096	6.00917	5.6529	5.33389	5.0466	4.78655	4.55006	4.33409
85	6.16253	5.79959	5.47465	5.18206	4.91722	4.67639	4.45645	4.25482	4.06932
86	5.60209	5.30527	5.03661	4.79228	4.56915	4.36456	4.17633	4.00257	3.84171
87	5.14442	4.89744	4.67186	4.46501	4.27466	4.09892	3.93619	3.78508	3.64441
88	4.76442	4.55596	4.36409	4.18692	4.02283	3.87043	3.72852	3.59606	3.47215
89	4.44456	4.26648	4.10151	3.94826	3.80552	3.67226	3.54758	3.43067	3.32085
90	4.17221	4.01852	3.87535	3.74166	3.61653	3.49918	3.38891	3.28511	3.18723

Table 30. Error factor (cont.)

θ / ϕ	36	37	38	39	40	41	42	43	44
0	3.09479	3.00736	2.92455	2.84603	2.77148	2.70063	2.63322	2.56903	2.50785
1	2.98564	2.90685	2.83202	2.76087	2.69315	2.62863	2.5671	2.50839	2.45231
2	2.8882	2.81694	2.74909	2.68442	2.62273	2.56382	2.50754	2.45371	2.40221
3	2.80095	2.7363	2.6746	2.61566	2.55932	2.50542	2.45382	2.40439	2.35702
4	2.72264	2.66382	2.60756	2.55372	2.50216	2.45274	2.40536	2.3599	2.31626
5	2.65221	2.59855	2.54715	2.49787	2.45059	2.40521	2.36164	2.31977	2.27954
6	2.58876	2.53972	2.49266	2.44747	2.40406	2.36234	2.32222	2.28363	2.24651
7	2.53154	2.48664	2.44349	2.402	2.36209	2.32369	2.28673	2.25114	2.21688
8	2.47991	2.43874	2.39913	2.36099	2.32427	2.28891	2.25483	2.22201	2.19037
9	2.43332	2.39553	2.35913	2.32406	2.29025	2.25767	2.22626	2.19597	2.16678
10	2.3913	2.35658	2.32312	2.29084	2.25972	2.2297	2.20075	2.17283	2.14591
11	2.35344	2.32153	2.29076	2.26106	2.23241	2.20477	2.1781	2.15239	2.1276
12	2.31939	2.29007	2.26177	2.23446	2.2081	2.18267	2.15814	2.13449	2.11169
13	2.28885	2.26191	2.23591	2.21081	2.18659	2.16322	2.14069	2.11899	2.09808
14	2.26155	2.23683	2.21296	2.18992	2.1677	2.14628	2.12564	2.10577	2.08666
15	2.23728	2.21461	2.19274	2.17164	2.1513	2.13171	2.11286	2.09474	2.07735
16	2.21582	2.19509	2.17509	2.15582	2.13726	2.11941	2.10227	2.08583	2.07009
17	2.19703	2.17811	2.15988	2.14234	2.12548	2.10929	2.09379	2.07896	2.06481
18	2.18075	2.16354	2.147	2.1311	2.11587	2.10128	2.08735	2.07408	2.06148
19	2.16686	2.15129	2.13635	2.12203	2.10836	2.09531	2.08291	2.07117	2.06009
20	2.15526	2.14125	2.12785	2.11506	2.1029	2.09135	2.08045	2.07019	2.06061
21	2.14586	2.13336	2.12145	2.11014	2.09945	2.08937	2.07993	2.07116	2.06306
22	2.13861	2.12756	2.1171	2.10724	2.09798	2.08936	2.08137	2.07406	2.06745
23	2.13344	2.12382	2.11477	2.10633	2.0985	2.0913	2.08477	2.07893	2.07381
24	2.13033	2.12209	2.11445	2.10741	2.10099	2.09523	2.09015	2.08579	2.08219
25	2.12924	2.12239	2.11613	2.11048	2.10549	2.10117	2.09756	2.0947	2.09264
26	2.13018	2.12469	2.11982	2.11558	2.11201	2.10915	2.10703	2.10571	2.10525
27	2.13315	2.12903	2.12555	2.12273	2.12061	2.11923	2.11865	2.11892	2.1201
28	2.13817	2.13543	2.13336	2.13198	2.13134	2.1315	2.1325	2.13441	2.1373
29	2.14528	2.14394	2.1433	2.1434	2.14429	2.14602	2.14867	2.1523	2.157
30	2.15452	2.15461	2.15545	2.15707	2.15954	2.16293	2.16729	2.17273	2.17933
31	2.16596	2.16753	2.16989	2.1731	2.17722	2.18233	2.18851	2.19586	2.20449
32	2.17969	2.18279	2.18673	2.1916	2.19746	2.20439	2.21249	2.22188	2.23267
33	2.1958	2.20049	2.2061	2.21271	2.2204	2.22927	2.23943	2.251	2.26413
34	2.21441	2.22078	2.22815	2.23661	2.24625	2.25719	2.26955	2.28347	2.29914
35	2.23567	2.24381	2.25305	2.26347	2.27521	2.28837	2.30311	2.31959	2.33802
36	2.25974	2.26976	2.28099	2.29354	2.30752	2.3231	2.34042	2.3597	2.38115
37	2.28681	2.29886	2.31223	2.32706	2.34348	2.36168	2.38183	2.40417	2.42896
38	2.31711	2.33133	2.34702	2.36433	2.38341	2.40448	2.42774	2.45347	2.48195
39	2.35091	2.36748	2.38569	2.4057	2.4277	2.45193	2.47863	2.50811	2.54073
40	2.38849	2.40763	2.42859	2.45157	2.47679	2.50452	2.53505	2.56873	2.60598
41	2.4302	2.45215	2.47615	2.50241	2.5312	2.56282	2.59763	2.63603	2.67851
42	2.47645	2.5015	2.52885	2.55876	2.59153	2.62752	2.66713	2.71086	2.75929
43	2.52771	2.55619	2.58727	2.62125	2.65849	2.69939	2.74446	2.79426	2.84948
44	2.58451	2.61682	2.65207	2.69063	2.7329	2.77939	2.83066	2.88741	2.95047
45	2.6475	2.68409	2.72405	2.76778	2.81577	2.86862	2.92701	2.99178	3.06392
46	2.71741	2.75884	2.80412	2.85373	2.90827	2.96843	3.03505	3.10913	3.19189
47	2.79513	2.84205	2.89339	2.94974	3.01181	3.08044	3.15663	3.24162	3.33691
48	2.88171	2.93489	2.99319	3.05731	3.12811	3.2066	3.29403	3.39191	3.50212

Table 30. Error factor (cont.)

θ / ϕ	36	37	38	39	40	41	42	43	44
42	2.47645	2.5015	2.52885	2.55876	2.59153	2.62752	2.66713	2.71086	2.75929
43	2.52771	2.55619	2.58727	2.62125	2.65849	2.69939	2.74446	2.79426	2.84948
44	2.58451	2.61682	2.65207	2.69063	2.7329	2.77939	2.83066	2.88741	2.95047
45	2.6475	2.68409	2.72405	2.76778	2.81577	2.86862	2.92701	2.99178	3.06392
46	2.71741	2.75884	2.80412	2.85373	2.90827	2.96843	3.03505	3.10913	3.19189
47	2.79513	2.84205	2.89339	2.94974	3.01181	3.08044	3.15663	3.24162	3.33691
48	2.88171	2.93489	2.99319	3.05731	3.12811	3.2066	3.29403	3.39191	3.50212
49	2.97838	3.03876	3.1051	3.17825	3.25925	3.34936	3.45009	3.56336	3.69152
50	3.08664	3.15537	3.23107	3.3148	3.40783	3.51171	3.62837	3.76019	3.91021
51	3.20832	3.28679	3.37349	3.46971	3.57706	3.69747	3.83338	3.98786	4.16486
52	3.34564	3.43557	3.5353	3.64644	3.771	3.91146	4.07095	4.25349	4.46428
53	3.50134	3.6049	3.72022	3.84937	3.99488	4.15998	4.34877	4.56658	4.82048
54	3.67887	3.79879	3.933	4.08412	4.25548	4.4513	4.67709	4.9401	5.25013
55	3.88258	4.02238	4.17974	4.35809	4.56182	4.79662	5.07002	5.39218	5.77712
56	4.11808	4.28236	4.46851	4.68111	4.92611	5.21135	5.54744	5.94902	6.43698
57	4.39268	4.58755	4.81013	5.06665	5.36537	5.71743	6.13829	6.64995	7.28491
58	4.71614	4.94993	5.21949	5.53354	5.90394	6.34708	6.88643	7.5567	8.41154
59	5.10176	5.38608	5.71763	6.10907	6.57801	7.1497	7.86167	8.77218	9.97688
60	5.56814	5.91967	6.33532	6.83419	7.44375	8.20506	9.18227	10.48158	12.29236
61	6.14211	6.58572	7.11941	7.77345	8.59336	9.65084	11.06582	13.05516	16.05546
62	6.86386	7.43826	8.14483	9.03472	10.1894	11.74689	13.96118	17.35648	23.21658
63	7.79642	8.56538	9.53947	10.81289	12.54781	15.04932	18.96717	25.97412	42.0861
64	9.04462	10.12093	11.54097	13.49983	16.37462	21.00114	29.67613	51.82671	227.6151
65	10.79652	12.4001	14.64646	18.01749	23.63692	34.87258	68.5223	999.999	66.73631
66	13.42665	16.05002	20.10004	27.17177	42.64965	103.42	220.1038	52.07142	29.1316
67	17.80301	22.81709	32.13954	55.49207	220.5863	106.8436	42.24777	26.03523	18.66039
68	26.49949	39.60415	80.59918	999.999	69.49033	35.25259	23.39633	17.38359	13.74997
69	52.03376	151.1488	158.0197	50.95721	30.04681	21.13773	16.20347	13.07037	10.9054
70	999.999	83.10591	39.92118	26.04089	19.19522	15.11885	12.41506	10.49128	9.05317
71	55.84661	32.62165	22.87616	17.51596	14.12573	11.78882	10.08099	8.77888	7.75374
72	27.45073	20.32229	16.05671	13.2185	11.1945	9.67881	8.50173	7.5616	6.79374
73	18.22492	14.78214	12.39078	10.63345	9.28793	8.22499	7.3644	6.65368	6.05709
74	13.66334	11.63595	10.10596	8.91064	7.9513	7.16459	6.50801	5.95195	5.47519
75	10.94749	9.6115	8.54847	7.68274	6.96426	6.3586	5.84131	5.39453	5.00494
76	9.14902	8.20236	7.42094	6.76514	6.20708	5.72659	5.30868	4.94203	4.61787
77	7.87275	7.16706	6.56863	6.05486	5.60909	5.21879	4.87433	4.56819	4.29443
78	6.92197	6.37587	5.90311	5.48995	5.12589	4.80277	4.51414	4.25485	4.02074
79	6.18773	5.75283	5.37016	5.03092	4.72819	4.45646	4.21128	3.98902	3.78668
80	5.60483	5.25055	4.93468	4.65135	4.39586	4.16435	3.95367	3.76119	3.58472
81	5.13184	4.8379	4.57295	4.33297	4.11464	3.91521	3.73238	3.56422	3.40909
82	4.74119	4.4936	4.26838	4.06269	3.87414	3.70071	3.5407	3.39267	3.25535
83	4.41382	4.20261	4.009	3.83091	3.66659	3.51454	3.37347	3.24228	3.12
84	4.13612	3.95401	3.78595	3.63042	3.48609	3.35184	3.22666	3.10972	3.00025
85	3.89812	3.73965	3.59257	3.45571	3.32807	3.20879	3.09709	2.9923	2.89384
86	3.69237	3.55337	3.42371	3.30249	3.18893	3.08237	2.98219	2.88788	2.79894
87	3.51314	3.39038	3.27536	3.16737	3.06581	2.97015	2.87992	2.79467	2.71405
88	3.35601	3.24694	3.14433	3.04765	2.9564	2.87016	2.78855	2.71124	2.6379
89	3.21749	3.12007	3.02809	2.94113	2.8588	2.78076	2.70671	2.63636	2.56946
90	3.09479	3.00736	2.92455	2.84603	2.77148	2.70063	2.63322	2.56903	2.50785

Table 30. Error factor (cont.)

θ / ϕ	45	56	47	48	48	50	51	52	53
0	2.44949	2.39379	2.34058	2.28974	2.24112	2.19462	2.15012	2.10752	2.06673
1	2.39871	2.34746	2.29842	2.25148	2.20653	2.16347	2.1222	2.08265	2.04474
2	2.35291	2.30568	2.26042	2.21703	2.17543	2.13552	2.09724	2.06051	2.02527
3	2.31159	2.26802	2.22621	2.18607	2.14754	2.11054	2.07501	2.0409	2.00815
4	2.27437	2.23412	2.19546	2.15832	2.12262	2.08831	2.05535	2.02367	1.99325
5	2.24087	2.20368	2.16792	2.13353	2.10045	2.06865	2.03808	2.00869	1.98047
6	2.21079	2.17642	2.14333	2.1115	2.08087	2.0514	2.02307	1.99584	1.96969
7	2.18388	2.1521	2.12151	2.09205	2.0637	2.03643	2.01021	1.98502	1.96084
8	2.1599	2.13053	2.10226	2.07503	2.04883	2.02363	1.99941	1.97616	1.95386
9	2.13865	2.11154	2.08543	2.0603	2.03612	2.01289	1.99058	1.96918	1.9487
10	2.11997	2.09498	2.07091	2.04776	2.0255	2.00414	1.98365	1.96404	1.94532
11	2.10371	2.08071	2.05858	2.03731	2.01689	1.99731	1.97859	1.96071	1.94369
12	2.08975	2.06863	2.04834	2.02887	2.01021	1.99237	1.97534	1.95915	1.9438
13	2.07798	2.05866	2.04013	2.02238	2.00543	1.98926	1.9739	1.95936	1.94566
14	2.06832	2.05072	2.03389	2.01781	2.0025	1.98797	1.97424	1.96133	1.94927
15	2.06069	2.04476	2.02956	2.01511	2.00141	1.9885	1.97638	1.96509	1.95467
16	2.05505	2.04073	2.02713	2.01426	2.00216	1.99084	1.98033	1.97066	1.96189
17	2.05135	2.0386	2.02656	2.01527	2.00474	1.99501	1.9861	1.97808	1.97098
18	2.04957	2.03836	2.02787	2.01813	2.00918	2.00104	1.99376	1.9874	1.98202
19	2.04969	2.04001	2.03106	2.02287	2.0155	2.00897	2.00335	1.99869	1.99507
20	2.05172	2.04356	2.03615	2.02953	2.02375	2.01886	2.01493	2.01203	2.01025
21	2.05567	2.04903	2.04317	2.03814	2.03399	2.03079	2.02861	2.02753	2.02767
22	2.06157	2.05647	2.05218	2.04877	2.0463	2.04484	2.04447	2.04531	2.04746
23	2.06946	2.06592	2.06324	2.0615	2.06076	2.06111	2.06265	2.0655	2.06979
24	2.07939	2.07745	2.07644	2.07642	2.07749	2.07974	2.08329	2.08827	2.09484
25	2.09144	2.09116	2.09186	2.09365	2.09661	2.10087	2.10655	2.11381	2.12284
26	2.10569	2.10713	2.10964	2.11332	2.11828	2.12467	2.13262	2.14234	2.15402
27	2.12226	2.12549	2.1299	2.13558	2.14268	2.15134	2.16175	2.17411	2.18868
28	2.14127	2.1464	2.1528	2.16062	2.17	2.18111	2.19417	2.20942	2.22716
29	2.16286	2.17	2.17854	2.18864	2.20048	2.21425	2.2302	2.24862	2.26984
30	2.18721	2.19649	2.20733	2.2199	2.2344	2.25107	2.27019	2.29209	2.31718
31	2.21452	2.22611	2.23943	2.25467	2.27207	2.29192	2.31453	2.3403	2.3697
32	2.24502	2.25911	2.27511	2.29328	2.31387	2.33722	2.3637	2.39379	2.42803
33	2.27899	2.29578	2.31473	2.3361	2.36021	2.38745	2.41826	2.45318	2.49288
34	2.31673	2.33648	2.35866	2.38358	2.4116	2.44318	2.47884	2.51923	2.56514
35	2.3586	2.38162	2.40737	2.43622	2.46862	2.50507	2.54621	2.59281	2.64581
36	2.40503	2.43165	2.46138	2.49463	2.53194	2.5739	2.62127	2.67498	2.73615
37	2.45649	2.48713	2.5213	2.55951	2.60236	2.65059	2.70509	2.76698	2.83763
38	2.51356	2.5487	2.58787	2.63168	2.68085	2.73625	2.79897	2.87034	2.95207
39	2.57689	2.6171	2.66195	2.71214	2.76854	2.8322	2.90445	2.98693	3.08172
40	2.64729	2.69324	2.74454	2.80204	2.86679	2.94005	3.02345	3.11902	3.22935
41	2.72566	2.77817	2.83688	2.90282	2.97726	3.06176	3.15832	3.26946	3.39847
42	2.81311	2.87315	2.94043	3.01619	3.10198	3.19975	3.31198	3.44185	3.59358
43	2.91097	2.97972	3.05697	3.14424	3.24346	3.35704	3.48812	3.64078	3.82048
44	3.02084	3.09974	3.1887	3.28959	3.40482	3.53745	3.69148	3.87221	4.08688
45	3.14466	3.2355	3.33833	3.4555	3.59003	3.74587	3.9282	4.14406	4.40317
46	3.28484	3.38985	3.50926	3.64608	3.80418	3.98868	4.20645	4.46699	4.78371
47	3.44437	3.56635	3.70583	3.86666	4.05391	4.27435	4.53727	4.8558	5.24898
48	3.62701	3.76956	3.93362	4.12422	4.34807	4.61437	4.93599	5.33157	5.82915

Table 30. Error factor (cont.)

θ / ϕ	45	46	47	48	49	50	51	52	53
42	2.81311	2.87315	2.94043	3.01619	3.10198	3.19975	3.31198	3.44185	3.59358
43	2.91097	2.97972	3.05697	3.14424	3.24346	3.35704	3.48812	3.64078	3.82048
44	3.02084	3.09974	3.1887	3.28959	3.40482	3.53745	3.69148	3.87221	4.08688
45	3.14466	3.2355	3.33833	3.4555	3.59003	3.74587	3.9282	4.14406	4.40317
46	3.28484	3.38985	3.50926	3.64608	3.80418	3.98868	4.20645	4.46699	4.78371
47	3.44437	3.56635	3.70583	3.86666	4.05391	4.27435	4.53727	4.8558	5.24898
48	3.62701	3.76956	3.93362	4.12422	4.34807	4.61437	4.93599	5.33157	5.82915
49	3.83758	4.00538	4.19996	4.42802	4.6987	5.02474	5.42452	5.92549	6.57061
50	4.08231	4.28156	4.51467	4.79078	5.12262	5.52842	6.03534	6.68559	7.54862
51	4.36948	4.60853	4.8912	5.23027	5.64402	6.15951	6.81869	7.69005	8.89378
52	4.71023	5.00067	5.34852	5.77223	6.29908	6.97109	7.85668	9.07511	10.85454
53	5.11999	5.4783	5.91418	6.45533	7.14436	8.05036	9.29331	11.1014	13.9686
54	5.62072	6.07117	6.62988	7.34046	8.27356	9.55151	11.40632	14.3378	19.65705
55	6.24481	6.82467	7.56184	8.52943	9.85395	11.77521	14.80938	20.30846	33.30259
56	7.04206	7.81153	8.82197	10.20618	12.21629	15.39672	21.18027	34.94918	109.803
57	8.09323	9.15621	10.61536	12.74063	16.11902	22.31336	37.33228	126.3601	84.48579
58	9.53851	11.09081	13.36303	17.00324	23.76992	40.69318	158.9086	78.09446	30.53446
59	11.64455	14.10335	18.08729	25.64416	45.45533	234.0895	70.34223	29.85801	18.66341
60	14.98847	19.42516	28.08161	52.39852	999.999	62.34069	28.82664	18.48597	13.4631
61	21.09549	31.31575	63.09686	999.999	54.78695	27.53736	18.15595	13.41129	10.54981
62	35.74237	81.23235	253.0942	48.01502	26.08479	17.69945	13.27469	10.54304	8.69066
63	117.832	136.2155	42.12053	24.55117	17.14452	13.06401	10.4821	8.70297	7.40392
64	90.70542	37.07061	23.00175	16.51857	12.79126	10.3725	8.67754	7.42497	6.46257
65	32.77607	21.48419	15.84658	12.4688	10.22052	8.61762	7.41813	6.48766	5.7456
66	20.03059	15.15007	12.10859	10.03284	8.52696	7.38551	6.49126	5.77242	5.1826
67	14.44662	11.72168	9.81611	8.40959	7.32954	6.4748	5.78213	5.20995	4.72983
68	11.31783	9.57675	8.26963	7.25288	6.43999	5.77578	5.22333	4.75706	4.35866
69	9.32067	8.11115	7.15826	6.38868	5.75459	5.22354	4.77266	4.38543	4.04959
70	7.938	7.04845	6.32279	5.71993	5.21149	4.77724	4.40235	4.07572	3.78886
71	6.92611	6.24429	5.67321	5.18823	4.77153	4.40991	4.09339	3.81426	3.56649
72	6.15511	5.61589	5.15483	4.75633	4.4087	4.10301	3.83231	3.59112	3.37506
73	5.54942	5.11241	4.73248	4.39934	4.10504	3.84335	3.60932	3.39894	3.20897
74	5.06208	4.70087	4.38253	4.10002	3.84778	3.62135	3.41712	3.2321	3.06387
75	4.66238	4.35896	4.0885	3.84603	3.62757	3.42984	3.25016	3.08629	2.93635
76	4.32936	4.07105	3.83856	3.62832	3.43739	3.26335	3.10415	2.95809	2.82371
77	4.04827	3.82585	3.624	3.44008	3.27191	3.11765	2.97573	2.84482	2.72378
78	3.8084	3.61501	3.43825	3.27613	3.12699	2.98942	2.8622	2.74429	2.63478
79	3.60178	3.43223	3.27627	3.13241	2.99935	2.876	2.76141	2.65474	2.55527
80	3.4224	3.27266	3.13415	3.00573	2.88639	2.77526	2.67159	2.57471	2.48403
81	3.26558	3.13249	3.00878	2.89354	2.786	2.68545	2.59129	2.50299	2.42007
82	3.12768	3.00872	2.89766	2.79378	2.69645	2.60513	2.51932	2.43859	2.36254
83	3.0058	2.89894	2.79878	2.70475	2.61634	2.53312	2.45467	2.38065	2.31073
84	2.8976	2.80118	2.71049	2.62506	2.54449	2.46842	2.3965	2.32846	2.26403
85	2.80117	2.71384	2.63143	2.55356	2.47991	2.41018	2.3441	2.28142	2.22192
86	2.71497	2.63559	2.56046	2.48928	2.42178	2.35771	2.29685	2.23899	2.18396
87	2.6377	2.56532	2.49664	2.4314	2.36939	2.3104	2.25424	2.20075	2.14977
88	2.56827	2.5021	2.43915	2.37923	2.32215	2.26773	2.21583	2.1663	2.11901
89	2.50579	2.44514	2.38733	2.33218	2.27954	2.22927	2.18123	2.13532	2.09142
90	2.44949	2.39379	2.34058	2.28974	2.24112	2.19462	2.15012	2.10752	2.06673

Table 30. Error factor (cont.)

θ / ϕ	54	55	56	57	58	59	60	61	62
0	2.02767	1.99027	1.95444	1.92014	1.88729	1.85584	1.82574	1.79695	1.76942
1	2.0084	1.97357	1.94018	1.90819	1.87754	1.8482	1.82011	1.79325	1.76757
2	1.99146	1.95903	1.92794	1.89813	1.86958	1.84223	1.81607	1.79107	1.76719
3	1.97671	1.94655	1.91762	1.88988	1.86332	1.8379	1.8136	1.79039	1.76828
4	1.96405	1.93602	1.90914	1.88339	1.85873	1.83516	1.81266	1.79122	1.77083
5	1.95337	1.92737	1.90245	1.87859	1.85578	1.83401	1.81327	1.79356	1.77488
6	1.94459	1.92053	1.89749	1.87546	1.85444	1.83443	1.81541	1.79742	1.78045
7	1.93766	1.91546	1.89423	1.87398	1.85471	1.83642	1.81912	1.80283	1.78758
8	1.93252	1.91211	1.89265	1.87414	1.85658	1.84	1.82441	1.80984	1.79633
9	1.92913	1.91047	1.89273	1.87593	1.86007	1.84519	1.83132	1.81849	1.80676
10	1.92747	1.91052	1.89448	1.87936	1.86521	1.85204	1.8399	1.82885	1.81895
11	1.92753	1.91226	1.8979	1.88448	1.87202	1.86059	1.85023	1.84101	1.83301
12	1.92931	1.91571	1.90303	1.8913	1.88057	1.87091	1.86237	1.85504	1.84903
13	1.93282	1.92089	1.90989	1.89988	1.89092	1.88307	1.87642	1.87108	1.86716
14	1.93809	1.92783	1.91854	1.91029	1.90313	1.89717	1.8925	1.88924	1.88755
15	1.94515	1.93659	1.92905	1.92259	1.91732	1.91332	1.91073	1.90969	1.91038
16	1.95406	1.94723	1.94148	1.9369	1.93358	1.93166	1.93127	1.9326	1.93586
17	1.96488	1.95984	1.95595	1.95331	1.95205	1.95232	1.95429	1.95817	1.96422
18	1.97769	1.9745	1.97255	1.97196	1.97289	1.9755	1.98	1.98664	1.99575
19	1.99259	1.99133	1.99142	1.99301	1.99626	2.00139	2.00863	2.0183	2.03076
20	2.00969	2.01046	2.01272	2.01662	2.02238	2.03023	2.04047	2.05346	2.06964
21	2.02913	2.03206	2.03662	2.04301	2.05148	2.0623	2.07582	2.09248	2.11281
22	2.05107	2.05629	2.06333	2.07242	2.08383	2.09791	2.11507	2.13582	2.1608
23	2.07569	2.08338	2.0931	2.10511	2.11976	2.13743	2.15863	2.18396	2.2142
24	2.1032	2.11356	2.12619	2.14142	2.15963	2.1813	2.20701	2.23751	2.27373
25	2.13385	2.14712	2.16294	2.18171	2.20387	2.23001	2.26081	2.29718	2.34023
26	2.16793	2.18437	2.20372	2.22641	2.25299	2.28415	2.32072	2.36379	2.41472
27	2.20576	2.22571	2.24895	2.27603	2.30758	2.34442	2.38757	2.43835	2.49843
28	2.24773	2.27156	2.29916	2.33115	2.36832	2.41164	2.46235	2.52205	2.59283
29	2.29428	2.32244	2.35493	2.39248	2.43605	2.4868	2.54625	2.61637	2.69976
30	2.34594	2.37896	2.41696	2.46084	2.51173	2.57107	2.64071	2.72309	2.82148
31	2.4033	2.44181	2.48609	2.53721	2.59656	2.66588	2.74748	2.84442	2.96084
32	2.4671	2.51184	2.56329	2.62277	2.69194	2.77298	2.86876	2.98314	3.12143
33	2.53817	2.59005	2.64977	2.71894	2.79963	2.89453	3.00726	3.14276	3.30795
34	2.61753	2.67762	2.74695	2.82747	2.92176	3.03321	3.16643	3.32781	3.5265
35	2.70639	2.77601	2.85657	2.95049	3.061	3.19241	3.35068	3.54422	3.78533
36	2.80621	2.88698	2.98078	3.09067	3.22072	3.3765	3.56581	3.79991	4.09569
37	2.91879	3.01269	3.12226	3.25136	3.40523	3.59114	3.81949	4.10568	4.4735
38	3.04631	3.15585	3.28439	3.43687	3.62014	3.84386	4.12218	4.47668	4.94189
39	3.19152	3.31986	3.47146	3.65278	3.87287	4.14486	4.48848	4.93484	5.53595
40	3.35785	3.50904	3.68906	3.90645	4.17348	4.50835	4.9394	5.51311	6.31153
41	3.54971	3.72905	3.94459	4.20787	4.53589	4.95467	5.50629	6.26342	7.36323
42	3.77281	3.9873	4.24799	4.57084	4.98001	5.51404	6.23818	7.27258	8.86514
43	4.03469	4.29385	4.61307	5.01501	5.53532	6.2334	7.2162	8.6976	11.17651
44	4.34553	4.66256	5.05943	5.56944	6.24733	7.18979	8.585	10.8545	15.17718
45	4.71939	5.11317	5.61596	6.27881	7.19034	8.51913	10.63015	14.48797	23.74607
46	5.17629	5.6747	6.32708	7.21575	8.49429	10.48568	14.00487	21.87117	54.90583
47	5.74569	6.39177	7.26472	8.50661	10.4091	13.68049	20.60271	44.86071	174.2261
48	6.47286	7.33654	8.5536	10.39241	13.48444	19.75245	39.16167	999.999	33.69785

Table 30. Error factor (cont.)

θ / ϕ	54	55	56	57	58	59	60	61	62
42	3.77281	3.9873	4.24799	4.57084	4.98001	5.51404	6.23818	7.27258	8.86514
43	4.03469	4.29385	4.61307	5.01501	5.53532	6.2334	7.2162	8.6976	11.17651
44	4.34553	4.66256	5.05943	5.56944	6.24733	7.18979	8.585	10.8545	15.17718
45	4.71939	5.11317	5.61596	6.27881	7.19034	8.51913	10.63015	14.48797	23.74607
46	5.17629	5.6747	6.32708	7.21575	8.49429	10.48568	14.00487	21.87117	54.90583
47	5.74569	6.39177	7.26472	8.50661	10.4091	13.68049	20.60271	44.86071	174.2261
48	6.47286	7.33654	8.5536	10.39241	13.48444	19.75245	39.16167	999.999	33.69785
49	7.43106	8.63392	10.43052	13.39723	19.21187	35.6918	999.999	40.4934	18.68309
50	8.74716	10.52062	13.40671	18.91634	33.55417	187.5671	48.49781	20.78305	12.95047
51	10.66172	13.50613	18.82763	32.31406	133.8104	57.57212	22.91354	14.00569	9.93175
52	13.69301	18.92495	31.74734	111.7845	67.22092	24.98593	15.02789	10.58416	8.073
53	19.20042	31.74189	102.0273	76.46071	26.89217	15.98326	11.2034	8.52533	6.81644
54	32.25599	99.14379	83.87926	28.51596	16.83666	11.77336	8.95024	7.15358	5.9125
55	101.5995	88.04708	29.74975	17.55488	12.27848	9.33883	7.46851	6.17652	5.23272
56	88.16733	30.51385	18.11024	12.70494	9.68284	7.75579	6.42242	5.44705	4.70429
57	30.77145	18.48372	13.04173	9.97522	8.01052	6.6466	5.64637	4.88306	4.2828
58	18.66709	13.28162	10.21052	8.22861	6.84592	5.82816	5.04921	4.43511	3.93968
59	13.42163	10.38527	8.40698	7.01778	5.9903	5.20091	4.57665	4.07166	3.65566
60	10.49811	8.54371	7.16029	6.13103	5.33665	4.70608	4.19435	3.77163	3.41732
61	8.63811	7.27228	6.24912	5.4552	4.82225	4.30672	3.8795	3.5204	3.215
62	7.35338	6.3438	5.55569	4.92428	4.4079	3.97845	3.61636	3.30753	3.04156
63	6.41486	5.63761	5.01155	4.49722	4.06782	3.70453	3.39373	3.12532	2.89166
64	5.70084	5.0837	4.57422	4.14709	3.7844	3.47309	3.20343	2.96803	2.76115
65	5.14066	4.63865	4.21591	3.85555	3.54516	3.27546	3.03933	2.83124	2.64683
66	4.69047	4.2741	3.91771	3.60963	3.34104	3.10518	2.89674	2.71153	2.54616
67	4.32164	3.97076	3.66628	3.39993	3.16529	2.95734	2.77204	2.60617	2.45709
68	4.01468	3.71502	3.45195	3.21946	3.01278	2.82812	2.66237	2.51302	2.37796
69	3.75584	3.49703	3.26754	3.06291	2.87955	2.71453	2.56545	2.43031	2.30744
70	3.53518	3.30948	3.1076	2.92618	2.76247	2.61418	2.47943	2.35662	2.24439
71	3.34529	3.14682	2.96794	2.80607	2.65907	2.52516	2.40282	2.29076	2.18789
72	3.18059	3.00478	2.84526	2.70001	2.56736	2.44588	2.33436	2.23176	2.13717
73	3.03674	2.88001	2.73694	2.60595	2.48571	2.37507	2.27305	2.17879	2.09156
74	2.91035	2.76985	2.64088	2.52222	2.41278	2.31164	2.21801	2.13117	2.0505
75	2.79875	2.67214	2.55537	2.44743	2.34747	2.25472	2.16852	2.0883	2.01353
76	2.69976	2.58516	2.479	2.38046	2.28885	2.20353	2.12397	2.04968	1.98023
77	2.61161	2.50747	2.4106	2.32035	2.23614	2.15746	2.08385	2.0149	1.95025
78	2.53288	2.43789	2.34922	2.26631	2.1887	2.11596	2.0477	1.98359	1.92331
79	2.46235	2.37544	2.29402	2.21766	2.14596	2.07856	2.01514	1.95542	1.89913
80	2.39904	2.31928	2.24433	2.17382	2.10744	2.04487	1.98585	1.93013	1.87749
81	2.3421	2.26871	2.19955	2.13431	2.07273	2.01455	1.95954	1.90749	1.8582
82	2.29083	2.22314	2.15918	2.09871	2.04149	1.9873	1.93596	1.88728	1.8411
83	2.24462	2.18206	2.12281	2.06666	2.01341	1.96288	1.91491	1.86934	1.82603
84	2.20295	2.14503	2.09005	2.03784	1.98823	1.94106	1.8962	1.85352	1.81288
85	2.1654	2.11168	2.06059	2.01199	1.96571	1.92165	1.87968	1.83968	1.80155
86	2.13157	2.08169	2.03417	1.98887	1.94568	1.90449	1.8652	1.82771	1.79193
87	2.10115	2.05478	2.01053	1.96829	1.92796	1.88944	1.85266	1.81753	1.78397
88	2.07385	2.03071	1.98947	1.95007	1.91239	1.87638	1.84196	1.80905	1.77759
89	2.04943	2.00926	1.97083	1.93406	1.89887	1.86521	1.83301	1.8022	1.77275
90	2.02767	1.99027	1.95444	1.92014	1.88729	1.85584	1.82574	1.79695	1.76942

Table 30. Error factor (cont.)

θ / ϕ	63	64	65	66	67	68	69	70	71
0	1.74312	1.718	1.69404	1.6712	1.64946	1.62879	1.60916	1.59057	1.57297
1	1.74306	1.71968	1.69741	1.67624	1.65613	1.63709	1.6191	1.60215	1.58625
2	1.74443	1.72276	1.70217	1.68266	1.66421	1.64683	1.63053	1.61531	1.6012
3	1.74724	1.72726	1.70836	1.69052	1.67376	1.6581	1.64355	1.63015	1.61794
4	1.7515	1.73322	1.71601	1.69988	1.68485	1.67097	1.65827	1.64681	1.63666
5	1.75725	1.74068	1.72519	1.71081	1.69758	1.68557	1.67482	1.66544	1.65753
6	1.76453	1.74969	1.73596	1.7234	1.71206	1.70201	1.69336	1.68623	1.68077
7	1.7734	1.76033	1.74843	1.73775	1.72839	1.72046	1.71407	1.70939	1.70664
8	1.78393	1.77268	1.76268	1.75399	1.74675	1.74107	1.73714	1.73517	1.73544
9	1.79619	1.78685	1.77883	1.77226	1.76728	1.76405	1.76282	1.76385	1.76752
10	1.81028	1.80294	1.79703	1.79272	1.79018	1.78964	1.79138	1.79577	1.80327
11	1.82633	1.82109	1.81744	1.81556	1.81569	1.8181	1.82315	1.83131	1.84319
12	1.84445	1.84146	1.84024	1.84101	1.84406	1.84974	1.8585	1.87094	1.88784
13	1.86482	1.86424	1.86564	1.86931	1.87559	1.88492	1.89788	1.91521	1.9379
14	1.88761	1.88964	1.89391	1.90077	1.91064	1.92408	1.94181	1.96475	1.99419
15	1.91303	1.9179	1.92532	1.93572	1.94963	1.96772	1.9909	2.02035	2.05769
16	1.94132	1.9493	1.96022	1.97458	1.99303	2.01643	2.0459	2.08293	2.12962
17	1.97276	1.98419	1.999	2.01781	2.04143	2.07092	2.10768	2.15363	2.21144
18	2.00769	2.02294	2.04211	2.06597	2.0955	2.13203	2.17732	2.23382	2.30501
19	2.04647	2.06601	2.09011	2.11972	2.15605	2.20077	2.25612	2.32524	2.41264
20	2.08956	2.11393	2.14363	2.17983	2.22407	2.2784	2.34569	2.43001	2.53731
21	2.13747	2.16731	2.20343	2.24726	2.30072	2.36642	2.44803	2.55085	2.68284
22	2.19082	2.22691	2.27042	2.32313	2.38745	2.4667	2.56565	2.69127	2.85432
23	2.25032	2.2936	2.34569	2.40882	2.48603	2.58161	2.70176	2.85583	3.05854
24	2.31685	2.36844	2.43057	2.50602	2.59868	2.71412	2.86054	3.05061	3.30494
25	2.39144	2.45273	2.52667	2.61683	2.7282	2.86808	3.04748	3.2839	3.60684
26	2.47533	2.54801	2.63602	2.7439	2.87816	3.04851	3.26999	3.56729	3.98384
27	2.57006	2.65624	2.76113	2.89059	3.05323	3.26215	3.53832	3.91748	4.46589
28	2.67749	2.77982	2.90517	3.06124	3.25955	3.51815	3.86698	4.35947	5.10121
29	2.79995	2.9218	3.07227	3.26159	3.50548	3.8294	4.27734	4.93243	5.97275
30	2.94038	3.08608	3.26778	3.49931	3.8026	4.21452	4.80212	5.7014	7.2363
31	3.10251	3.27774	3.49885	3.78496	4.16744	4.70152	5.49413	6.78291	9.223
32	3.29121	3.50351	3.77524	4.13346	4.62447	5.33452	6.44447	8.40851	12.78267
33	3.51285	3.77251	4.11061	4.5666	5.21153	6.18739	7.82495	11.1131	20.9533
34	3.77606	4.0974	4.52467	5.11752	5.99034	7.39378	10.00288	16.47409	58.7296
35	4.09272	4.4963	5.04702	5.83916	7.06895	9.22298	13.92989	32.06424	72.78142
36	4.4797	4.99607	5.7241	6.82173	8.6552	12.31066	23.07096	999.999	22.49665
37	4.96175	5.6383	6.63334	8.23249	11.20663	18.60308	67.83162	35.60465	13.33633
38	5.57679	6.49102	7.91406	10.42025	15.96633	38.32814	71.87033	17.35567	9.50428
39	6.38587	7.67376	9.84474	14.25374	27.91714	999.999	23.51882	11.50351	7.40554
40	7.49415	9.41745	13.0748	22.66545	112.5171	33.99577	14.09072	8.62711	6.08529
41	9.09938	12.23396	19.55049	55.74443	55.32384	17.52482	10.08463	6.92202	5.18116
42	11.62277	17.52983	38.97908	120.4705	22.23359	11.83307	7.87416	5.79733	4.52539
43	16.14858	31.07818	999.999	28.97429	13.94181	8.95548	6.47722	5.00234	4.0297
44	26.57626	138.7133	39.21886	16.49809	10.17955	7.22348	5.51741	4.41251	3.64313
45	75.65787	56.23994	19.61034	11.55857	8.03725	6.06989	4.81946	3.95895	3.33427
46	89.02714	23.41035	13.10133	8.91737	6.65778	5.24883	4.29071	3.6005	3.08267
47	28.05154	14.81042	9.85961	7.27749	5.69799	4.63647	3.87757	3.31101	2.87444
48	16.67836	10.85564	7.92353	6.16326	4.99367	4.16362	3.54689	3.07308	2.69983

Table 30. Error factor (cont.)

θ / ϕ	63	64	65	66	67	68	69	70	71
42	11.62277	17.52983	38.97908	120.4705	22.23359	11.83307	7.87416	5.79733	4.52539
43	16.14858	31.07818	999.999	28.97429	13.94181	8.95548	6.47722	5.00234	4.0297
44	26.57626	138.7133	39.21886	16.49809	10.17955	7.22348	5.51741	4.41251	3.64313
45	75.65787	56.23994	19.61034	11.55857	8.03725	6.06989	4.81946	3.95895	3.33427
46	89.02714	23.41035	13.10133	8.91737	6.65778	5.24883	4.29071	3.6005	3.08267
47	28.05154	14.81042	9.85961	7.27749	5.69799	4.63647	3.87757	3.31101	2.87444
48	16.67836	10.85564	7.92353	6.16326	4.99367	4.16362	3.54689	3.07308	2.69983
49	11.89222	8.58826	6.63988	5.35909	4.45635	3.78861	3.27705	2.8747	2.55179
50	9.26173	7.12191	5.72887	4.75307	4.03417	3.48483	3.05337	2.70729	2.4251
51	7.60228	6.09848	5.05064	4.28131	3.69468	3.23449	2.86552	2.56458	2.3158
52	6.46283	5.3456	4.52751	3.90472	3.41657	3.02527	2.70601	2.44186	2.22084
53	5.6342	4.77006	4.11288	3.59801	3.18525	2.84832	2.56931	2.33555	2.13786
54	5.0061	4.31701	3.7771	3.3441	2.99039	2.69718	2.4512	2.24284	2.06495
55	4.51489	3.9521	3.50039	3.13104	2.82449	2.56696	2.34846	2.16156	2.00061
56	4.12125	3.6527	3.26908	2.95023	2.68196	2.45395	2.25855	2.08994	1.9436
57	3.79959	3.4033	3.07338	2.79531	2.55855	2.35525	2.17946	2.02656	1.89292
58	3.53254	3.19292	2.90613	2.66147	2.45097	2.26857	2.10958	1.97028	1.84772
59	3.30787	3.01356	2.76195	2.54502	2.35665	2.19209	2.04758	1.92014	1.80733
60	3.11677	2.85925	2.63674	2.44309	2.27354	2.12431	1.9924	1.87535	1.77116
61	2.95268	2.72548	2.5273	2.35339	2.19998	2.06405	1.94315	1.83526	1.73871
62	2.81064	2.60873	2.43112	2.27409	2.13463	2.0103	1.89908	1.79931	1.70958
63	2.68684	2.50624	2.34618	2.2037	2.07638	1.96223	1.85958	1.76704	1.68341
64	2.57828	2.41582	2.27086	2.14102	2.02433	1.91916	1.82412	1.73803	1.65989
65	2.4826	2.3357	2.20382	2.08503	1.97771	1.8805	1.79225	1.71197	1.63878
66	2.39789	2.26445	2.14398	2.0349	1.93587	1.84576	1.7636	1.68854	1.61985
67	2.32259	2.20088	2.09042	1.98992	1.89827	1.81452	1.73784	1.66751	1.6029
68	2.25545	2.14401	2.04239	1.94952	1.86446	1.78643	1.7147	1.64866	1.58777
69	2.19541	2.09302	1.99925	1.91318	1.83405	1.76116	1.69393	1.63181	1.57432
70	2.14159	2.04723	1.96044	1.88048	1.80669	1.73848	1.67533	1.61678	1.56242
71	2.09326	2.00605	1.92552	1.85106	1.7821	1.71813	1.65872	1.60346	1.55198
72	2.0498	1.96898	1.89409	1.8246	1.76002	1.69994	1.64395	1.59171	1.54289
73	2.01069	1.93561	1.86581	1.80083	1.74026	1.68372	1.63088	1.58144	1.53509
74	1.97546	1.90557	1.84039	1.77952	1.72261	1.66934	1.61941	1.57255	1.52851
75	1.94375	1.87856	1.81757	1.76046	1.70692	1.65666	1.60943	1.56498	1.52309
76	1.91521	1.8543	1.79715	1.74349	1.69305	1.64559	1.60086	1.55867	1.5188
77	1.88957	1.83256	1.77894	1.72846	1.68089	1.63602	1.59364	1.55356	1.51559
78	1.86658	1.81315	1.76277	1.71524	1.67034	1.62788	1.5877	1.54961	1.51345
79	1.84602	1.79588	1.74851	1.70371	1.6613	1.62112	1.583	1.5468	1.51236
80	1.82772	1.78063	1.73603	1.69378	1.6537	1.61566	1.5795	1.54509	1.5123
81	1.81151	1.76724	1.72525	1.68538	1.6475	1.61147	1.57718	1.54449	1.51329
82	1.79726	1.75563	1.71606	1.67843	1.64263	1.60852	1.57601	1.54498	1.51531
83	1.78485	1.74568	1.7084	1.67289	1.63906	1.60679	1.576	1.54657	1.51841
84	1.77419	1.73733	1.70221	1.66872	1.63676	1.60627	1.57713	1.54926	1.52258
85	1.76519	1.73052	1.69744	1.66587	1.63573	1.60694	1.57942	1.55309	1.52788
86	1.75778	1.72518	1.69406	1.66433	1.63594	1.60881	1.58288	1.55808	1.53433
87	1.75191	1.72129	1.69204	1.66409	1.6374	1.61191	1.58755	1.56426	1.542
88	1.74753	1.7188	1.69136	1.66515	1.64013	1.61624	1.59345	1.5717	1.55094
89	1.7446	1.71771	1.69203	1.66752	1.64414	1.62186	1.60064	1.58044	1.56124
90	1.74312	1.718	1.69404	1.6712	1.64946	1.62879	1.60916	1.59057	1.57297

Table 30. Error factor (cont.)

θ / ϕ	72	73	74	75	76	77	78	79	80
0	1.55637	1.54074	1.52607	1.51234	1.49955	1.48768	1.47673	1.46667	1.45752
1	1.5714	1.55759	1.54486	1.53322	1.52271	1.51338	1.5053	1.49857	1.49335
2	1.58821	1.5764	1.56581	1.55651	1.54861	1.54224	1.53757	1.53489	1.53457
3	1.60699	1.59736	1.58916	1.58252	1.57763	1.57472	1.57416	1.57643	1.58227
4	1.62792	1.62071	1.6152	1.6116	1.6102	1.61141	1.61579	1.62418	1.63782
5	1.65123	1.64672	1.64426	1.64416	1.64686	1.65297	1.66338	1.67938	1.703
6	1.67718	1.67573	1.67675	1.68071	1.68825	1.70025	1.71804	1.7436	1.7801
7	1.7061	1.7081	1.71314	1.72185	1.73514	1.75428	1.78121	1.81889	1.87218
8	1.73833	1.74429	1.75399	1.7683	1.78848	1.81634	1.85467	1.90787	1.9834
9	1.7743	1.78483	1.79997	1.82093	1.84943	1.88805	1.94076	2.0141	2.1195
10	1.81452	1.83035	1.85191	1.88082	1.91947	1.97146	2.04251	2.14234	2.28867
11	1.85959	1.88161	1.91078	1.9493	2.00043	2.06923	2.164	2.29929	2.50303
12	1.91023	1.93955	1.97783	2.02803	2.09466	2.18486	2.31076	2.49449	2.7812
13	1.9673	2.00528	2.05455	2.11912	2.20522	2.32305	2.49055	2.74218	3.15341
14	2.03185	2.08021	2.14286	2.22527	2.33615	2.49025	2.71459	3.0644	3.67212
15	2.10518	2.16606	2.24517	2.35001	2.4929	2.69552	2.99965	3.49733	4.43724
16	2.18889	2.26504	2.36461	2.49804	2.68301	2.95208	3.37206	4.10472	5.6652
17	2.28496	2.37993	2.50529	2.67572	2.91717	3.27992	3.8756	5.01038	7.92931
18	2.39595	2.51438	2.67269	2.89195	3.21112	3.71084	4.58882	6.49068	13.41132
19	2.52511	2.67319	2.87433	3.15945	3.58896	4.29856	5.66817	9.31446	44.80709
20	2.67671	2.86286	3.12081	3.4972	4.08964	5.14173	7.47654	16.72223	33.18003
21	2.85646	3.09236	3.42749	3.93472	4.78036	6.44321	11.09134	85.05025	12.14903
22	3.0721	3.37448	3.81759	4.52059	5.78803	8.6972	21.76987	27.48693	7.47843
23	3.3345	3.72804	4.32791	5.34085	7.38436	13.50554	999.999	11.87311	5.43738
24	3.65934	4.182	5.02047	6.56373	10.27517	30.63733	23.15839	7.61084	4.30109
25	4.0701	4.78324	6.00858	8.56852	17.04403	111.4543	11.43699	5.63286	3.58232
26	4.60368	5.61313	7.52375	12.42827	50.80252	19.79137	7.62924	4.49795	3.09021
27	5.32146	6.82621	10.12422	22.83253	51.50021	10.89796	5.75336	3.76642	2.73464
28	6.33374	8.75647	15.58576	144.8972	17.12139	7.55185	4.64277	3.25887	2.46755
29	7.86063	12.28444	34.20208	33.29907	10.30292	5.8051	3.91261	2.88838	2.26091
30	10.41398	20.72943	171.5807	14.9691	7.39844	4.73753	3.39887	2.60774	2.09733
31	15.52049	67.30234	24.47037	9.68736	5.79648	4.02113	3.01985	2.38907	1.96539
32	30.70903	53.78717	13.20936	7.18819	4.78597	3.5097	2.73027	2.21487	1.85735
33	999.999	19.24666	9.07637	5.73712	4.09361	3.12819	2.50301	2.0736	1.76773
34	31.79479	11.75274	6.93843	4.7931	3.59191	2.83412	2.32084	1.95732	1.69258
35	15.79129	8.48648	5.63689	4.13271	3.21338	2.60164	2.17229	1.86043	1.62897
36	10.53391	6.66388	4.76466	3.64691	2.91896	2.41412	2.04942	1.77883	1.57469
37	7.92775	5.50527	4.1419	3.27612	2.68445	2.26036	1.94657	1.70949	1.52804
38	6.37643	4.7067	3.67682	2.98503	2.49408	2.13256	1.85961	1.65011	1.48768
39	5.35088	4.12508	3.31769	2.75141	2.33712	2.02512	1.78544	1.5989	1.45258
40	4.62511	3.68424	3.03312	2.56054	2.20603	1.93392	1.72169	1.55446	1.4219
41	4.08634	3.33985	2.80296	2.40229	2.09535	1.85584	1.66655	1.5157	1.39497
42	3.67202	3.06441	2.61369	2.26947	2.00102	1.78851	1.61856	1.48174	1.37124
43	3.34464	2.8399	2.45589	2.15684	1.91998	1.73009	1.57658	1.45185	1.35025
44	3.08037	2.65407	2.3228	2.06048	1.84988	1.67911	1.53971	1.42545	1.33164
45	2.8633	2.49826	2.20945	1.97741	1.78886	1.63441	1.50718	1.40206	1.3151
46	2.68246	2.36621	2.11209	1.90532	1.73548	1.59504	1.4784	1.38128	1.30037
47	2.52998	2.25326	2.02788	1.84239	1.68855	1.56024	1.45285	1.36278	1.28723
48	2.40012	2.15587	1.95456	1.78718	1.64713	1.52938	1.43011	1.34628	1.2755

Table 30. Error factor (cont.)

θ / ϕ	72	73	74	75	76	77	78	78	80
42	3.67202	3.06441	2.61369	2.26947	2.00102	1.78851	1.61856	1.48174	1.37124
43	3.34464	2.8399	2.45589	2.15684	1.91998	1.73009	1.57658	1.45185	1.35025
44	3.08037	2.65407	2.3228	2.06048	1.84988	1.67911	1.53971	1.42545	1.33164
45	2.8633	2.49826	2.20945	1.97741	1.78886	1.63441	1.50718	1.40206	1.3151
46	2.68246	2.36621	2.11209	1.90532	1.73548	1.59504	1.4784	1.38128	1.30037
47	2.52998	2.25326	2.02788	1.84239	1.68855	1.56024	1.45285	1.36278	1.28723
48	2.40012	2.15587	1.95456	1.78718	1.64713	1.52938	1.43011	1.34628	1.2755
49	2.28856	2.07134	1.89038	1.73854	1.61043	1.50194	1.40983	1.33155	1.26503
50	2.19201	1.99751	1.83393	1.69551	1.57784	1.47748	1.39172	1.31838	1.25567
51	2.10791	1.93271	1.78408	1.65732	1.5488	1.45564	1.37553	1.3066	1.24733
52	2.03425	1.87558	1.73988	1.62333	1.52288	1.43611	1.36105	1.29609	1.23989
53	1.96941	1.825	1.70059	1.593	1.4997	1.41863	1.34809	1.28669	1.23329
54	1.9121	1.78007	1.66555	1.56589	1.47895	1.40297	1.3365	1.27833	1.22744
55	1.86125	1.74005	1.63425	1.54163	1.46037	1.38896	1.32615	1.27089	1.2223
56	1.816	1.70431	1.60623	1.51988	1.44371	1.37643	1.31693	1.26431	1.21779
57	1.77562	1.67233	1.58112	1.50038	1.42879	1.36523	1.30874	1.25852	1.2139
58	1.73951	1.64368	1.55859	1.4829	1.41544	1.35525	1.3015	1.25347	1.21056
59	1.70716	1.61797	1.53839	1.46724	1.40352	1.34639	1.29513	1.24909	1.20776
60	1.67814	1.5949	1.52027	1.45322	1.3929	1.33857	1.28957	1.24536	1.20547
61	1.65208	1.5742	1.50403	1.44071	1.38348	1.33169	1.28478	1.24224	1.20367
62	1.62869	1.55562	1.4895	1.42957	1.37516	1.32571	1.2807	1.2397	1.20234
63	1.60768	1.53897	1.47653	1.41969	1.36787	1.32056	1.27731	1.23772	1.20147
64	1.58883	1.52409	1.465	1.41099	1.36155	1.3162	1.27457	1.23629	1.20106
65	1.57195	1.51082	1.4548	1.40339	1.35612	1.3126	1.27246	1.23538	1.20109
66	1.55687	1.49903	1.44583	1.3968	1.35155	1.30971	1.27096	1.23499	1.20157
67	1.54343	1.48862	1.438	1.39119	1.3478	1.30752	1.27005	1.23513	1.20251
68	1.53152	1.47949	1.43126	1.38649	1.34484	1.30601	1.26974	1.23578	1.20391
69	1.52103	1.47156	1.42555	1.38267	1.34264	1.30517	1.27002	1.23696	1.20578
70	1.51186	1.46477	1.42081	1.3797	1.34118	1.30498	1.27088	1.23867	1.20815
71	1.50394	1.45905	1.41701	1.37756	1.34045	1.30545	1.27235	1.24093	1.21103
72	1.4972	1.45436	1.41412	1.37622	1.34045	1.30658	1.27442	1.24377	1.21444
73	1.49158	1.45067	1.41211	1.37568	1.34117	1.30838	1.27712	1.24719	1.21843
74	1.48704	1.44793	1.41096	1.37592	1.34262	1.31087	1.28047	1.25125	1.22302
75	1.48355	1.44614	1.41068	1.37697	1.34482	1.31406	1.2845	1.25597	1.22827
76	1.48106	1.44527	1.41125	1.37881	1.34778	1.31799	1.28925	1.26139	1.23423
77	1.47957	1.44532	1.41268	1.38147	1.35152	1.32268	1.29476	1.26758	1.24095
78	1.47907	1.44629	1.41498	1.38496	1.35609	1.32818	1.30108	1.27459	1.24851
79	1.47954	1.44819	1.41817	1.38933	1.36151	1.33454	1.30827	1.28249	1.257
80	1.48099	1.45103	1.42228	1.39459	1.36783	1.34182	1.3164	1.29137	1.26652
81	1.48344	1.45484	1.42734	1.40081	1.37511	1.35008	1.32555	1.30132	1.27717
82	1.48691	1.45964	1.43339	1.40803	1.38342	1.35941	1.33582	1.31246	1.2891
83	1.49141	1.46547	1.44048	1.41631	1.39283	1.3699	1.34733	1.32493	1.30246
84	1.49699	1.47239	1.44868	1.42574	1.40345	1.38166	1.3602	1.33888	1.31745
85	1.50369	1.48045	1.45805	1.43639	1.41536	1.39481	1.37459	1.35449	1.33428
86	1.51157	1.48971	1.46868	1.44838	1.4287	1.40951	1.39067	1.37198	1.35322
87	1.52069	1.50027	1.48068	1.46182	1.4436	1.42592	1.40865	1.39161	1.37459
88	1.53113	1.51222	1.49415	1.47685	1.46025	1.44426	1.42878	1.41368	1.39877
89	1.54299	1.52567	1.50923	1.49363	1.47882	1.46475	1.45136	1.43855	1.42623
90	1.55637	1.54074	1.52607	1.51234	1.49955	1.48768	1.47673	1.46667	1.45752

Table 30. Error factor (cont.)

θ / ϕ	81	82	83	84	85	86	87	88	89	90
0	1.44926	1.44188	1.43538	1.42975	1.425	1.42111	1.41809	1.41594	1.41464	1.2247
1	1.48985	1.48843	1.48965	1.49451	1.5049	1.52493	1.56554	1.66818	2.23662	1
2	1.5372	1.5437	1.55565	1.57591	1.61029	1.67269	1.80624	2.23825	999.999	1
3	1.59282	1.60996	1.63696	1.6801	1.7532	1.89319	2.24096	4.13496	2.23443	1
4	1.65873	1.69027	1.73864	1.81646	1.95397	2.24474	3.17502	999.999	1.41421	1
5	1.73756	1.78887	1.86813	1.99987	2.24957	2.86474	6.15509	4.09729	1.20226	1
6	1.83288	1.91175	2.03669	2.25543	2.71482	4.17084	999.999	2.22957	1.11861	1
7	1.94965	2.06771	2.2623	2.62893	3.52685	8.31645	5.9623	1.66473	1.0777	1
8	2.0949	2.27015	2.57532	3.21348	5.23048	205.497	3.12871	1.41423	1.0548	1
9	2.27895	2.54045	3.03148	4.23177	10.7249	7.70754	2.22158	1.28167	1.04076	1
10	2.5176	2.91506	3.74514	6.38214	131.645	4.02231	1.79612	1.20352	1.03154	1
11	2.83627	3.46137	4.99409	13.5677	9.2427	2.80113	1.55956	1.15382	1.02517	1
12	3.27856	4.31962	7.67403	91.5269	4.8672	2.21061	1.41428	1.12038	1.0206	1
13	3.92621	5.83765	17.1745	10.4922	3.36949	1.87252	1.31883	1.09687	1.0172	1
14	4.95224	9.18158	67.3373	5.63131	2.6292	1.65917	1.25294	1.07974	1.01461	1
15	6.79819	22.1828	11.4061	3.90482	2.19689	1.51561	1.20565	1.06689	1.01259	1
16	11.0255	51.6384	6.28879	3.03414	1.91898	1.41441	1.17065	1.05701	1.01098	1
17	30.0270	11.9693	4.39041	2.51755	1.7287	1.34051	1.14406	1.04927	1.00969	1
18	40.8765	6.82092	3.41258	2.18068	1.59244	1.28497	1.12342	1.04309	1.00863	1
19	12.2014	4.81318	2.82372	1.94698	1.49151	1.24225	1.1071	1.03809	1.00775	1
20	7.2177	3.75452	2.43497	1.77757	1.4147	1.20874	1.09398	1.03398	1.00702	1
21	5.16387	3.10718	2.16228	1.65064	1.35496	1.182	1.08329	1.03056	1.0064	1
22	4.0524	2.67475	1.96261	1.55305	1.30764	1.16034	1.07448	1.0277	1.00587	1
23	3.36159	2.36837	1.81161	1.47643	1.26956	1.14259	1.06713	1.02528	1.00542	1
24	2.89454	2.14202	1.6945	1.41522	1.2385	1.12787	1.06095	1.02322	1.00503	1
25	2.5604	1.96945	1.60183	1.36559	1.21286	1.11554	1.0557	1.02145	1.00469	1
26	2.31147	1.83462	1.52725	1.32484	1.19149	1.10512	1.05122	1.01991	1.0044	1
27	2.12025	1.72717	1.46637	1.291	1.17349	1.09624	1.04736	1.01858	1.00414	1
28	1.96984	1.64015	1.41608	1.26262	1.15822	1.08863	1.04402	1.01742	1.00391	1
29	1.84923	1.5687	1.37408	1.23863	1.14517	1.08207	1.04111	1.0164	1.00371	1
30	1.75098	1.50934	1.3387	1.21817	1.13394	1.07637	1.03857	1.01551	1.00354	1
31	1.66989	1.45954	1.30863	1.20062	1.12422	1.07141	1.03634	1.01472	1.00338	1
32	1.60219	1.41738	1.28291	1.18547	1.11576	1.06706	1.03438	1.01402	1.00324	1
33	1.54513	1.38141	1.26075	1.17231	1.10837	1.06323	1.03265	1.01341	1.00312	1
34	1.49663	1.35051	1.24155	1.16084	1.10189	1.05987	1.03111	1.01286	1.00301	1
35	1.45509	1.32381	1.22484	1.15079	1.09618	1.05689	1.02976	1.01237	1.00291	1
36	1.41927	1.3006	1.21022	1.14195	1.09114	1.05425	1.02855	1.01194	1.00283	1
37	1.38822	1.28033	1.19738	1.13415	1.08668	1.05191	1.02748	1.01156	1.00275	1
38	1.36115	1.26256	1.18607	1.12725	1.08272	1.04984	1.02654	1.01123	1.00269	1
39	1.33745	1.24691	1.17606	1.12114	1.07921	1.04799	1.0257	1.01093	1.00263	1
40	1.31661	1.2331	1.1672	1.11571	1.07609	1.04636	1.02496	1.01068	1.00258	1
41	1.29822	1.22086	1.15933	1.11088	1.07331	1.04491	1.02431	1.01045	1.00254	1
42	1.28195	1.20999	1.15234	1.10659	1.07085	1.04363	1.02374	1.01026	1.00251	1
43	1.26751	1.20033	1.14611	1.10277	1.06867	1.0425	1.02324	1.0101	1.00248	1
44	1.25468	1.19173	1.14056	1.09938	1.06674	1.04152	1.02282	1.00996	1.00246	1
45	1.24324	1.18406	1.13562	1.09637	1.06504	1.04066	1.02246	1.00985	1.00244	1
46	1.23305	1.17723	1.13124	1.09371	1.06356	1.03993	1.02216	1.00977	1.00243	1
47	1.22395	1.17114	1.12734	1.09136	1.06227	1.03931	1.02192	1.00971	1.00243	1
48	1.21584	1.16573	1.12389	1.08931	1.06116	1.03879	1.02174	1.00967	1.00243	1

Table 30. Error factor (cont.)

θ / ϕ	81	82	83	84	85	86	87	88	89	90
42	1.28195	1.20999	1.15234	1.10659	1.07085	1.04363	1.02374	1.01026	1.00251	1
43	1.26751	1.20033	1.14611	1.10277	1.06867	1.0425	1.02324	1.0101	1.00248	1
44	1.25468	1.19173	1.14056	1.09938	1.06674	1.04152	1.02282	1.00996	1.00246	1
45	1.24324	1.18406	1.13562	1.09637	1.06504	1.04066	1.02246	1.00985	1.00244	1
46	1.23305	1.17723	1.13124	1.09371	1.06356	1.03993	1.02216	1.00977	1.00243	1
47	1.22395	1.17114	1.12734	1.09136	1.06227	1.03931	1.02192	1.00971	1.00243	1
48	1.21584	1.16573	1.12389	1.08931	1.06116	1.03879	1.02174	1.00967	1.00243	1
49	1.2086	1.16092	1.12086	1.08753	1.06022	1.03837	1.0216	1.00966	1.00244	1
50	1.20216	1.15666	1.1182	1.086	1.05944	1.03806	1.02153	1.00967	1.00246	1
51	1.19644	1.15291	1.11589	1.0847	1.05881	1.03783	1.0215	1.00971	1.00248	1
52	1.19138	1.14963	1.11391	1.08363	1.05834	1.0377	1.02153	1.00977	1.00251	1
53	1.18692	1.14678	1.11224	1.08277	1.058	1.03766	1.02161	1.00985	1.00254	1
54	1.18301	1.14434	1.11085	1.08212	1.05781	1.03771	1.02174	1.00996	1.00258	1
55	1.17963	1.14228	1.10975	1.08166	1.05775	1.03785	1.02193	1.0101	1.00263	1
56	1.17673	1.14058	1.10891	1.0814	1.05783	1.03808	1.02217	1.01026	1.00269	1
57	1.17429	1.13922	1.10833	1.08133	1.05804	1.0384	1.02247	1.01045	1.00275	1
58	1.17228	1.1382	1.108	1.08145	1.0584	1.03883	1.02283	1.01068	1.00283	1
59	1.17069	1.13751	1.10793	1.08176	1.0589	1.03935	1.02326	1.01094	1.00291	1
60	1.1695	1.13713	1.10811	1.08227	1.05955	1.03998	1.02376	1.01123	1.00301	1
61	1.16871	1.13707	1.10853	1.08298	1.06035	1.04073	1.02433	1.01157	1.00312	1
62	1.1683	1.13732	1.10922	1.08389	1.06131	1.04159	1.02498	1.01195	1.00324	1
63	1.16827	1.13789	1.11016	1.08502	1.06245	1.04259	1.02572	1.01238	1.00338	1
64	1.16862	1.13878	1.11138	1.08637	1.06377	1.04372	1.02657	1.01286	1.00354	1
65	1.16935	1.13999	1.11288	1.08796	1.06528	1.04502	1.02752	1.01341	1.00371	1
66	1.17048	1.14155	1.11468	1.08981	1.06702	1.04648	1.02859	1.01403	1.00391	1
67	1.17201	1.14347	1.11679	1.09194	1.06898	1.04813	1.0298	1.01473	1.00414	1
68	1.17395	1.14576	1.11924	1.09436	1.0712	1.04999	1.03116	1.01552	1.0044	1
69	1.17632	1.14844	1.12204	1.09711	1.07371	1.05208	1.0327	1.01641	1.00469	1
70	1.17915	1.15155	1.12524	1.10021	1.07653	1.05444	1.03444	1.01743	1.00503	1
71	1.18246	1.15511	1.12886	1.10371	1.07971	1.05711	1.03641	1.0186	1.00542	1
72	1.18628	1.15915	1.13295	1.10764	1.08329	1.06011	1.03865	1.01993	1.00588	1
73	1.19066	1.16374	1.13756	1.11207	1.08731	1.06351	1.0412	1.02146	1.0064	1
74	1.19563	1.1689	1.14273	1.11704	1.09186	1.06737	1.04412	1.02324	1.00702	1
75	1.20124	1.17472	1.14855	1.12264	1.09699	1.07177	1.04748	1.0253	1.00776	1
76	1.20757	1.18124	1.15508	1.12895	1.10281	1.07678	1.05135	1.02773	1.00863	1
77	1.21468	1.18856	1.16242	1.13607	1.10942	1.08254	1.05586	1.03059	1.00969	1
78	1.22265	1.19678	1.17067	1.14412	1.11696	1.08918	1.06114	1.03401	1.01099	1
79	1.23159	1.206	1.17998	1.15325	1.12559	1.09688	1.06735	1.03813	1.01259	1
80	1.24161	1.21636	1.19049	1.16365	1.13552	1.10586	1.07474	1.04315	1.01461	1
81	1.25284	1.22803	1.20239	1.17553	1.147	1.11642	1.08361	1.04934	1.0172	1
82	1.26545	1.24119	1.21592	1.18917	1.16036	1.12891	1.09437	1.0571	1.0206	1
83	1.27963	1.25607	1.23135	1.20489	1.176	1.14384	1.10758	1.067	1.02518	1
84	1.2956	1.27296	1.24902	1.22314	1.19446	1.16187	1.12402	1.07988	1.03155	1
85	1.31364	1.29218	1.26935	1.24444	1.21641	1.18386	1.14483	1.09706	1.04077	1
86	1.33408	1.31415	1.29288	1.26947	1.24278	1.21106	1.17165	1.12065	1.05483	1
87	1.35731	1.33939	1.32026	1.29914	1.27478	1.24519	1.20698	1.15421	1.07773	1
88	1.38383	1.36852	1.35235	1.33461	1.31408	1.28875	1.25475	1.20412	1.11868	1
89	1.41423	1.40234	1.39025	1.37743	1.36304	1.34547	1.32141	1.28264	1.20241	1
90	1.44926	1.44188	1.43538	1.42975	1.425	1.42111	1.41809	1.41594	1.41464	1.22475

APPENDIX II

TEST DATA

Test data, with approximately zero error, were established for the purpose of producing further sets of data of known error. The subsequent data sets were used in the development and testing of techniques for the automated reproduction of three dimensional coordinates. The configuration of the camera system was arbitrary but consisted of eight cameras positioned evenly around a laboratory test region 1.5m x 1.0m x 0.5m in size. The average object distances varied between 8 and 10.5 meters, but all cameras had a principal distance of 0.10 m. The laboratory space boundary was defined by eight points which were also the camera calibration points. The set up is presented in Figure 20 with relevant measurements in Tables 31 and 32.

Figure 20. Test data set up.

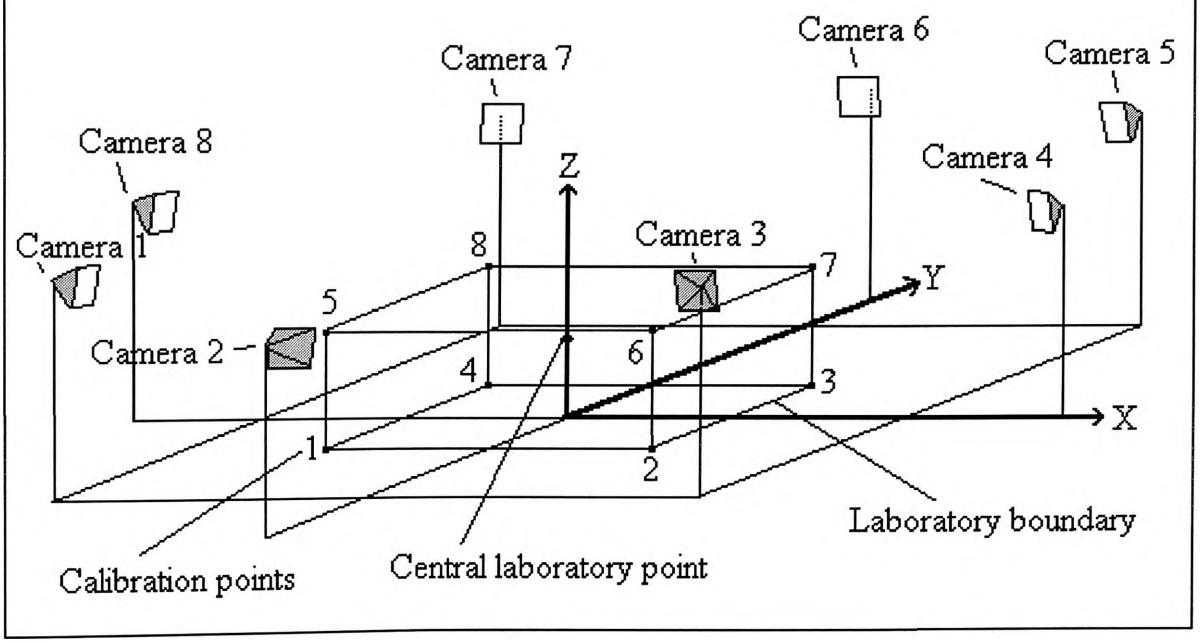

Table 31. Laboratory boundary.

Lab Point	Coordinate (m)		
	X	Y	Z
1	-0.5	-0.10	0.05
2	1.00	-0.10	0.05
3	1.00	0.40	0.05
4	-0.50	0.40	0.05
5	-0.50	-0.10	1.00
6	1.00	-0.10	1.00
7	1.00	0.40	1.00
8	-0.50	0.40	1.00
Central Point	0.50	0.30	0.75

Table 32. Camera positions.

Camera	Principal Distance (m)	Perspective Centre*			Unit Vector along Principal Axis*		
		X	Y	Z	X	Y	Z
1	0.10	-7.0	-7.0	1.8	0.713018	0.694004	-0.099823
2	0.10	0.0	-9.0	1.8	0.533479	0.992272	-0.112031
3	0.10	7.0	-7.0	1.8	-0.661195	0.742572	-0.106808
4	0.10	10.0	0.0	1.8	-0.993458	0.031372	-0.109803
5	0.10	7.0	7.0	1.8	-0.691950	-0.713240	-0.111777
5	0.10	0.0	9.0	1.8	0.569646	-0.991184	-0.119626
7	0.10	-7.0	7.0	1.8	0.741730	-0.662612	-0.103842
8	0.10	-9.0	0.0	1.8	0.993458	0.031372	-0.109803

*All coordinates in metres.

The calculation of camera image coordinates first required the calculation of the intersection of each laboratory point's collinear line with the image plane of the respective camera expressed relative to the laboratory coordinate system. Knowing the position of the axis system on the image plane, a coordinate transformation then produced the local image coordinates for each laboratory point in the respective

camera. The laboratory space coordinates of the intersection of the collinear lines with each camera, as well as the respective image coordinates following the coordinate transformation, are presented in Tables 33 - 40. The two dimensional image coordinate data were the Y and Z coordinates of the image plane coordinates. The camera DLT coefficients are presented in Table 41, the Conjugate Point Errors (CPE) for the eight cameras in Table 42, and the markers reproduced and LPSE are presented in Table 43.

Table 33. Camera 1 - image plane coordinates relative to laboratory space and image plane of the eight calibration markers.

Lab Point	Lab Coordinates			Image Plane Coordinates		
	X	Y	Z	X	Y	Z
1	-6.932277	-6.928110	1.781767	0.000366	11.740185	4.749141
2	-6.925005	-6.935317	1.783595	0.000584	21.926029	6.577120
3	-6.927368	-6.932816	1.784112	0.000366	18.502581	7.093987
4	-6.934640	-6.925590	1.782403	0.000810	8.304294	5.385341
5	-6.931601	-6.927392	1.791582	0.000759	11.698179	14.563951
6	-6.924333	-6.934737	1.792433	0.000415	21.979420	15.415561
7	-6.926737	-6.932232	1.792674	0.000866	18.524164	15.655994
8	-6.934011	-6.924874	1.791878	0.000254	8.229930	14.860450

Table 34) Camera 2; image plane coordinates relative to laboratory space and image plane of the eight calibration markers.

Lab Point	Lab Coordinates			Image Plane Coordinates		
	X	Y	Z	X	Y	Z
1	-0.005555	-8.901118	1.780557	-0.000862	7.212623	4.759760
2	0.011012	-8.901989	1.780728	0.000021	23.698629	4.931297
3	0.010442	-8.901846	1.781727	-0.000397	23.124903	5.929661
4	-0.005265	-8.901019	1.781573	-0.000979	7.495311	5.775549
5	-0.005622	-8.899935	1.791005	0.000092	7.083532	15.208447
6	0.011143	-8.900826	1.791085	-0.000091	23.766222	15.288622
7	0.010559	-8.900743	1.791553	0.000349	23.182476	15.755664
8	-0.005325	-8.899897	1.791481	-0.000034	7.376213	15.683611

Table 35. Camera 3 - image plane coordinates relative to laboratory space and image plane of the eight calibration markers.

Lab Point	Lab Coordinates			Image Plane Coordinates		
	X	Y	Z	X	Y	Z
1	6.926969	-6.932811	1.782959	-0.000355	5.193901	6.640214
2	6.935329	-6.925629	1.781138	-0.000517	16.151100	4.818497
3	6.937818	-6.923309	1.781864	-0.000142	19.533007	5.544425
4	6.929517	-6.930457	1.783554	-0.000400	8.642539	7.234722
5	6.926240	-6.932141	1.792132	-0.000168	5.095978	15.813151
6	6.934615	-6.924807	1.791282	-0.000661	16.163765	14.962757
7	6.937157	-6.922494	1.791621	-0.000397	19.581160	15.301617
8	6.928839	-6.929787	1.792409	-0.000044	8.581970	16.090250

Table 36. Camera 4 - image plane coordinates relative to laboratory space and image plane of the eight calibration markers.

Lab Point	Lab Coordinates			Image Plane Coordinates		
	X	Y	Z	X	Y	Z
1	9.901133	-0.000942	1.783522	0.000195	2.962847	7.502244
2	9.901425	-0.001095	1.780833	-0.000188	2.819354	4.812763
3	9.901594	0.004374	1.780865	0.000086	8.257744	4.845627
4	9.901278	0.003761	1.783546	0.000087	7.639075	7.526627
5	9.900152	-0.000951	1.792392	-0.000142	2.922811	16.372707
6	9.900286	-0.001108	1.791137	0.000188	2.771026	15.116722
7	9.900459	0.004424	1.791152	-0.000368	8.272269	15.132033
8	9.900301	0.003798	1.792404	-0.000208	7.645414	16.384014

Table 37. Camera 5 - image plane coordinates relative to laboratory space and image plane of the eight calibration markers.

Lab Point	Lab Coordinates			Image Plane Coordinates		
	X	Y	Z	X	Y	Z
1	6.928225	6.932053	1.783252	0.000517	22.176830	7.429907
2	6.936247	6.924559	1.781405	0.000292	11.270140	5.582828
3	6.933736	6.927110	1.780673	0.000071	14.825552	4.850495
4	6.925688	6.934606	1.782661	0.000530	25.752489	6.838154
5	6.927488	6.931355	1.792265	0.000386	22.219593	16.442770
6	6.935520	6.923698	1.791403	0.000109	11.193054	15.580103
7	6.932950	6.926245	1.791060	0.000064	14.787787	15.237484
8	6.924898	6.933910	1.791989	0.000608	25.835047	16.166557

Table 38. Camera 6 - image plane coordinates relative to laboratory space and image plane of the eight calibration markers.

Lab Point	Lab Coordinates			Image Plane Coordinates		
	X	Y	Z	X	Y	Z
1	-0.005434	8.901093	1.780980	-0.000479	31.020647	5.942199
2	0.010769	8.902004	1.781155	-0.000998	14.908413	6.117078
3	0.011376	8.902167	1.780092	-0.000256	14.297355	5.054749
4	-0.005744	8.901207	1.779897	-0.000606	31.320847	4.859300
5	-0.005502	8.899857	1.791196	-0.000452	31.158520	16.158741
6	0.010902	8.900790	1.791278	-0.001084	14.845366	16.240656
7	0.011525	8.900886	1.790780	-0.000735	14.222728	15.742695
8	-0.005820	8.899900	1.790688	-0.001303	31.470613	15.650906

Table 39. Camera 7 - image plane coordinates relative to laboratory space and image plane of the eight calibration markers.

Lab Point	Lab Coordinates			Image Plane Coordinates		
	X	Y	Z	X	Y	Z
1	-6.933042	6.926861	1.781973	0.000167	23.881943	5.356988
2	-6.926064	6.934381	1.783826	-0.000026	13.679747	7.210612
3	-6.923728	6.937076	1.783315	0.000220	10.134094	6.699707
4	-6.930676	6.929609	1.781336	0.000206	20.275822	4.719889
5	-6.932354	6.926110	1.791674	0.000109	23.983618	15.058531
6	-6.925383	6.933777	1.792538	0.000598	13.677253	15.922542
7	-6.923004	6.936478	1.792300	0.000496	10.097086	15.684662
8	-6.929938	6.928861	1.791377	0.000167	20.342470	14.761210

Table 40. Camera 8 - image plane coordinates relative to laboratory space and image plane of the eight calibration markers.

Lab Point	Lab Coordinates			Image Plane Coordinates		
	X	Y	Z	X	Y	Z
1	-8.901545	-0.001158	1.779730	-0.000169	12.239504	3.710260
2	-8.901220	-0.000988	1.782714	-0.000305	12.080292	6.693858
3	-8.901373	0.003945	1.782740	-0.000076	7.174916	6.720714
4	-8.901724	0.004625	1.779767	-0.000877	6.488642	3.746891
5	-8.900341	-0.001172	1.790620	-0.000742	12.291335	14.600570
6	-8.900192	-0.000998	1.792015	-0.000658	12.122761	15.995546
7	-8.900348	0.003986	1.792028	-0.000095	7.166338	16.008152
8	-8.900524	0.004681	1.790637	-0.000899	6.470191	14.617767

Table 41. Test data, DLT coefficients.

Camera							
1	2	3	4	5	6	7	8
8.057392	10.970978	6.422073	-0.376740	-8.346438	-10.7246	-5.578152	1.212952
-6.002474	1.371640	7.711554	9.826633	5.613270	-2.793334	-8.330841	-10.84359
-0.159270	-0.220882	-0.159538	-0.075939	-0.200960	-0.261856	-0.14527	-0.096081
14.672402	12.742438	9.313993	3.903699	19.484764	25.611671	19.528564	11.089638
1.633859	0.141531	-1.562818	-2.351306	-1.666732	0.155589	1.731428	2.606824
1.590557	2.629813	1.755145	0.074386	-1.718562	-2.708070	-1.546957	0.082146
9.742443	10.653508	9.729325	9.609426	9.692859	10.618811	9.740084	10.654251
5.033953	4.492293	5.714183	6.214997	6.244873	5.260249	5.415321	4.283977
0.071088	0.005849	-0.065991	-0.098054	-0.068941	0.006232	0.074039	0.108707
0.069219	0.108657	0.074122	0.003109	-0.071113	-0.108490	-0.066159	0.003410
-0.009960	-0.012271	-0.010642	-0.010853	-0.011159	-0.013095	-0.010380	-0.012010

Table 42. Test data - CPE.

Camera	Conjugate Point Error	
	mean (m)	Std.Deviation (m)
camera 1	0.000125	0.000066
camera 2	0.000085	0.000026
camera 3	0.000160	0.000049
camera 4	0.000101	0.000028
camera 5	0.000142	0.000050
camera 6	0.000112	0.000042
camera 7	0.000157	0.000039
camera 8	0.000083	0.000016

Table 43. Test data - laboratory calibration markers reproduced and LPSE.

Lab Point	Lab Coordinates *		
	X	Y	Z
Lab point 1	-0.500000	-0.099994	0.050001
Lab point 2	1.000003	-0.099992	0.049997
Lab point 3	1.000003	0.399994	0.050003
Lab point 4	-0.500004	0.399993	0.049999
Lab point 5	-0.499997	-0.100008	1.000002
Lab point 6	0.999995	-0.100005	1.000000
Lab point 7	1.000000	0.400004	1.000000
Lab point 8	-0.499998	0.400010	0.999997
LPSE	0.000003 ± 0.000000 m		

* Actual laboratory coordinates of markers are presented in Table 31.

APPENDIX III

THREE DIMENSIONAL REPRODUCTION ALGORITHM - SCHEMATIC

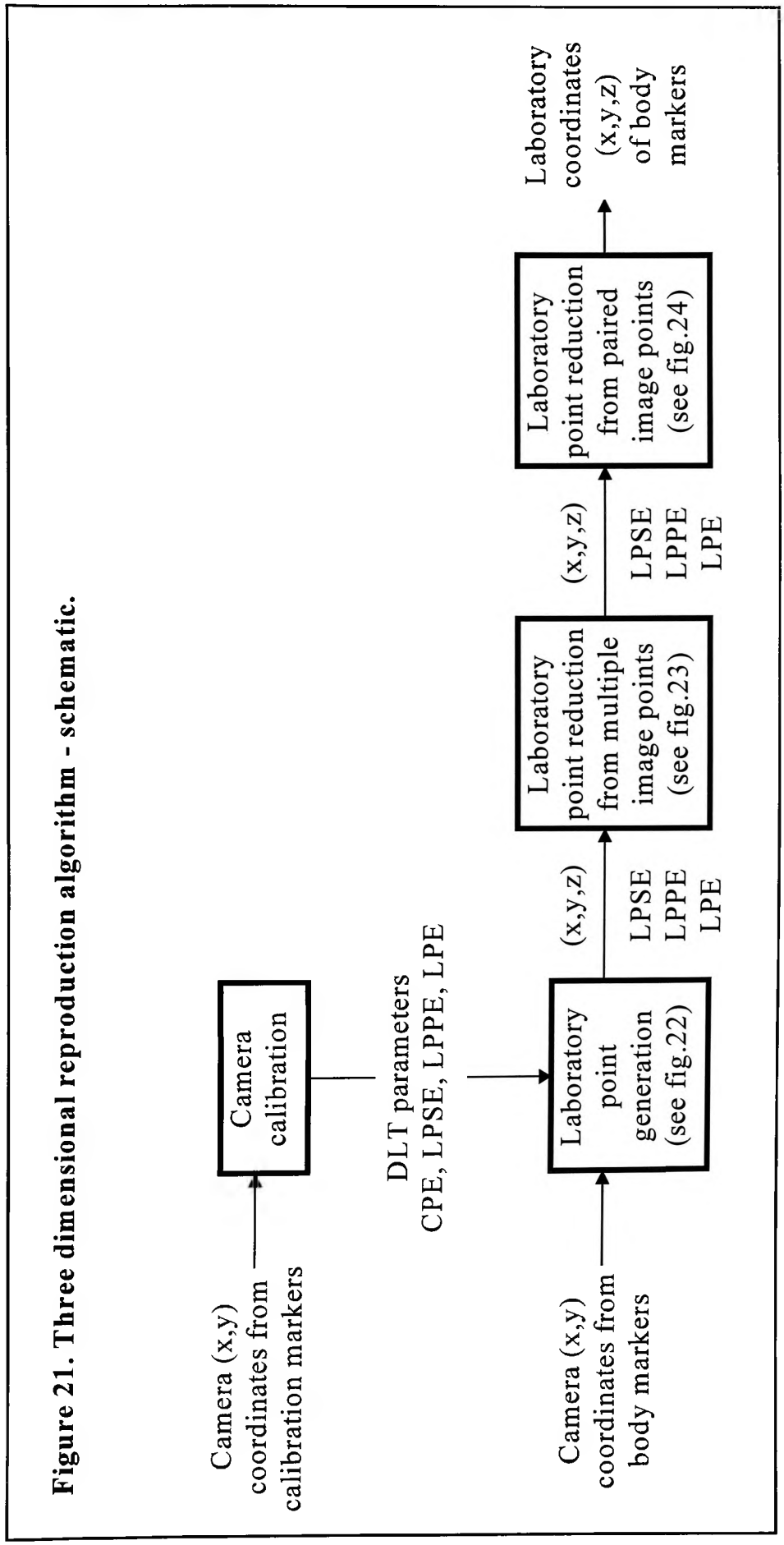

Figure 21. Three dimensional reproduction algorithm - schematic.

Figure 22. Three dimensional point generation - schematic

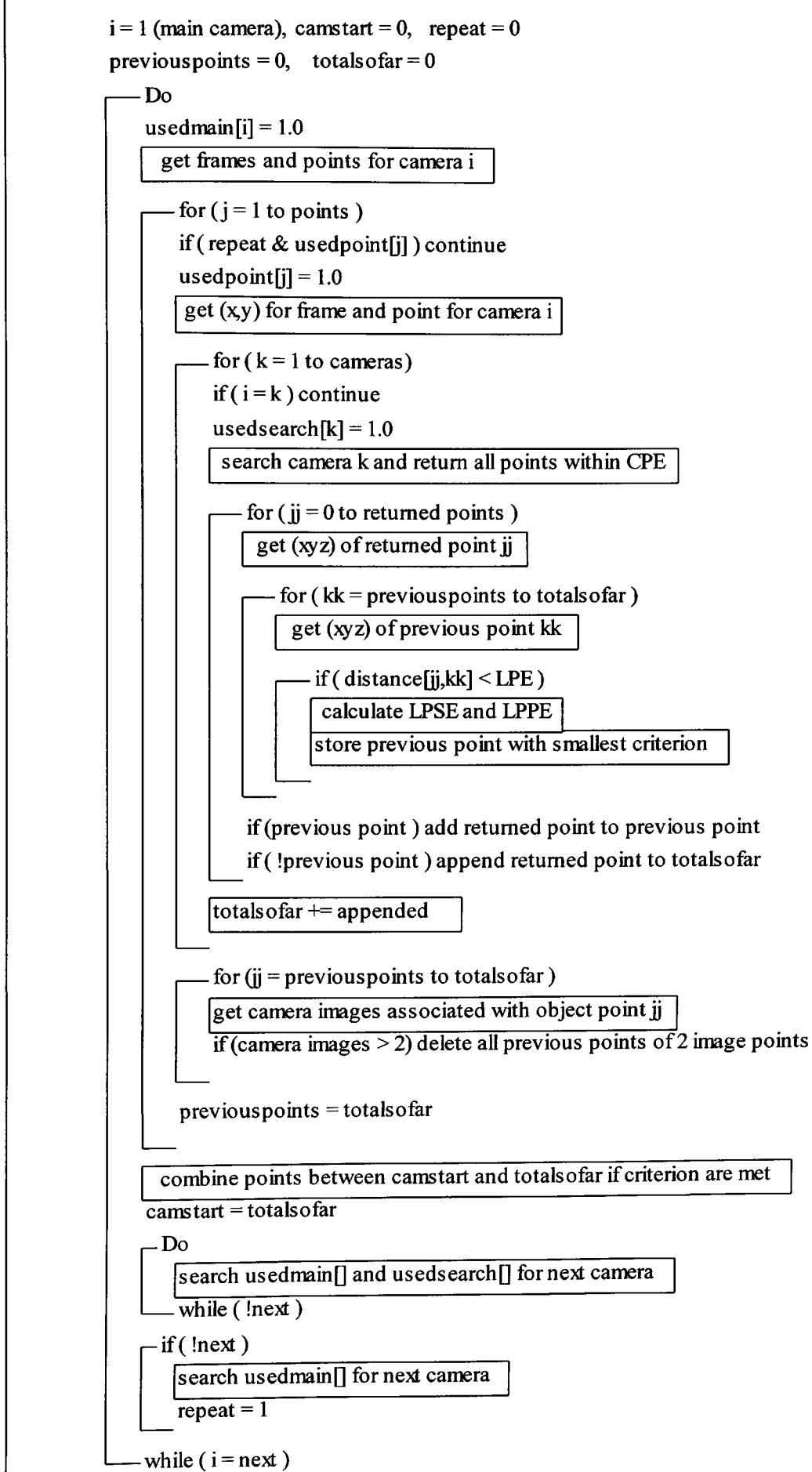

Figure 23. Three dimensional point reduction : amongst object points from multiple image points.

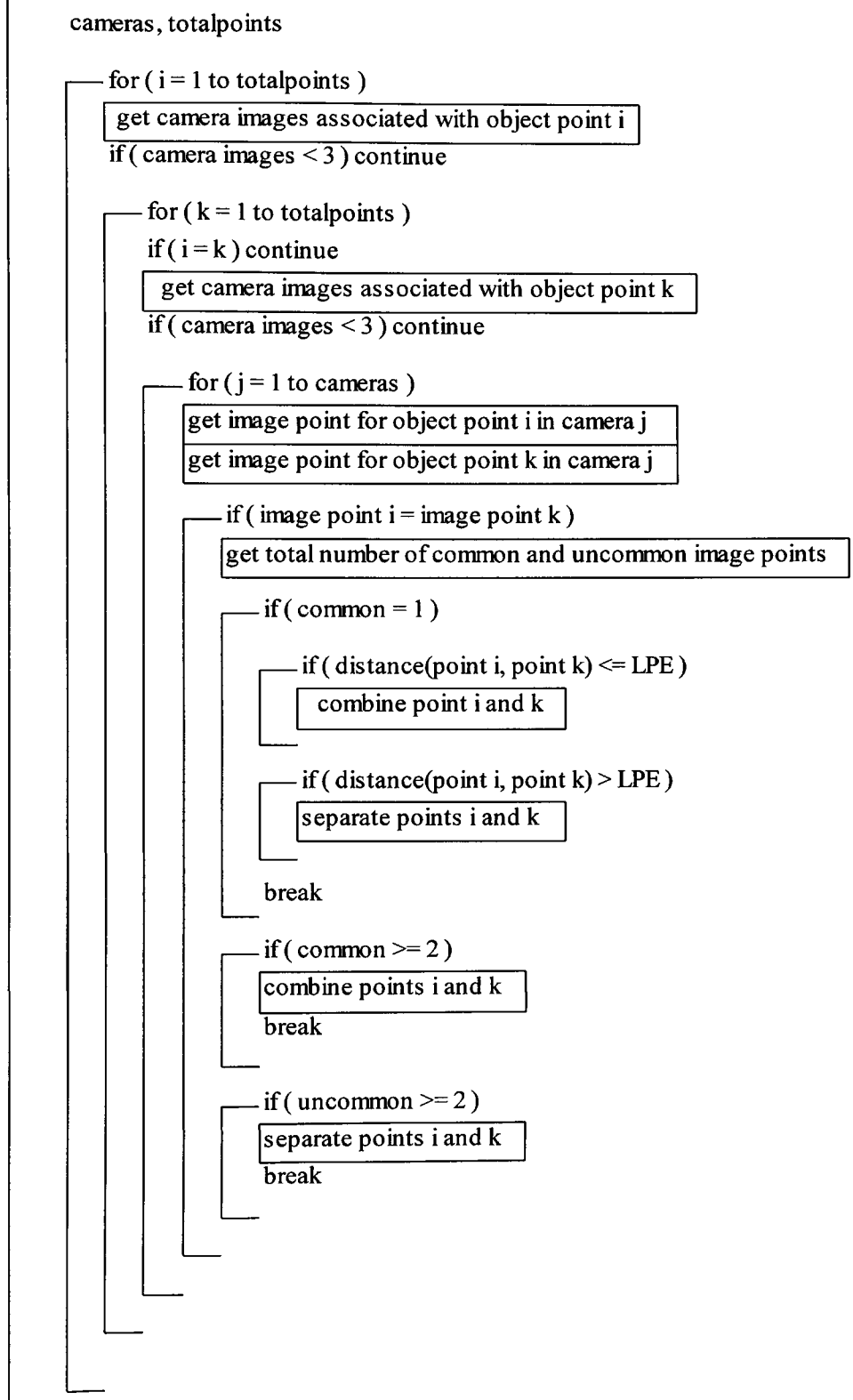

Figure 24. Three dimensional point reduction : amongst object points of paired image points.

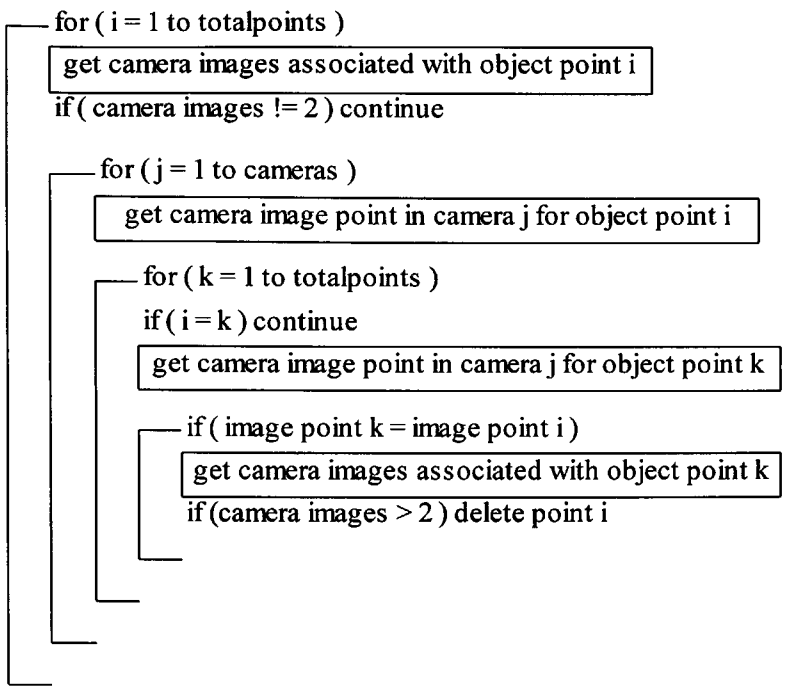

APPENDIX IV

VIDEO DATA

The video data consisted of four camera views of an eight marker calibration cube and a set of 55 body markers. The laboratory coordinates of the calibration markers are given in Table 44 and the respective digitised image coordinates of the calibration cube for each camera are in Table 45. The DLT parameters follow in Table 46. The CPE errors of the four cameras are presented in Table 47 and the markers reproduced and LPSE are presented in Table 48. The image coordinates for the body markers in each respective camera are listed in Table 49. Finally the conjugate image points for each body marker and the reproduced laboratory coordinate are given in Table 50.

Table 44. Calibration cube.

Calibration Marker	Coordinate		
	X	Y	Z
1	00.00	00.00	0.039
2	0.749	00.00	0.038
3	0.749	00.50	0.039
4	00.00	00.50	0.038
5	00.01	0.004	0.786
6	0.748	00.00	0.786
7	0.749	00.50	0.787
8	00.01	0.502	0.786

Table 45. Camera image coordinates of calibration markers.

Marker	Camera 1		Camera 2		Camera 3		Camera 4	
	X	Y	X	Y	X	Y	X	Y
1	116.08	88.00	71.20	115.41	111.00	124.80	144.18	64.46
2	153.66	97.67	109.25	105.00	72.22	117.67	98.00	72.25
3	122.50	100.80	141.91	109.19	103.16	113.34	67.81	67.64
4	84.66	91.84	103.08	118.00	141.00	121.50	114.86	58.47
5	113.66	152.84	73.50	174.80	111.00	179.25	145.58	128.42
6	151.85	156.15	111.27	172.09	70.88	178.00	99.00	130.25
7	120.50	155.80	145.36	171.55	102.35	177.29	69.07	130.29
8	81.50	151.80	105.14	174.15	140.83	179.00	116.09	128.41

Table 46. Video data, DLT parameters.

DLT parameter	Camera			
	1	2	3	4
1	72.6420	34.1021	-61.4585	-47.9893
2	-51.4674	75.7943	45.1005	-77.2885
3	-7.8696	-0.7631	-3.6160	0.0239
4	116.3281	71.2728	111.2424	144.0869
5	27.5385	-29.2734	-25.0476	20.7757
6	20.8480	20.1931	-18.9989	-21.3534
7	81.1971	73.8173	67.6006	83.0803
8	84.6791	112.3311	122.1177	61.1471
9	0.1489	-0.1495	-0.1304	0.1420
10	0.1392	0.1231	-0.1010	-0.1640
11	-0.0362	-0.0324	-0.0291	-0.0201

Table 47. Video data, Conjugate Point Error.

	Camera 1	Camera 2	Camera 3	Camera 4
CPE*	0.0849±0.0549	0.1221±0.0542	0.1182±0.0467	0.0896±0.0314

*The camera view was 240 x 240 pixels for all cameras.

Table 48. Video data, calibration markers reproduced and LPSE.

Marker Point	Coordinate * (m)		
	X	Y	Z
point 1	0.0001	-0.0008	0.0391
point 2	0.7490	-0.0011	0.0382
point 3	0.7473	0.5015	0.0392
point 4	0.0015	0.5005	0.0374
point 5	0.0092	0.0060	0.7855
point 6	0.7487	0.0001	0.7862
point 7	0.7500	0.4996	0.7863
point 8	0.0092	0.5003	0.7870
LPSE	0.0036 m ± 0.0035 m		

* Actual laboratory coordinates are presented in Table 44.

Table 49. Video data, camera image coordinates of body markers .

	Camera 1		Camera 2		Camera 3		Camera 4	
	X	Y	X	Y	X	Y	X	Y
1	124.674	220.474	138.868	245.046	137.565	255.177	79.792	199.270
2	89.887	215.552	175.452	238.904	152.781	221.176	37.856	206.778
3	123.927	190.179	118.869	210.168	140.465	222.334	97.184	166.215
4	124.801	165.633	197.964	206.600	132.480	195.584	6.182	173.705
5	102.703	174.498	117.769	183.829	103.792	196.953	96.705	140.716
6	123.606	171.290	211.759	206.945	118.580	197.195	65.748	152.707
7	95.653	170.099	139.232	189.255	105.578	157.090	75.964	147.158
8	125.179	139.057	168.661	187.716	131.734	155.055	42.219	148.655
9	118.474	139.207	155.263	190.156	113.776	124.219	57.705	108.437
10	105.066	137.412	167.798	189.454	131.529	123.758	47.668	107.915
11	119.714	108.657	144.659	151.829	94.126	118.735	75.688	77.309
12	113.018	109.222	151.775	152.011	103.389	117.554	68.159	76.302
13	100.563	109.013	134.903	120.080	118.219	117.440	63.982	74.030
14	97.960	109.239	145.061	122.509	128.085	116.214	60.666	73.573
15	129.899	106.424	144.083	113.075	100.265	179.500	57.469	73.599
16	109.642	106.932	152.732	113.998	100.344	173.262	43.050	69.885
17	115.952	158.752	155.530	116.049	102.277	179.341	69.428	133.700
18	117.200	154.794	163.563	116.876	100.935	174.522	68.032	129.162
19	117.403	149.427	142.960	173.601	100.954	172.934	67.925	123.057
20	122.359	157.630	142.661	167.449	134.688	179.240	57.262	133.694
21	122.555	152.226	150.095	173.347	134.709	172.771	57.180	128.830
22	96.883	158.186	151.322	168.634	126.985	179.308	57.070	122.348
23	97.056	154.214	151.244	167.094	127.011	174.497	47.689	132.212
24	97.285	148.930	158.047	173.476	127.019	172.896	47.581	125.666
25	94.066	156.948	157.818	169.102	99.128	145.574	69.178	104.863
26	94.296	151.745	157.741	167.646	100.570	139.661	70.383	98.642
27	119.409	133.373	139.823	139.935	101.038	149.549	71.596	92.385
28	118.527	127.886	138.129	134.111	102.437	143.506	56.740	102.925
29	117.642	122.384	147.151	144.293	103.820	137.527	58.046	96.279
30	124.854	128.044	145.477	138.439	134.305	144.244	59.301	89.598
31	123.930	122.520	143.821	132.647	135.546	138.223	50.203	96.222
32	97.969	133.172	157.009	145.889	126.765	149.003	51.441	89.596
33	97.023	127.779	155.315	140.341	128.101	142.875		
34	96.123	122.376	153.697	134.840	129.369	136.807		
35	95.502	128.292						
36	94.609	123.037						

Table 50. Conjugate image points and reproduced laboratory coordinates.

Lab Point	Conjugate Image Points					Reproduced Coordinates		
	total	camera 1	camera 2	camera 3	camera 4	X	Y	Z
1	3	1.0000	1.0000	0.0000	1.0000	0.7233	0.3728	1.6197
2	4	2.0000	2.0000	1.0000	2.0000	0.7230	0.9797	1.6200
3	3	3.0000	3.0000	0.0000	3.0000	0.5373	0.2569	1.2238
4	3	4.0000	5.0000	0.0000	5.0000	0.5372	0.2569	0.9179
5	2	5.0000	0.0000	0.0000	6.0000	0.6074	0.6768	1.0442
6	3	6.0000	7.0000	0.0000	7.0000	0.7232	0.4187	0.9899
7	4	7.0000	8.0000	4.0000	8.0000	0.7229	0.9098	0.9901
8	2	8.0000	11.000	0.0000	0.0000	0.7929	0.4664	0.5579
9	3	9.0000	12.000	7.0000	0.0000	0.7926	0.5815	0.5581
10	2	10.000	0.0000	0.0000	9.0000	0.6773	0.7227	0.5403
11	3	11.000	13.000	0.0000	11.000	0.6531	0.4665	0.1620
12	3	12.000	0.0000	9.0000	12.000	0.6529	0.5819	0.1623
13	3	13.000	14.000	0.0000	13.000	0.5601	0.7225	0.1621
14	3	14.000	0.0000	10.000	14.000	0.5599	0.7699	0.1624
15	3	15.000	15.000	11.000	0.0000	0.8395	0.4425	0.1081
16	3	16.000	17.000	13.000	0.0000	0.7465	0.7225	0.1081
17	2	17.000	0.0000	0.0000	17.000	0.7003	0.5368	0.8282
18	2	18.000	0.0000	0.0000	18.000	0.7233	0.5368	0.7742
19	2	19.000	0.0000	0.0000	19.000	0.7233	0.5368	0.7022
20	3	20.000	19.000	15.000	0.0000	0.7467	0.4666	0.8101
21	3	21.000	20.000	16.000	0.0000	0.7467	0.4666	0.7381
22	2	22.000	0.0000	0.0000	20.000	0.6074	0.7927	0.8283
23	2	23.000	0.0000	0.0000	21.000	0.6074	0.7927	0.7743
24	2	24.000	0.0000	0.0000	22.000	0.6074	0.7927	0.7023
25	3	25.000	0.0000	20.000	23.000	0.6531	0.8870	0.8104
26	3	26.000	0.0000	21.000	24.000	0.6531	0.8870	0.7384
27	2	27.000	0.0000	0.0000	25.000	0.7232	0.5127	0.4862
28	2	28.000	0.0000	0.0000	26.000	0.7002	0.5127	0.4142
29	2	29.000	0.0000	0.0000	27.000	0.6772	0.5127	0.3422
30	3	30.000	27.000	25.000	0.0000	0.7466	0.4426	0.4141
31	3	31.000	28.000	26.000	0.0000	0.7226	0.4426	0.3421
32	2	32.000	0.0000	0.0000	28.000	0.6073	0.7927	0.4863
33	2	33.000	0.0000	0.0000	29.000	0.5833	0.7927	0.4143
34	2	34.000	0.0000	0.0000	30.000	0.5603	0.7927	0.3423
35	3	35.000	0.0000	30.000	31.000	0.6300	0.8629	0.4144
36	3	36.000	0.0000	31.000	32.000	0.6070	0.8630	0.3434
37	3	0.0000	4.0000	2.0000	4.0000	0.8620	1.2703	1.2418
38	2	0.0000	6.0000	3.0000	0.0000	1.0716	1.2700	1.2419
39	2	0.0000	9.0000	5.0000	0.0000	0.8163	0.5829	1.0079
40	2	0.0000	10.000	6.0000	0.0000	0.8162	0.7929	1.0079

Table 50. Conjugate image points and reproduced laboratory coordinates (cont.)

Lab Point	Conjugate Image Points					Reproduced Coordinates		
	total	camera 1	camera 2	camera 3	camera 4	X	Y	Z
40	2	0.0000	10.000	6.0000	0.0000	0.8162	0.7929	1.0079
41	2	0.0000	0.0000	8.0000	10.000	0.6765	0.8633	0.5403
42	3	0.0000	16.000	12.000	15.000	0.8393	0.5830	0.1080
43	3	0.0000	18.000	14.000	16.000	0.7462	0.8631	0.1080
44	2	0.0000	21.000	17.000	0.0000	0.7923	0.5369	0.8099
45	2	0.0000	22.000	18.000	0.0000	0.8163	0.5369	0.7559
46	2	0.0000	23.000	19.000	0.0000	0.8163	0.5369	0.7379
47	2	0.0000	24.000	22.000	0.0000	0.6693	0.7930	0.8099
48	2	0.0000	25.000	23.000	0.0000	0.6692	0.7930	0.7559
49	2	0.0000	26.000	24.000	0.0000	0.6692	0.7929	0.7379
50	2	0.0000	29.000	27.000	0.0000	0.7922	0.5128	0.4679
51	2	0.0000	30.000	28.000	0.0000	0.7692	0.5128	0.3959
52	2	0.0000	31.000	29.000	0.0000	0.7462	0.5128	0.3239
53	2	0.0000	32.000	32.000	0.0000	0.6761	0.7929	0.4679
54	2	0.0000	33.000	33.000	0.0000	0.6521	0.7929	0.3958
55	2	0.0000	34.000	34.000	0.0000	0.6291	0.7929	0.3238